早稲田大学審査学位論文

博士（スポーツ科学）

Morphological and mechanical properties of the human triceps surae aponeuroses and their functional roles in motor performance

人間の下腿三頭筋腱膜の形態的・力学的特性と身体運動パフォーマンスとの関連性

２０１９年７月

早稲田大学大学院　スポーツ科学研究科

単　西瑶

SHAN, Xiyao

研究指導教員：　川上　泰雄　教授

Preface

The human triceps surae muscle-tendon unit is a complex muscle group comprised of two biarticular gastrocnemii and one monoarticular soleus. All three muscles join to the common Achilles tendon distally, while intricated aponeuroses are located in both posterior and anterior surface regions of each muscle belly. The main function of triceps surae muscle-tendon unit is plantar flexion, and it plays an important role in human motor performance, such as walking. During human motor performance, the muscles work as actuators while the tendinous tissues (tendon and aponeurosis) work as spring, and both muscles and tendinous tissues interact with each other anatomically and functionally. The muscle-tendon interaction during motor performance works in such a way that the spring-like function of tendinous tissues contribute to energy saving and power enhancement. However, being as a substantially large and sheet-like tendinous tissues, the aponeurosis in the triceps surae can function both as a spring and muscle fibers' attachment base. A large number of studies have focused on the mechanical property of the Achilles tendon, but morphological and mechanical properties of the complicated aponeuroses still remain unclear. This thesis compiles a series of studies which were carried out on the morphological and mechanical properties of the human triceps surae aponeuroses *in vivo* and *ex-situ*, in an attempt to understand how this elastic sheet tissue contributes to human motor performance.

Table of contents

CHAPTER 1 Aponeuroses within the triceps surae

1-1 Introduction

The human triceps surae (TS), is a muscle group comprised of two biarticular gastrocnemii [medial and lateral gastrocnemius (MG and LG)] and one monoarticular soleus (SOL), contributing to human posture control and locomotion (Branthwaite et al., 2012; Honeine et al., 2013; Tokuno et al., 2007). It has aponeuroses in the proximal and distal sites, and the distal sites insert into the calcaneus by sharing the common Achilles tendon (Blitz and Eliot, 2007, 2008). The tendinous tissues (tendon and aponeuroses) play a significant role in human movements functioning as a spring and contributing to energy saving and power enhancement of the muscle-tendon unit (Fukunaga et al., 2002; Kawakami, 2012; Maganaris, 2002). Unlike the cord-like structure of tendon, the sheet-like structure of aponeurosis serves as an attachment site of muscle fascicles on the surface of a muscle belly, and can bear the pressure and tension during muscle contraction (Raiteri et al., 2016; Scott and Loeb, 1995).

To date, anisotropic and inhomogeneous properties of the TS aponeuroses have been reported (Muramatsu et al., 2001; Slane et al., 2017), and site-dependent differences of aponeuroses strains have been found during human movements through *in vivo* studies (Bojsen-Moller et al., 2004a; Finni et al., 2003; Magnusson et al., 2003). Few studies, however, focused on the site-dependent morphology and mechanical properties of TS aponeuroses. During muscle contraction, the aponeurosis is stretched both in the longitudinal (along the muscle's line of action) and transverse directions, and larger transverse deformability has been documented (Iwanuma et al., 2011).

Likewise, intrinsic bidirectional differences of aponeurosis have been confirmed in an animal cadaveric study (Azizi and Roberts, 2009), however, it remains unclear if intrinsic mechanical properties of human aponeurosis are direction-specific.

Recent advance of the ultrasound shear wave elastography (SWE) allows investigators to measure muscle and tendinous tissue stiffness during muscle contraction (Jeon et al., 2018; Mendes et al., 2018; Ryu and Jeong, 2017; Yoshitake et al., 2014), which has provided a method for investigating the muscle-tendon behavior during muscle contraction *in vivo*. Some studies (Ateş et al., 2015; Bouillard et al., 2012; Bouillard et al., 2011) reported a linear relationship of muscle stiffness and torque during muscle contractions, while others found a non-linear relationship for the mechanical properties of aponeurosis and exercise intensities (Arampatzis et al., 2007). Moreover, biaxial (longitudinal and transverse) strain of aponeurosis during muscle contraction was previously reported (Arellano et al., 2016). However, it remains unresolved whether the changes in stiffness are also direction-dependent.

Since the interaction between the foot and ground is extremely important for human beings' unique bipedal characteristics, the TS has achieved distinctive development (Hanna and Schmitt, 2011; Kumakura and Inokuchi, 1991). In addition, the essentiality of TS to walking which is human's most basic motor performance has been particularly recognized (Honeine et al., 2013), and the distinctive architectures of TS muscle and tendinous tissues (tendons and aponeuroses) are considered to be the results of adaptation to their required functions. Moreover, walking is one of the major daily physical activities of humans, and its performance is particularly important in the

elderly. However, walking performance has been shown to decline as people get older, and this can cause serious impact on life quality of the elderly (Yonei et al., 2008). Muscle strength of the TS and spring-like function of their tendinous tissues are known to play considerable roles in walking performance. In order to know how the tendinous tissues of the TS with various length and shapes function as springs, it is necessary to characterize their mechanical properties.

1-2 Terminology

1-2-1 Morphological property

Triceps surae

In this thesis, the triceps surae (TS) is a skeletal muscle (hereinafter muscle) group located in the posterior aspect of lower leg, comprised of three pennate muscles, which are medial gastrocnemius (MG), lateral gastrocnemius (LG) and soleus (SOL).

Triceps surae aponeuroses

Triceps surae aponeuroses are mainly distributed in eight regions: posterior and anterior regions of medial gastrocnemius (MG), lateral gastrocnemius (LG), medial part of soleus (SOL-med), lateral part of soleus (SOL-lat). In addition, aponeuroses in the anterior region of gastrocnemii and posterior region of soleus were named adjoining aponeuroses between gastrocnemii and soleus in chapter 3 and chapter 4 of this thesis.

Triceps surae muscle-aponeurosis-tendon unit

In this thesis, triceps surae muscle-aponeurosis-tendon unit (MTU, Fig. 1-1) is defined as a junctional complex connected by muscle fibers and connective tissue (e.g., aponeurosis and tendon) structures from proximal to distal. The muscle fibers and connective tissue structures within the MTU are not only simply combined with each other, but also interact anatomically and functionally (Kawakami, 2012).

Inter-muscular difference

In this thesis, inter-muscular difference is defined as difference of aponeurosis thickness between muscles (MG, LG and SOL), e.g., differences between gastrocnemii and soleus, or differences between medial gastrocnemius and lateral gastrocnemius.

Intra-muscular difference

Intra-muscular difference is defined as difference of aponeurosis thickness within a muscle (e.g., proximal and distal site of MG, posterior and anterior region of MG aponeuroses).

Inhomogeneity (site-dependence)

In this thesis, inhomogeneity feature is defined as site-dependent differences of aponeurosis thickness in chapter 2. The aponeurosis specimens were dissected from proximal, middle and distal site of each region of aponeurosis.

Muscle architecture

In this thesis, muscle architecture means the muscle fibers' geometrical arrangement within a muscle, such as pennation angle. Pennation angle of TS is defined as the angle of the muscle fascicle and the aponeurosis between gastrocnemii and soleus (Kawakami et al., 1998).

1-2-2 Mechanical property

Stiffness

In chapter 2, stiffness means the extent to which the aponeurosis specimen resists deformation in response to the applied tensile force. It was calculated from the slope of linear region of force-displacement curve. In chapter 3 and 4, the stiffness means the muscle or aponeurosis tissue property, which can show how stiffer the tissue is.

Young's modulus

In chapter 2, Young's modulus of aponeurosis specimen was calculated from the slope of linear region of stress-strain curve during the tensile test. In chapter 4, Young's modulus was calculated from the propagation speed of shear wave in tissue and the tissue density. Higher Young's modulus of tissue in this thesis means stiffer tissue.

Hysteresis

In chapter 2, the hysteresis was calculated from the areas under the loading and unloading force-displacement curve during tensile test. It can indicate the energy dissipation of aponeurosis specimen during loading and unloading process.

Shear wave velocity

Shear wave velocity (SWV) is determined by the propagation velocity of ultrasonic pulse in tissue and detected from the ultrasound shear wave elastography (SWE). In this thesis, SWS was used to determine aponeurosis and muscle stiffness *in vivo*.

Inhomogeneity (site-dependence)

In this thesis, inhomogeneity of mechanical property means differences from proximal to distal site. In chapter 2, the aponeurosis specimens were dissected from proximal, middle and distal site of each region of aponeurosis. In chapter 3 and 4, the proximal site was determined at the level of 30% lower leg length from the proximal end, and the distal site was determined at the level of distal end of gastrocnemii muscle-tendon junction point.

Anisotropy (direction-dependence)

In this thesis, anisotropy is defined as direction-dependent differences of mechanical properties of TS aponeuroses between longitudinal and transverse direction, thereinto, longitudinal direction corresponding to direction along the muscle's line of action, and transverse direction corresponding to direction orthogonal to the muscle's line of action.

Viscoelasticity

In this thesis, viscoelasticity of aponeurosis is determined as viscous and elastic characteristics undergoing deformation, and the hysteresis was used to identify the viscoelasticity of aponeurosis under tensile test in chapter 2.

1-2-3 Function

Muscle-aponeurosis interaction

Since aponeurosis serves as an attachment site of muscle fascicles on the surface of a muscle belly, muscle-aponeurosis interaction means the mutual influence between muscle fibers and aponeurosis during movement. Muscle plays like an actuator while the aponeurosis plays like a spring during motor performance.

Myofascial force transmission

Within the muscle-tendon unit, the forces produced from muscles fibers can not only serially transmit to the tendon, but also can transmit forces to the adjacent muscles through connective tissue (i.e., aponeurosis and facia) (Huijing and Baan, 2001; Huijing and Baan, 2003), later of which was defined as myofascial force transmission in this thesis.

Ex situ

The specimens of TS aponeuroses were dissected from human cadavers and they were applied to tensile test to determine the mechanical properties, which was termed

"*ex situ*" condition to test intrinsic aponeurosis mechanical properties in this thesis.

In vivo

The term "*in vivo*" in this thesis refers to the ultrasound experiment done in the living human TS muscles and aponeurosis.

1-3 Literature Review

The purpose of this thesis is to examine the site- and direction- dependent differences of morphological and mechanical properties of TS aponeuroses *ex situ* and *in vivo*, and how the muscle-aponeurosis behavior changes during muscle contraction, and to examine correlations between aponeuroses' stiffness and walking performance. The following topics will be overviewed in this literature review: 1) *Ex situ* and *in vivo* approaches in tissue morphological and mechanical properties, 2) architecture and function of the TS muscles and aponeuroses, 3) muscle-aponeurosis interaction during muscle contraction, and 4) mechanics of human TS muscles and aponeuroses in motor performance.

1-3-1 *Ex situ* and *in vivo* approaches in tissue morphological and mechanical properties

1-3-1-1 *Ex situ (cadaveric study)*

In order to enhance the understanding of the function of the soft tissues, a tensile test is an common and reliable measure to evaluate the mechanical properties of the soft

tissues, and has been applied to obtain the stiffness and/or Young's modulus of muscle, aponeurosis and tendon (Azizi et al., 2009; Louis-Ugbo et al., 2004; Morrow et al., 2010; Takaza et al., 2013). The basic idea of a tensile test is to fix a tissue sample by grips of the test instrument, dimensions (e.g., width, thickness, length) and cross-sectional area of the tissue sample are measured before tensile test, load and displacement are recorded during tensile test, the stiffness (N/mm) and tensile modulus (Young's modulus, MPa) were calculated from the slope of the linear region of the load-displacement relationship curve and stress-strain relationship curve respectively. However, previous studies on the tensile test of viscoelastic tissues (e.g., ligament and tendon) mentioned that the results could be affected by the experimental conditions and implemented procedure, the humidity, temperature and stretching speed of the machine should be carefully considered (Innocenti et al., 2017; Sta et al., 1999; Woo et al., 1991). In addition, Gras et al., (2012) reported that the parameters of tensile test were sensitive to experimental conditions rather than the changes in velocity. To our knowledge, although tensile test of muscles has been performed on both animals and humans (Gras et al., 2012; Morrow et al., 2010; Takaza et al., 2013), few studies focused on the tensile test of human aponeurosis. Even though the soft tissues such as ligaments and tendon have been tested, but only small dimension of tissue specimens were dissected which omitted the entire region of soft tissues.

1-3-1-2 *In vivo*

Magnetic resonance imaging (MRI) has been considered "gold standard" imaging

technique used to noninvasively measure the human muscle size. Previous studies have using MRI to assess the muscle adaptations in response to training in sport science (Fiatarone et al., 1990; Maeo et al., 2018a; Maeo et al., 2018b). In addition, except for the muscle size changes after training, studies on the tendinous tissues using MRI were also carried out recently (Backer et al., 2019; Haims et al., 2000; Prasetyono and Sisca, 2019). However, MRI are still limited to measurements at rest, even though Iwanuma et al. (2011) reported *in vivo* deformation of the Achilles tendon in the longitudinal and transverse directions during isometric contractions (Fig.1-2). For the muscle architecture changes during movement, real time ultrasonography (B-mode) provides a method to delineate the individual muscle architecture with higher validity and reliability. Previous studies used B-mode ultrasonography to investigate the muscle architectures at rest and during contractions (Ito et al., 1998; Kawakami et al., 1993; Kawakami et al., 1998). Additionally, B-mode ultrasonography was used to tract the muscle fascicle length changes during human walking (Arnold et al., 2013; Fukunaga et al., 2001), as well as the *in vivo* deformations of tendinous tissues during walking (Franz et al., 2015; Fukunaga et al., 2001).

Since the common ultrasonography has limitations to measure the biomechanical properties of tissue, a new ultrasonography technology named shear wave elastography (SWE) has been developed to quantify the mechanical properties of tissue by determining the propagation speed of shear wave through tissue (Fig. 1-3) (Bercoff et al., 2004). During the past few years, SWE was applied to assess the tissue stiffness (Brandenburg et al., 2014; Cortes et al., 2015; Martin et al., 2015; Taljanovic et al.,

2017; Zhang et al., 2016b), and spatial variations in shear wave velocity of muscles and tendons have been reported (DeWall et al., 2014; Slane et al., 2015; Slane et al., 2017; Yoshida et al., 2017). In addition, recent advance of the ultrasound SWE allows investigators to measure muscle and tendinous tissue stiffness during muscle contraction (Jeon et al., 2018; Mendes et al., 2018; Ryu and Jeong, 2017; Shinohara et al., 2010; Yoshitake et al., 2014), which has supplied a method for the investigation of the muscle-tendon behavior during muscle contraction *in vivo*.

SWE could be a promising tool to measure mechanical properties of muscle and tendon, and some studies reported the repeatability and validity of SWE in muscle-tendon measurement (Ateş et al., 2015; Baumer et al., 2017; Eby et al., 2013; Ting et al., 2015). Baumer et al. (2015) reported that the intraclass correlation coefficient (ICC) values of day-to-day reliability was greater than 0.33 for passive muscle, 0.65 for active muscle, 0.48 for passive tendon and 0.94 for active tendon. In addition, Ates et al. (2015) showed that the ICC values of measured muscle during isometric contractions were from 0.73 to 0.98. Otsuka et al. (2019) and Shiotani et al. (2019) reported that the SWE measurements were highly repeatable for human fascia lata (0.68-0.99) and plantar fascia (ICC > 0.93) tissues. Moreover, Eby et al. (2013) and Ting et al. (2015) demonstrated valid SWE results for muscles, however, the orientation of transducer and depth of detection should be taken into consideration for valid measurement.

1-3-2 Architecture and function of the triceps surae muscles and aponeuroses

1-3-2-1 The triceps surae architecture

The TS structure refers to the muscle size, shape and arrangement of fibers. The human TS is composed of two biarticular gastrocnemii (MG and LG) and one monoarticular soleus (Gray anatomy, 1995), and within soleus, the muscle belly has been shown to be divided into two portions, which are the posterior portion and anterior portion (Martin et al., 2001) (Fig. 1-4). Both gastrocnemii and soleus belong to pennate muscle depend on their muscle fibers architecture. As pennate muscle, muscle fascicles insert into the aponeurosis obliquely relative to the line of muscle action, and the pennation angle (PA) has been reported as an important factor of muscle function (Fukunaga et al., 1997b).

To date, data of muscle architecture such as PA derived from cadaver specimens (Friederich and Brand, 1990; Martin et al., 2001) has been used to understand the gross muscle fiber architectures. Friederich and Brand (1990) found the difference of PA between gastrocnemii (6.5-17.5 deg) and soleus (32deg) through measuring on a cadaver, while Martin et al., (2001) reported the different value of PA of gastrocnemii (21-32.5 deg) and soleus (30.3 ± 7.3 deg). However, cadaver studies do not allow us to understand its dynamic behavior (i.e., during muscle contraction).

In the last few decades, the technique of ultrasonography has been developed to directly measure the structural parameters of muscles *in vivo* (Chow et al., 2000; Fukunaga et al., 1997a; Kawakami et al., 1998; Kwah et al., 2013; Maganaris et al., 1998; Stenroth et al., 2012). Chow et al., (2000) found significant differences of muscle thickness and PA of the TS in males and females. Stenroth et al., (2012) reported that the TS muscle size was smaller ($p < 0.05$) and muscle fascicle length was shorter ($p <$

0.05) in old subjects than young counterparts. As Kwah et al., (2013) documented, the ultrasound measurements of muscle architecture are reliable (ICC were always > 0.5) in many experimental conditions, while for the validity, validity coefficient value can be over 0.7 only in certain conditions (e.g., rest state). Studies on muscle architecture during muscle contraction should consider the test validity. During muscle contraction, the changes of muscle fascicle length and PA were deduced to be related to muscle force-producing capabilities and elastic features of tendinous tissues (tendon and aponeurosis) (Kawakami et al., 1998).

1-3-2-2 Triceps surae aponeuroses and tendon structure

Within the muscle-aponeurosis-tendon unit, the tendinous tissue was divided into the free tendon and aponeurosis, later of which covered on the surface of muscle belly portion in a white, flat and sheet-like structure (Benjamin et al., 2008). The aponeurosis is composed of fibroblasts and ordered arrangement of collagenous fiber bundles. It provides attachment points for muscle fibers to attach to the tendon, and microscopy study has showed the connection between muscle fibers and connective tissues (Trotter et al., 1985) (Fig. 1-5). The human TS has aponeuroses in the proximal and distal aspects, covering both posterior and anterior region of gastrocnemii and soleus. The adjoining aponeuroses exist between gastrocnemii and soleus and ultimately insert into the calcaneus by sharing the common Achilles tendon (Blitz and Eliot, 2007, 2008; Oda et al., 2015) (Fig. 1-6 & 1-7).

Studies on the morphology of aponeurosis and tendon were mainly conducted by

using finite element simulation (Rehorn and Blemker, 2010) and cadaver study (Oda et al., 2015). Rehorn and Blemker (2010) developed computational model of aponeurosis to investigate how the aponeurosis morphology influences muscle stretch distribution, and the simplified model of aponeurosis architecture used uniform thickness throughout the whole length. However, the information of aponeurosis thickness distribution was not considered during previous simulation study. Thus, Oda et al. (2015) directedly measured the cross-sectional thickness of TS aponeuroses from a human cadaver. The results showed that higher thickness of aponeuroses was observed near the aponeurosis-bone and aponeurosis-tendon junction. Although studies to date have examined the thickness heterogeneity of aponeurosis, further studies are required to understand the morphology of TS aponeuroses and how it affects the muscle-tendon function.

1-3-2-3 Mechanical properties of the triceps surae

The TS mainly works as ankle plantar flexion, which lifts the heel up, contributing to human locomotion such as walking (Honeine et al., 2013). However, previous studies (Francis et al., 2013; Neptune et al., 2001) reported that gastrocnemius and soleus make different contributions to walking performance. Both studies found that gastrocnemius and soleus have opposite effect on forward progression of leg during walking. Function of the TS is greatly associated with the mechanical properties of muscle fibers (Kawakami et al., 1998). Therefore, differences of the mechanical properties of synergist muscles (inter-muscular differences) need to be clarified. For the inter-muscular differences of the TS, previous study found different passive stiffness among

GM, GL and SOL depending on the ankle positions (Lacourpaille et al., 2017). In addition to the inter-muscular differences, intra-muscular difference within a muscle was also examined (Giordano and Segal, 2006; Segal and Song, 2005). Both studies found that site-dependent differences of muscle activity exist within the individual muscle of the TS.

1-3-2-4 Mechanical properties of the triceps surae aponeuroses and tendon

The tendinous tissue (aponeurosis and tendon) has been proved to perform an important role in locomotion (Fukunaga et al., 2002). It plays a significant role in human movements functioning as a spring and contributing to energy saving and power enhancement of the muscle-tendon unit (Fukunaga et al., 2002; Kawakami, 2012; Maganaris, 2002). Unlike the uni-axial loading pattern on the cord-like structure of tendon during contraction, the sheet-like structure of aponeurosis serves as an attachment site of muscle fascicles on the surface of a muscle belly, and can bear the pressure and tension with more complicated shape changes during muscle contraction (Raiteri, 2018; Raiteri et al., 2016; Scott and Loeb, 1995). During muscle contraction, the aponeurosis is stretched both in the longitudinal (along the muscle's line of action) and the transverse directions, and higher transverse deformability has been documented in previous studies (Azizi and Roberts, 2009; Iwanuma et al., 2011; Maganaris et al., 2001). However, the aponeurosis strain was less (14%) during muscle contraction than the strain (24%) during passive tensile loading condition, which indicates that the aponeurosis stain could be affected by the muscle contraction (Bojsen-Møller and

Magnusson, 2019; Lieber et al., 2000). Furthermore, previous studies have reported anisotropic (different material properties in the transverse and longitudinal directions) and inhomogeneous properties of the TS aponeuroses (Muramatsu et al., 2001; Slane et al., 2017), and site-dependent differences between aponeuroses and tendon strains have been found during human movements through *in vivo* studies (Bojsen-Moller et al., 2004a; Finni et al., 2003; Magnusson et al., 2003). However, Muramatsu et al. (2001) reported that there was no significant difference in the maximal strain between aponeurosis (5.9 ± 1.6%) and Achilles tendon (5.1 ± 1.1%), and even no significant differences between proximal and distal region of aponeurosis. On the other hand, Iwanuma et al. (2011) the stain of Achilles tendon (3.3%) was higher than that of aponeurosis (1.1-1.6%) at submaximal contractions. The different functional roles during muscle contractions between the aponeurosis and tendon still remain unclear.

1-3-3 Muscle-aponeurosis interaction during muscle contraction

Within the muscle-tendon unit, muscle fibers and tendinous tissues act as contractile and elastic components, respectively (Lieber et al., 1992). And Lieber et al. (1992) demonstrated the interaction between the contractile and elastic components by the finding that internal muscle fiber shortening causes the elongation of tendon length during force development. In addition, another study further proved that the aponeurosis tissue plays a major role in muscle-tendon interaction (Kawakami and Lieber, 2000). Muscle-aponeurosis-tendon mechanical function is determined by interaction between muscle fibers and the connective tissues (Stenroth, 2016).

Depending on the thickness distribution of aponeuroses (Oda et al., 2015) and architecture of muscle fibers (Maganaris et al., 1998), the muscle-aponeurosis interaction could lead to non-uniform behaviors of muscle-tendon unit (Finni, 2006; Kawakami et al., 1998). Previous *in vivo* studies (Arampatzis et al., 2006; Ateş et al., 2018; Bojsen-Moller et al., 2004b) reported different muscle behaviors under different knee-joint positions during muscle contractions, and the TS was proved to activate differently from proximal to distal sites during submaximal plantarflexions (Giordano and Segal, 2006; Segal and Song, 2005). The architectural heterogeneity and different muscle activation may make the aponeurosis behavior more complicated.

The force generated by individual actin-myosin cross bridges is transmitted within the fiber both longitudinally and transversely, then the transmission of force reaches the aponeurosis, tendons, and joints, which causes the movement. Some studies (Ateş et al., 2015; Bouillard et al., 2012; Bouillard et al., 2011) reported linear relationship of muscle stiffness and torque during muscle contractions, while non-linear relationship of mechanical properties of aponeurosis and sports intensities was also reported (Arampatzis et al., 2007). This signifies that the relationship existing between muscle-aponeurosis stiffness and torque still remains unclear. Moreover, during isometric muscle contraction, the architecture of muscle changes with the increasing level of contraction, such as PA (Ito et al., 1998; Narici et al., 1996). The aponeurosis's length and width could be altered by the shape changes of muscle belly, which indicates mechanical loading of aponeuroses is more complex than that of tendons (Arellano et al., 2016; Scott and Loeb, 1995).

1-3-4 Mechanics of human triceps surae muscles and aponeuroses in motor performance

Human motor performance is regarded as a subfield of human performance, it can be affected by capacity of information processing and movement output. The movement output need not only agonist muscle contraction, but also control of synergist muscles (Kaurranen, 1999). As described above for the structural and functional features of human TS, it works as a major plantar flexor and generates forces for propelling forward and stabilizing the body in human common movement (e.g., walking, running) (Bassey et al., 1988; Hof et al., 2002; Honeine et al., 2013). During human walking, although the bi-articular gastrocnemii and mono-articular soleus were proved to have different mechanical behavior of muscle fascicles (Ishikawa et al., 2005), they all contract and were stretched during the gait cycle, which is regarded as a stretch-shorten cycle behavior in the muscle-tendon unit. Because of the interaction between muscle fascicles and tendinous tissues, spring-like behavior of tendinous tissues (i.e., tendon and aponeurosis) of these muscles also contributes to the maintenance of walking speed by storing and releasing elastic energy (Franz and Thelen, 2016; Fukunaga et al., 2001; Hof et al., 2002). The matching of muscle fibers as force generators and tendinous tissues as elastic springs can influence walking performance (Stenroth et al., 2017). Another previous study suggested that the relationships between musculotendinous properties and walking performance can be changed by aging (Stenroth et al., 2015). Such a change may be due to the reduced muscle strength and

altered mechanical properties of tendinous tissues with aging (Foster-Burns, 1999; Narici et al., 2008), which awaits empirical verification. In addition, it is unknown whether enlargement of inter-individual variability of walking ability in the elderly is attributable to the changes in muscle strength or tendinous tissue, or both.

1-4 Purpose

As mentioned in the literature review, little is known about the morphological and mechanical properties of human TS aponeuroses not only *in vivo* but also *ex situ*, and consensus was not reached on the muscle-aponeurosis changes of morphological and mechanical properties during muscle contraction. Therefore, the general purpose of this thesis is to investigate the intrinsic morphological and mechanical properties of TS aponeuroses *ex situ* and *in vivo*.

In Chapter 2, data on site- and direction-dependence of the material properties of human TS aponeuroses under biaxial tension with their functional implications are presented.

In Chapter 3, using ultrasound SWE to measure the architecture and stiffness of TS muscles and aponeuroses during different levels of muscle contractions, and examine the relationships between relative tendon length change and stiffness of muscles and aponeuroses.

In Chapter 4, using ultrasound SWE to examine the site- and direction-dependent differences of the TS muscles and aponeuroses in the elderly, and to investigate the relationships between TS aponeuroses stiffness and muscle strength and walking

performance.

In Chapter 5, the main findings of each chapter are listed. Then, the following sections are discussed: 1) generalization of the findings: site- and direction-dependence, 2) applicability of the findings, which are implications for muscle-tendon interaction and motor performance, 4) limitations. Finally, conclusion of this thesis and future direction are addressed.

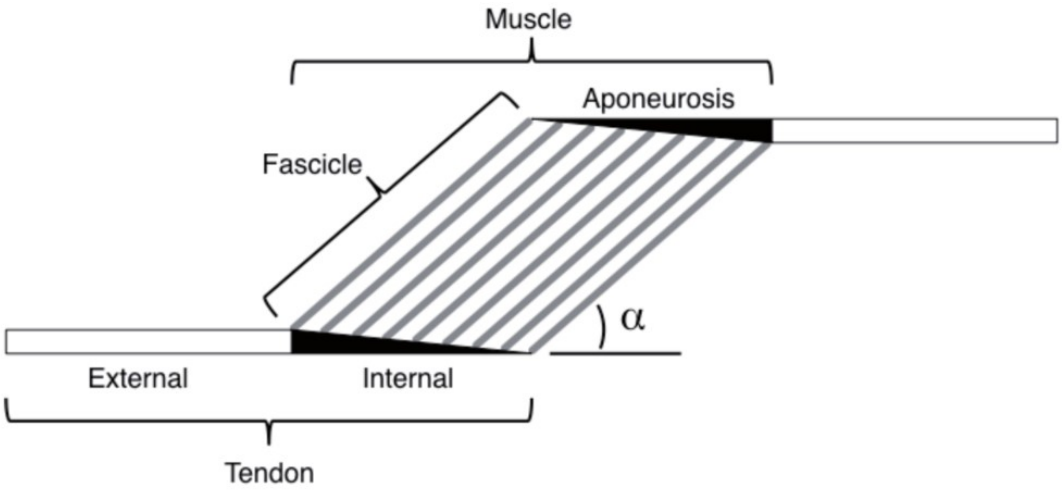

Fig. 1-1 Parallelogram model of a muscle-aponeurosis-tendon unit comprised of muscle fibers and connective tissues (aponeurosis and tendon). (Zajac 1989)

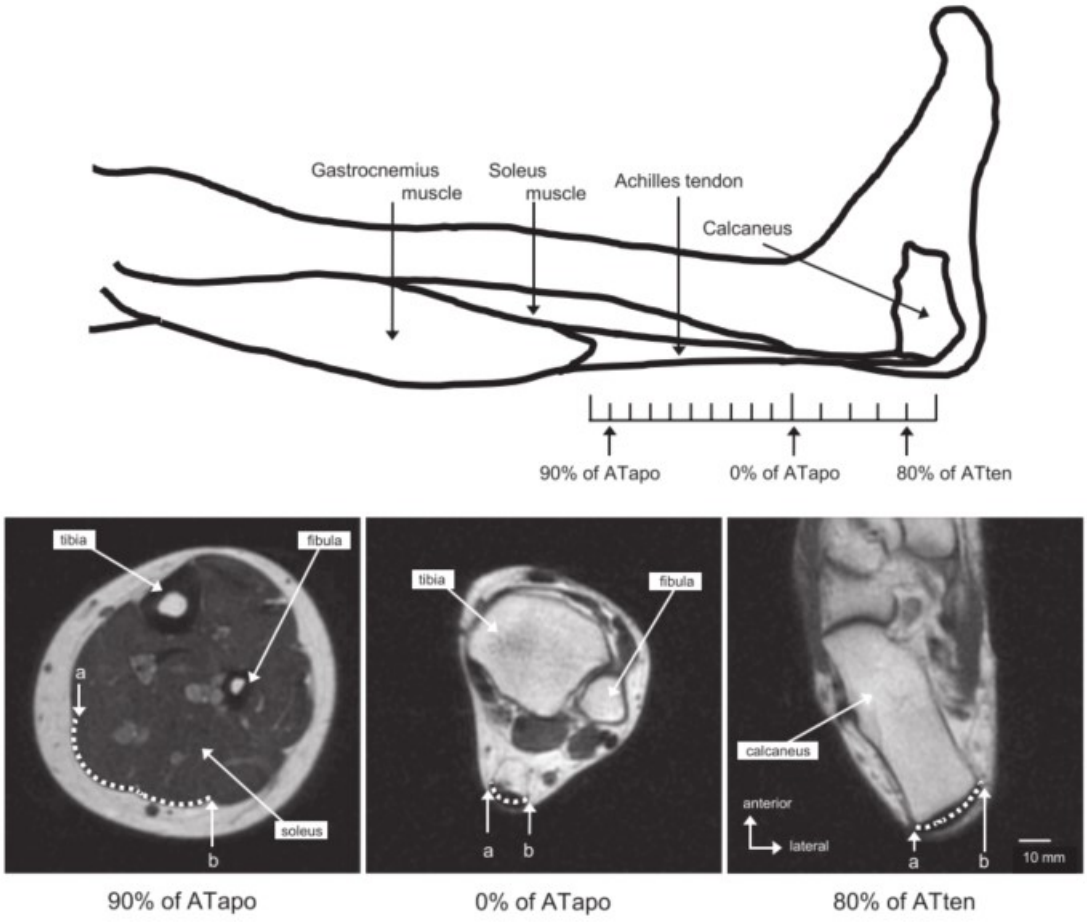

Fig. 1-2 Typical MR images at the positions corresponding to 0% (middle) and 90% (left) of aponeurosis length and 80% (right) of tendon length. Dashed lines: tendon width; a: medial edge; b: lateral edge. (Iwanuma et al., 2011)

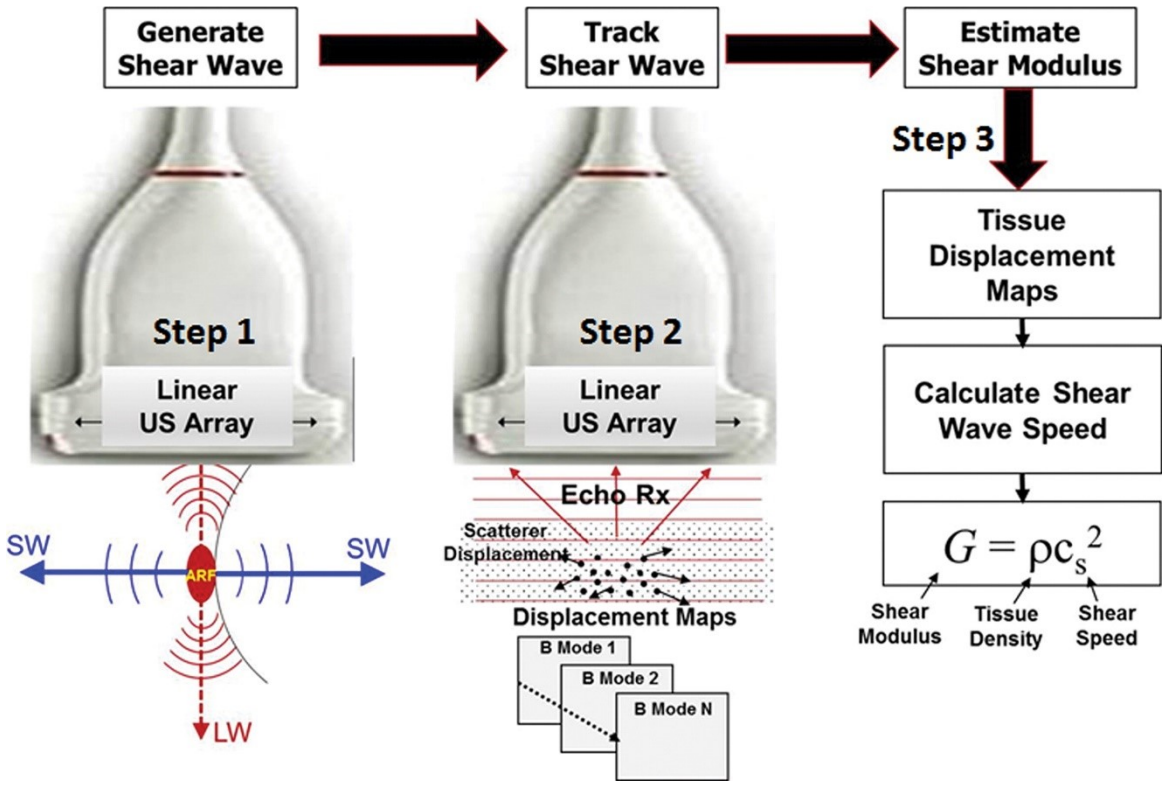

Fig. 1-3 Basic physics of shear wave elastography. (Mihra et al., 2017)

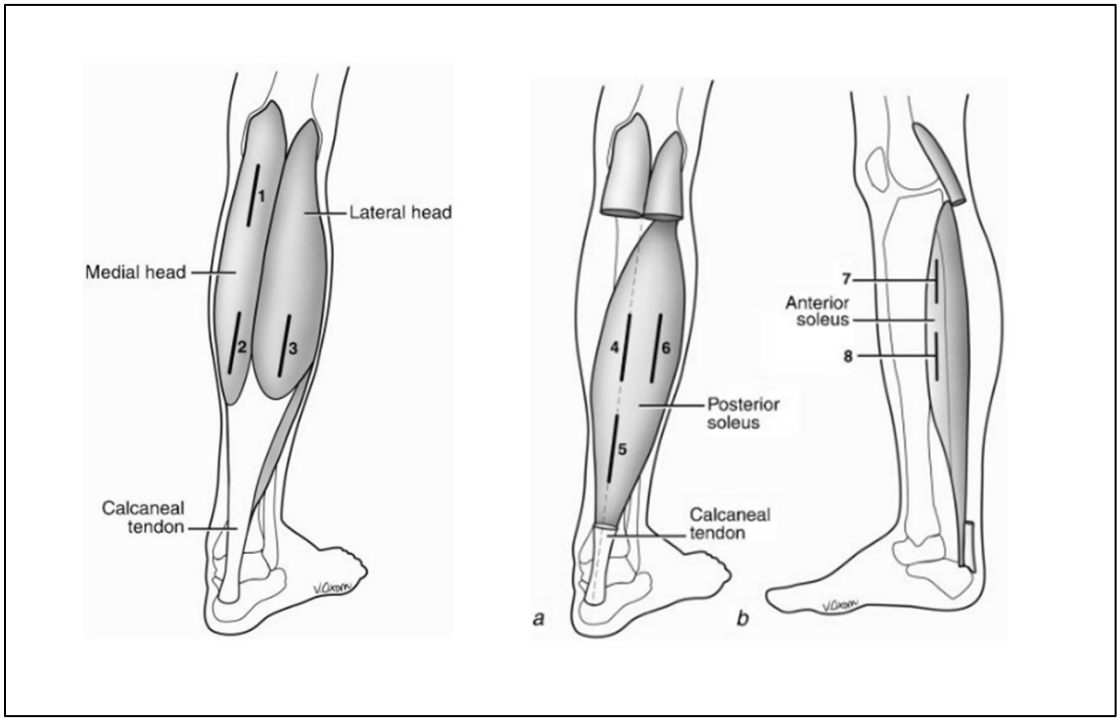

Fig. 1-4 Posterior view of the human triceps surae comprised of medial gastrocnemius (MG), lateral gastrocnemius (LG), posterior portion of soleus and anterior portion of soleus. (Martin et al., 2001)

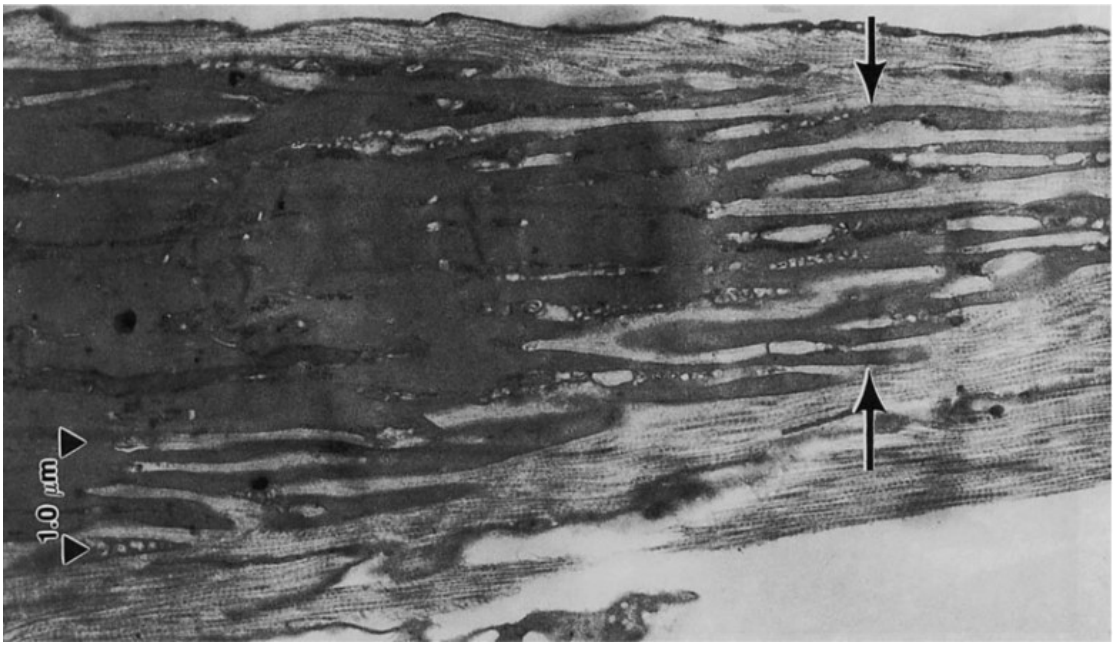

Fig. 1-5 Transmission electron micrograph of the muscle-tendon inter-face of a single plantaris muscle fiber. (Trotter et al., 1985)

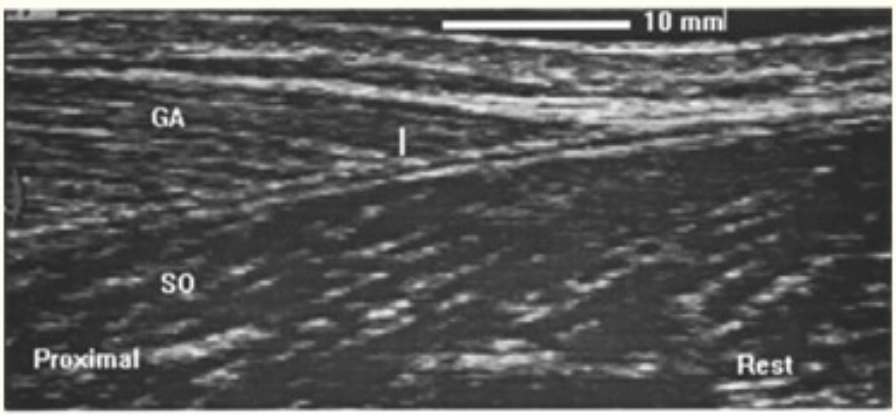

Fig. 1-6 Sonography of the triceps surae adjoining aponeuroses between gastrocnemius and soleus. GA, gastrocnemius muscle; SO, soleus muscle. The adjoining aponeuroses were seen on the ultrasound image as two distinct entities with a small separating space. (Magnusson et al., 2001)

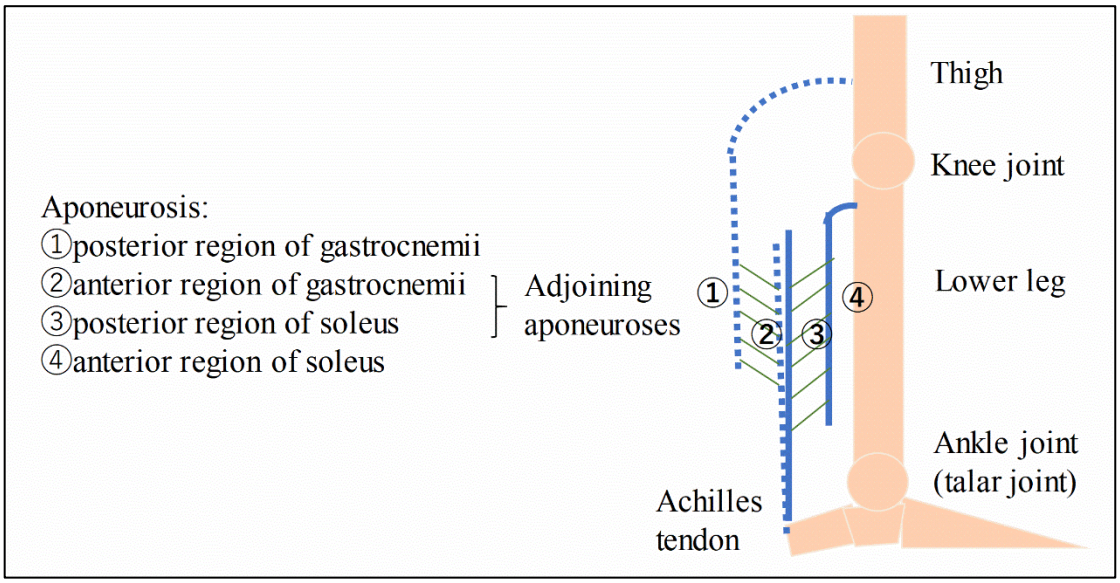

Fig. 1-7 Schematic representation of aponeuroses distribution in the triceps surae muscle-aponeuroses-tendon unit.

CHAPTER 2 Morphological and mechanical properties of the human triceps surae aponeuroses taken from elderly cadavers

2-1 Introduction

As mentioned in Chapter 1, although the aponeurosis is reported to stretched more in the transverse direction than in the longitudinal direction, the intrinsic bidirectional differences in the human aponeurosis mechanical properties still remain unclear. Previous studies have reported anisotropic (different material properties in the transverse and longitudinal directions) and inhomogeneous properties of the TS aponeuroses (Muramatsu et al., 2001; Slane et al., 2017), and site-dependent differences of aponeuroses strains have been found during human movements through *in vivo* studies (Bojsen-Moller et al., 2004a; Finni et al., 2003; Magnusson et al., 2003). Few studies, however, focused on the site-dependent morphology of TS aponeuroses. While a cadaveric study revealed the geometry and thickness distribution of the TS aponeuroses using one leg of an elderly male cadaver (Oda et al., 2015), there is still a paucity of information on the intrinsic morphological properties of human aponeurosis. Another previous study showed the gradient in aponeurosis thickness appeared to match the gradient in tension transmitted along aponeurosis structure (Scott and Loeb, 1995), therefore we hypothesized that thinner aponeuroses are more compliant than thicker aponeuroses. Additionally, it remains unknown whether or not the anisotropy, inhomogeneity and inter-muscular differences of human aponeuroses are due to differences of their morphological and mechanical properties. These issues cannot be

approached by *in vivo* studies where one cannot directly and accurately measure intrinsic morphological and mechanical properties of aponeuroses. This study therefore aimed to identify the intrinsic morphological and mechanical characteristics of the human TS aponeuroses, in particular, the site- and direction-dependent differences and differences between gastrocnemii and soleus.

2-2 Materials and Methods

2-2-1 Materials

This study was approved (2017-M001) by the ethics committee of Aichi Medical University. Twenty-five TS muscle-tendon units (324.2 ± 98.8 g, mean ± s.d.) were procured from 13 human donors (formalin fixed, 6 males, 7 females) aged 67-92 years (82.2 ± 10.1, mean ± s.d.). The sample size (n = 25) exceeded the necessary number of samples for this study (n = 24, determined by power analysis with the power: 0.80 and effect size f = 0.75) (Faul et al., 2007). The cadavers were donated to Aichi Medical University, Aichi, Japan. Before they died, the donors signed the informed consent agreeing to body donation and its use for research. The cadavers were embalmed by using 20% formaldehyde, a Porti-boy pump with cannula was used to inject embalming fluid into the body through the femoral artery (toward the feet) and common carotid artery (toward the cephalad). Once embalming was completed, the body was placed in a sealed plastic body bag and stored at room temperature (Hayashi et al., 2014). Specimens of aponeuroses were excised from eight regions: posterior and anterior regions of gastrocnemius medialis (GM), gastrocnemius lateralis (GL), medial part of

soleus (SOL-med), lateral part of soleus (SOL-lat). In each region, three size-matched rectangular pieces of aponeuroses (2-4 cm x 2-4 cm) were harvested from the proximal, middle and distal sites (Figs. 2-1B, 1C, 1D). The muscles and aponeuroses specimens were kept moist by using Alcohol (50% by volume) throughout the dissection process (Otsuka et al., 2018).

2-2-2 Measurements

The average thickness of each aponeurosis specimen was calculated after measuring the thickness at four different sites (Fig. 2-1E) of each specimen by using a digital vernier caliper (LIXIL VIVA, Japan) (Hwang et al., 2012; Kumar et al., 2011). It was not possible to perfectly remove muscle fibers from each sample (otherwise we could break it) but we took great care to trim them as much as we could while not destroying the aponeurosis, and to avoid inclusion of remaining fibers during thickness measurement. For each site, we repeated at least 3 times to avoid variations between trials, then the value of thickness was recorded. The specimen's average thickness and width (or length) were used to calculate the cross-sectional area of the specimen. The uniaxial tensile test was implemented by using an instrument (IMADA CO., LTD, Japan) that was equipped with one test stand and two sets of force gauges (1: ZTA-500N, 1000Hz; 2: ZTA-5N, 1000Hz, Fig. 2A). Before placing and fixing each specimen of aponeurosis on the instrument, sandpapers (5 cm × 0.5 cm) were glued to the top and bottom ends of the specimen to prevent slipping from the thin film grips during the tensile test (Lynch et al., 2003) and the synchronous loading-unloading curve that was

displayed real-time during measurement to ensure slippage did not occur. In such a case with an irregular shape of the curve, the test was repeated after adjusting the grip interface. The specimens of aponeuroses were loaded longitudinally (along the muscle's line of action) and transversely, to avoid the order effect of testing in one to the other directions, the order of testing on the two directions was randomized and counterbalanced (Otsuka et al., 2018). According to the previous study (Azizi et al., 2009) and our pilot experiment, the aponeuroses were expected to be stiffer in the longitudinal than the transverse direction. Thus, the force gauge 1 (ZTA-500N) and 2 (ZTA-5N) were used for the longitudinal and transverse direction test respectively. The load and displacement during the tensile test were displayed simultaneously in the kit software. The speed was set at 25 $mm \cdot min^{-1}$ (Otsuka et al., 2018) both for the stretch and relaxation, and five identical cycles were performed during the cyclic tensile test. All the tensile tests were carried out at a room temperature (20-26℃).

2-2-3 Analyses

The data of all tested specimens were used for the analyses unless the specimens were damaged during dissection or tensile test processes. Out of the five cycles of the tensile test, forces obtained from the first and second cycles were slightly smaller due to the initial aponeuroses settling within the film grips of the force measurement instrument. We used only the third cycle for analysis in order not to introduce possible force reduction in the last two cycles (4th and 5th) (Azizi et al., 2009). The stress (σ) and strain (ε) were calculated using the following equations.

$$\sigma = F/A \tag{2-1}$$

$$\varepsilon = (l - L)/L \tag{2-2}$$

Where F is the tensile force, A is the initial (unloaded) cross-sectional area of each specimen, l and L are the final and initial lengths of the aponeurosis, respectively. The initial length (resting length) of each specimen was determined using the same threshold force (when the load cell reached 0.1N).

For the load-displacement and stress-strain curves, the linear region was identified based on a previous study (Mogi et al., 2013) as follows: First, loads were normalized to the maximum load and then elongation was recorded at relative loads of 10%, 20%, 30%, 40%, 50%, 60%, 70%, 80%, 90%, and 100%. Secondly, from the relationship between the relative loads and elongations, slopes at adjacent data points were calculated to find the transition point (when the slope is zero) from the toe- to linear-region (Fig. 2-2B). The stiffness (N/mm) and tensile modulus (MPa) were calculated from the slope of the linear region of the load-displacement relationship curve and stress-strain relationship curve respectively (Figs. 2-2C, 2D), and were used as mechanical variables of the aponeuroses. The mechanical hysteresis was calculated in the same way as in a previous study (Maganaris and Paul, 2000) using equation (2-3).

$$Hysteresis\ (\%) = \left[\left(S_{loading} - S_{unloading}\right)/S_{loading}\right] \times 100 \tag{2-3}$$

Where $S_{loading}$ is the area under the loading curve and $S_{unloading}$ is the area under the unloading curve (Fig. 2-2E). All calculations were performed by using the software

Origin 9.0 (OriginLab, Northampton, MA, USA).

We did not find significant sex differences in any of the measurements and the derived parameters, therefore we pooled the data for males and females.

2-2-4 Statistics

All the data are shown as mean ± standard deviation. Accounting for unequal sample size (number of specimens) between sites, and variations among and within individuals, a one-way factorial mixed-model ANOVA (analysis of variance) with individual as a random effect and sites (proximal, middle and distal) as fixed factors was used to determine the site-dependent differences in thickness. To test the site- and direction-dependent differences in stiffness, Young's modulus and hysteresis, a two-way factorial mixed-model ANOVA with individual as a random effect and fixed factors [sites (proximal, middle, distal) and directions (longitudinal and transverse)] was performed. To compare across regions (posterior and anterior) within a muscle and then compare the differences among muscles (GM, GL, SOL-med and SOL-lat), the average [proximal/middle/distal (P/M/D)] thickness and Young's modulus were calculated, and a two-way factorial mixed-model ANOVA with individual as a random effect and fixed factors [muscles (GM, GL, SOL-med and SOL-lat) and regions (posterior and anterior)] was used. A post-hoc test (Bonferroni) was performed when appropriate. All the statistical analyses were performed using SPSS Statistics 24.0 (IBM SPSS Statistics, SPSS Inc., Chicago, USA). The significance level was set at $\alpha < 0.05$.

2-3 Results

2-3-1 Thickness

In the posterior and anterior regions of GM and GL, significant differences among the proximal (P), middle (M) and distal (D) sites were showed [posterior region of GM: P (0.52 ± 0.21 mm) > M (0.46 ± 0.18 mm) > D (0.40 ± 0.20 mm), posterior region of GL: P (0.59 ± 0.23 mm) > M (0.47 ± 0.20 mm) > D (0.39 ± 0.20 mm), anterior region of GM: D (0.57 ± 0.15 mm) > M (0.53 ± 0.17 mm) > P (0.47 ± 0.15 mm), and anterior region of GL: D (0.45 ± 0.16 mm) > P (0.38 ± 0.15 mm), $p < 0.01$]. In the posterior regions of SOL-med and SOL-lat, the proximal site was significantly thinner than the distal site [SOL-med: D (0.39 ± 0.13 mm) > P (0.33 ± 0.16 mm), SOL-lat: D (0.41 ± 0.18 mm) > P (0.36 ± 0.17 mm), $p < 0.05$], and there was no significant difference among sites in the anterior regions of SOL-med and SOL-lat (Fig. 2-3).

For the average (across the P/M/D sites) thickness of aponeuroses in the posterior and anterior regions of the TS (GM, GL, SOL-med and SOL-lat), there was significant muscle × region interaction ($p<0.001$) while the main effects of muscle ($p<0.001$) and region ($p<0.001$) were both significant (Fig. 2-4). In the posterior regions, GL = GM > SOL-med = SOL-lat ($p<0.01$, Fig. 2-4), and in the anterior regions, GM = SOL-lat > GL = SOL-med ($p < 0.05$, Fig. 2-4).

2-3-2 Stiffness

Stiffness in all regions of the TS aponeuroses showed significant differences between the longitudinal and transverse directions ($p < 0.001$, Table 2-1). Significant

differences in the longitudinal stiffness among the proximal, middle and distal sites were showed in the posterior (P = M > D, $p < 0.01$) and anterior (P = M > D, $p < 0.01$) regions of GM and anterior region (P < M = D, $p < 0.05$) of GL (Table 2-1).

2-3-3 Young's modulus

For the Young's modulus, there was no significant interaction between sites and directions in any regions of TS aponeuroses, while the values in the longitudinal direction were significantly higher than those in the transverse direction in all regions ($p < 0.001$, Table 2-2).

For the average (across the P/M/D sites) Young's modulus of aponeuroses in posterior and anterior regions of the TS, in the longitudinal direction, the muscle × region interaction showed no significance while the main effect of muscle was significant (posterior region: GL > GM = SOL-med = SOL-lat, and anterior region: GL > GM = SOL-med = SOL-lat, $p < 0.001$, Fig. 2-5). In the transverse direction, the Young's modulus of posterior region of SOL-lat was significantly higher than GM ($p < 0.001$), GL ($p = 0.003$), and SOL-med ($p = 0.012$) (Fig. 2-5).

2-3-4 Hysteresis

The hysteresis in the transverse direction was significantly larger than in the longitudinal direction at the middle and distal sites of posterior region of GM ($p < 0.001$), proximal and middle sites of anterior region of GL ($p = 0.001$), all three sites of posterior region of GL ($p = 0.01$) and SOL-med ($p = 0.001$), anterior region of SOL-

med (p = 0.002) and SOL-lat (p = 0.009). In contrast, the hysteresis in the distal site of anterior region of GL was higher in the longitudinal than the transverse direction (p = 0.005, Table 2-3).

2-4 Discussion

In the present study, we measured morphological and mechanical properties of the human TS aponeuroses by using uniaxial tensile tests, and found the site- and direction-dependent differences in anisotropy and heterogeneity of aponeurotic tissues. In addition, differences of material properties of aponeuroses in synergist muscles (gastrocnemii and soleus) were provided which would help us better understand the contributing factors for the force transmission in muscle-aponeurosis-tendon complex.

2-4-1 Site-dependent differences of morphological and mechanical properties of aponeurosis

In each region of the TS aponeuroses, except for the anterior regions of soleus, the thickness distributed inhomogeneously from the proximal to distal sites (Figs. 2-3 and 2-6), which is consistent with the previous study (Oda et al., 2015) that showed site differences of soleus aponeuroses thickness. Being continuous with the free portion of the tendon and further extending upon the muscle belly, the aponeurosis not only acts to transmit forces in its longitudinal direction, but also bears all the possible tension and deformation of the contracting muscle belly in the longitudinal as well as transverse direction (Huijing, 1999). A flat sheet-like structure with anisotropic stiffness covering

the muscle belly surface would contribute to such contraction-induced muscle behavior.

As for the longitudinal direction of the aponeurosis, the aponeurotic parts around the proximal and distal ends of muscle belly would experience forces developed from the majority of muscle fibers, while the parts near the termination of the aponeurosis experience forces with far fewer fibers (Magnusson et al., 2001). During muscle contraction, the aponeurosis would be stretched more around the ends of muscle belly while less around the termination of the aponeurosis. If however the aponeurosis exhibits a similar stretch regardless of its part, it should have higher stiffness around the muscle belly ends and less around its termination. This is exactly consistent with our findings of site-dependent differences of stiffness within the gastrocnemius aponeurosis (Table 2-1). On the other hand, The Young's modulus did not show site-dependent differences in any regions, although there were tendencies in the values being smaller around terminations of both anterior and posterior aponeuroses of the gastrocnemius (Table 2-2). Thus, the reason for the site-dependent differences in aponeurosis stiffness, is due to different aponeurosis thicknesses rather than a difference in the material property. A previous study reported that the longitudinal stiffness of aponeurosis influences the muscle fascicle behavior and probably favors the magnitude of force production (Raiteri, 2018), which indicates that the aponeurosis would act to control the muscle fascicle behavior during movement.

2-4-2 Differences of aponeuroses between gastrocnemii and soleus in morphological and mechanical properties

Compared to other regions of gastrocnemii and soleus, thinner thickness but higher Young's modulus in the anterior region of GL aponeurosis (longitudinal) and posterior region of SOL-lat aponeurosis (transverse) are somewhat unexpected findings (Fig. 2-4 and 2-5). Such findings were not found in any other region of GM aponeurosis and SOL-med aponeurosis. The anterior region of GL aponeurosis and posterior region of SOL-lat aponeurosis are adjoining aponeuroses which connect to the Achilles tendon serially. The medial-lateral differences in thickness and Young's modulus may reflect different muscle-aponeurosis interaction between synergist muscles (GM, GL and soleus), which affects the muscle force transmission to the tendon differently, and contributes differently to the limb movement control between medial and lateral side. A previous cadaveric study on site specificity of structural and mechanical properties of human fascia lata found that higher transverse Young's modulus accompany with higher proportion of transversely directed fibers (Otsuka et al., 2018). Such differences in aponeuroses morphology and mechanical properties may be related to the unique arrangement of collagenous bundles (Lake et al., 2010; Miller et al., 2012) in the adjoining aponeuroses, which awaits future investigation.

2-4-3 Direction-dependent differences of mechanical properties

The differences of mechanical properties (stiffness and Young's modulus) of human TS aponeuroses between longitudinal (along the muscle-tendon unit's line of action) and transverse (orthogonal to the muscle-tendon unit's line of action) directions found in the current study are consistent with the features of a turkey's aponeuroses

(Azizi et al., 2009) and human fascia lata (Otsuka et al., 2018). All previous studies indicate that the aponeuroses are more compliant in the transverse direction, and our study further showed that the stiffness and Young's modulus in the transverse direction were much smaller (<1%) than the values in the longitudinal direction, regardless of regions (Table 2-1 and 2-2). As previously documented (Azizi et al., 2009), most of the collagen fiber bundles of aponeurosis appear to be arrayed longitudinally, so the loading regime of aponeurosis is greatly limited to the longitudinal direction. This may cause the distinct differences between longitudinal and transverse directions in strain. Higher stiffness and Young's modulus of the aponeurosis in the longitudinal direction, may reflect its role as a mechanical spring within the muscle-tendon unit, whilst being more compliant in the transverse direction possibly helps to accommodate the expansion of the contracting muscle belly in this direction. Compared with the results of turkey's aponeuroses, the transverse Young's modulus of human aponeurosis was much lower. One of the possible reasons may be that they used frozen turkey materials while our samples were tested following formalin fixation which may have altered the tissue properties. Another possibility may be the differences in the magnitude of the transverse strain between species (humans: 6-21% (Iwanuma et al., 2011; Maganaris et al., 2001), turkeys: 8% (Azizi and Roberts, 2009)). On the other hand, another study (Otsuka et al., 2018) on human formalin-fixed fascia lata showed similar results of Young's modulus in the longitudinal direction (71.6-275.9 MPa) as well as in the transverse direction (3.2-41.9 MPa). The anisotropy of the aponeuroses is also far more pronounced in the current study than that reported in a previous *in vivo* human study

(Iwanuma et al., 2011). The Young's modulus determined for the linear region of the stress-strain curve in this study was 100-500 MPa (at 3-5% strain) in the longitudinal direction which was about 100 times higher than in the transverse direction (0.5-3 MPa, at 5-30% strain), whereas an *in vivo* study reported values of the longitudinal strain being only 5-10 times larger than the transverse strain (Iwanuma et al., 2011). Their study also found no significant differences in the strains of aponeurosis between 30% maximal voluntary contraction (MVC) and 60% MVC along the longitudinal (1.1 and 1.6%) or transverse (5.0-11.4% and 5.0-13.9%) direction. The elastic feature of aponeurosis in the present study was found in the isolated condition, thus the *in vivo* finding of their study could be due to the condition where contracting muscle fibers were attaching onto the aponeurosis. In this condition, the aponeurosis mechanical properties might be modulated by the stiffened, contracting muscle fibers. The maximal load of aponeurosis during the tensile test of the present study was about 37.8 ± 18.3 N with the strain at 4.9 ± 1.4%. Previous *in vivo* studies reported that the aponeurosis strain was 1.1-1.6% during 30%-60%MVC muscle contractions (Iwanuma et al., 2011) and 5.9-7% during maximal voluntary contraction (Arampatzis et al., 2007; Maganaris et al., 2001; Muramatsu et al., 2001). Regarding the aponeurosis strain, the magnitude of elongation in our study is comparable to those under the maximal voluntary contraction *in vivo*. Thus the present findings on inter- and intra-muscle variability in aponeurosis mechanical properties and their anisotropy may relate to the situations of highly active muscle contractions in humans. However, due to substantially variable reported values of aponeurosis strains *in vivo*, and a large number of estimations and

assumptions in the parameters to be used for individual muscle forces, we do not feel justified to attempt describing the muscle-aponeurosis behavior during exercises. Future studies to accurately determine individual muscle forces will lead to reasonable and useful modeling of the functional roles of aponeuroses in motor performance.

2-4-4 Viscoelasticity of triceps surae aponeuroses

The aponeurosis serially connects to tendon which enables it to transmit the forces produced from muscle fibers to tendon, and finally to the bones. However, the work produced by muscle fibers cannot be fully transmitted to the bone due to the viscoelasticity of aponeurosis and tendon tissues. The energy dissipation during loading and unloading process is called hysteresis, and tendon hysteresis has been measured in *in vivo* human studies (Farris et al., 2011; Foure et al., 2012; Foure et al., 2010; Kubo et al., 2002) with diverse values between studies. A previous study suggested that hysteresis is a quite sensitive measure largely influenced by the method utilized (Finni et al., 2012). In our results, the energy dissipation along longitudinal and transverse directions was different, with the former being smaller than the latter (Table 2-3). The aponeuroses were much softer transversely, and during the unloading phase, more energy was lost (dissipated as heat), so the efficiency (unloading energy/ loading energy) decreased. Since the amount of hysteresis may influence the efficiency of muscle contraction with the same conformation (Foure et al., 2012; Herzog et al., 2012; Kostyukov et al., 1995), lower hysteresis in the longitudinal direction may make the muscle more efficient, which can relate to the high efficiency of human stretch-

shortening cycle movement such as walking where the TS are the major agonists (Hof et al., 2002).

2-5 Conclusions

In the present study, site-related differences of thickness were found from proximal to distal in TS aponeuroses, with different morphology and mechanical properties among aponeuroses of synergist muscles. The reason for site-dependent differences in stiffness is due to a reduced aponeurosis thickness rather than a reduction in the material property. The anisotropic elastic feature (differences between longitudinal and transverse directions in stiffness and Young's modulus) of the aponeuroses were more pronounced than *in vivo* observations, suggesting inherent material design of the aponeurosis that matches three-dimensional contractile behavior of muscle fibers.

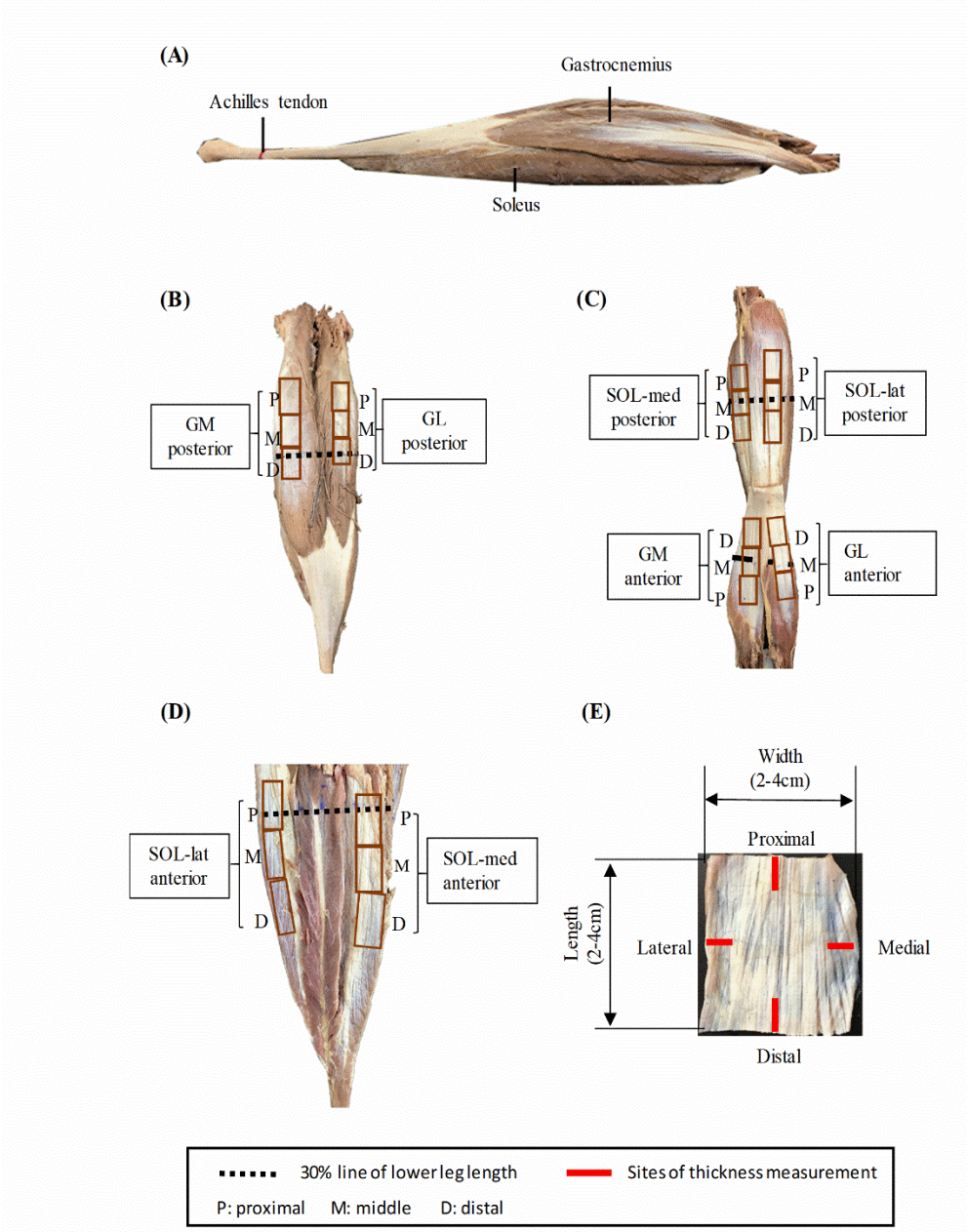

Fig. 2-1. Specimen preparation, three size-matched rectangular specimens of aponeuroses were dissected from three sites of each region. (A) Lateral sagittal view of triceps surae muscle-tendon unit with aponeuroses. (B) Posterior view of posterior part of gastrocnemii. (C) Posterior view of anterior part of gastrocnemii and posterior part of soleus. (D) Anterior view of anterior part of soleus. (E) One typical specimen of aponeurosis. GM gastrocnemius medialis, GL gastrocnemius lateralis, SOL-med medial part of soleus, SOL-lat lateral part of soleus.

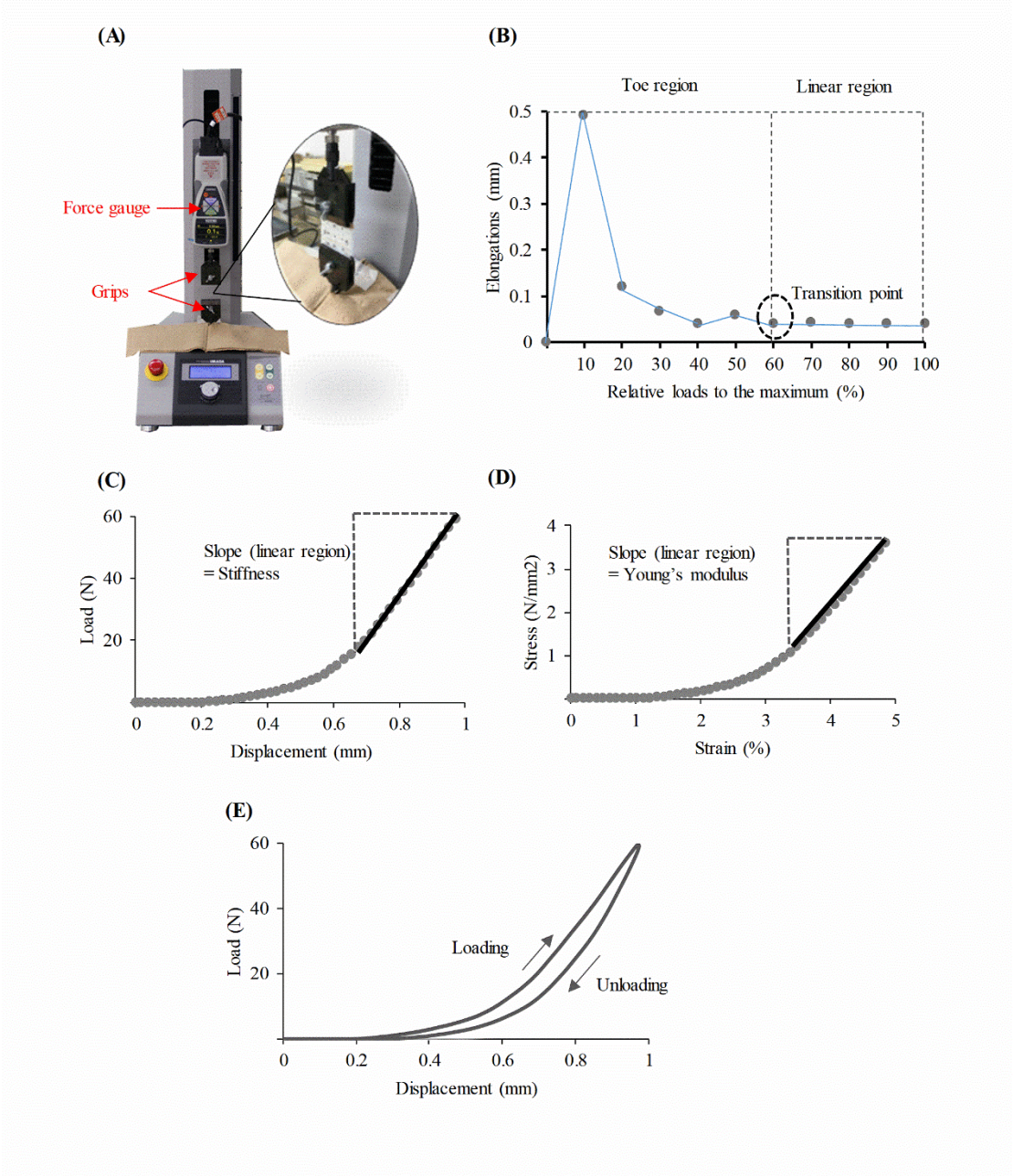

Fig. 2-2. Mechanical testing and data process. (A) A tensile test machine with an inset showing a gripped specimen. (B) A relationship curve between relative loads (to maximal) and elongations. (C) A representative load-displacement curve recorded by the tensile test. (D) A representative stress-strain curve recorded by the tensile test. (E) A representative load-displacement curve during tensile test. The arrows indicate loading and unloading directions.

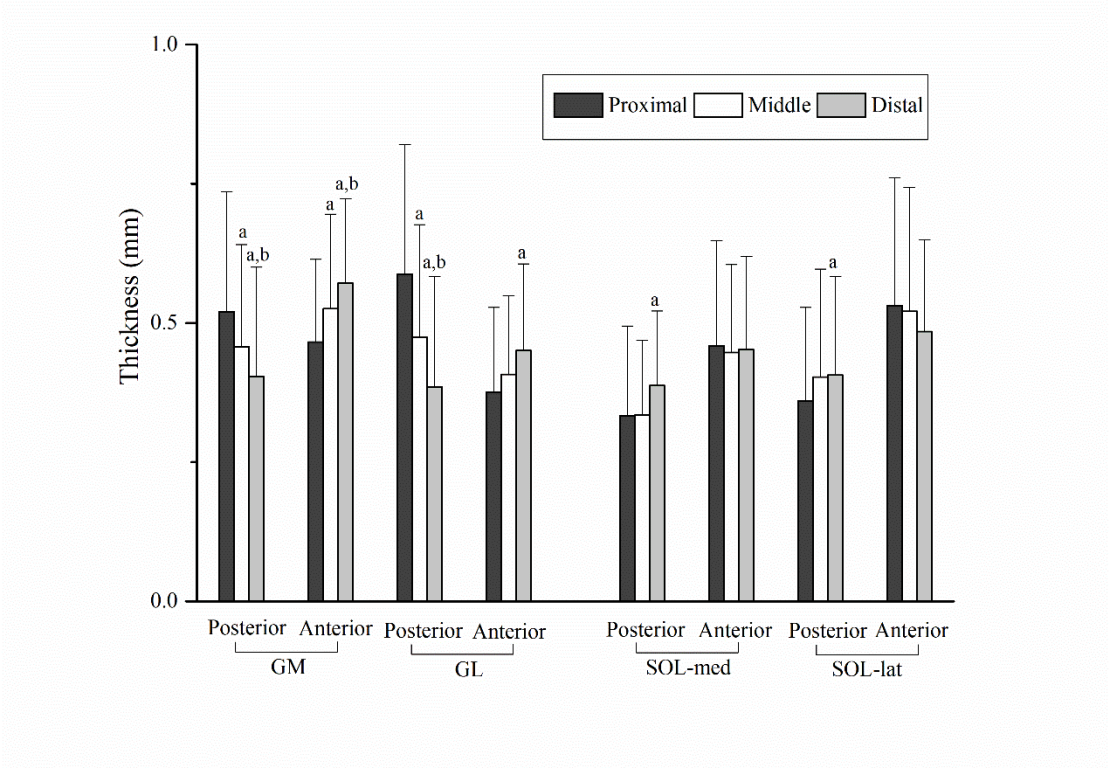

Fig. 2-3. **Average (mean + s.d.) thickness of aponeuroses from proximal to distal sites in each region**. a: denotes different from proximal site, $p < 0.05$; b: denotes different from middle site, $p < 0.05$. GM gastrocnemius medialis, GL gastrocnemius lateralis, SOL-med medial part of soleus, SOL-lat lateral part of soleus.

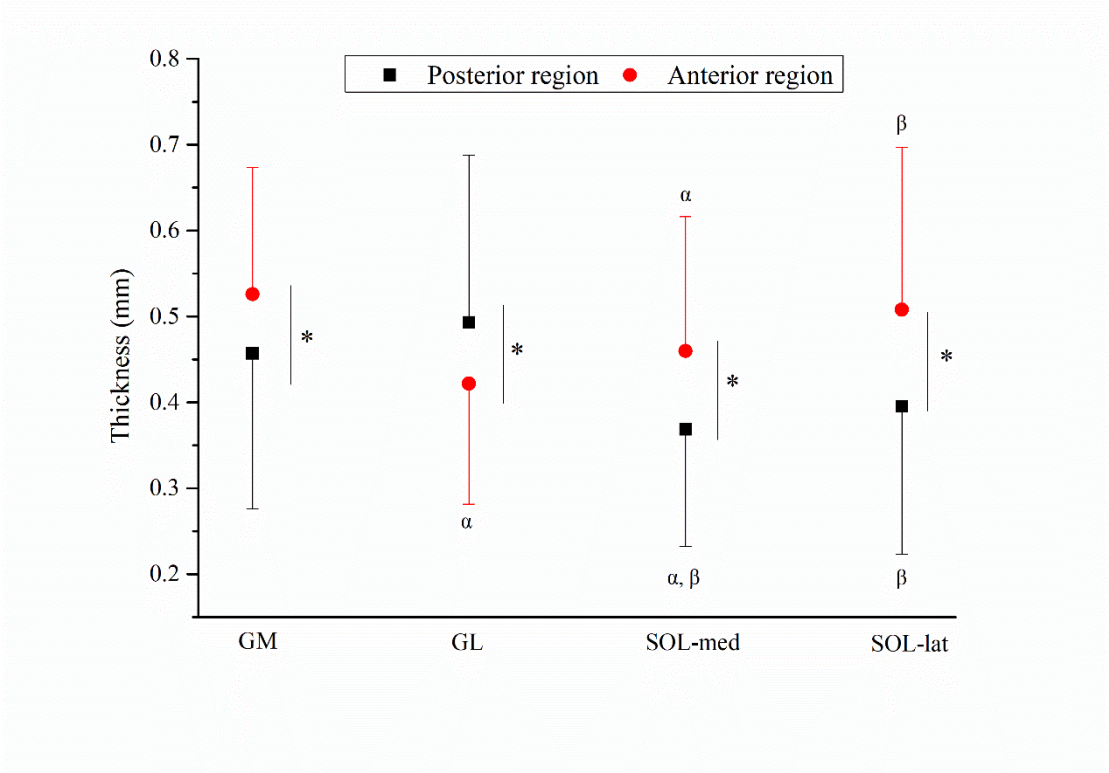

Fig. 2-4. Average (proximal/middle/distal sites, mean ± s.d.) thickness of aponeuroses in posterior and anterior regions of the triceps surae. *: denotes differences between posterior and anterior regions, $p < 0.05$; α: denotes different from GM, $p < 0.05$; β: denotes different from GL, $p < 0.05$. GM gastrocnemius medialis, GL gastrocnemius lateralis, SOL-med medial part of soleus, SOL-lat lateral part of soleus.

Table 2-1. Mean and standard deviations (s.d.) of the stiffness values for the tested specimens (N/mm)

	GM-posterior		GM-anterior		SOL-med-posterior		SOL-med-anterior	
	L	T	L	T	L	T	L	T
Proximal	114.2±36.7	0.7±1.4[#]	107.1±33.3	0.9±0.9[#]	83.7±27.3	0.9±0.7[#]	74±26.6	0.9±1.5[#]
Middle	114.3±37.5	0.4±0.7[#]	125.4±40.1	0.6±0.5[#]	89.6±38	0.9±1.1[#]	78.7±32.3	0.7±0.6[#]
Distal	83.3±34.8[a,b]	0.3±0.4[#]	143.6±45.2[a]	0.8±1.1[#]	106.9±35.9	0.8±0.7[#]	69±26.5	1±0.9[#]
	GL-posterior		GL-anterior		SOL-lat-posterior		SOL-lat-anterior	
	L	T	L	T	L	T	L	T
Proximal	108.2±35	0.7±0.6[#]	102±45.9	0.8±0.9[#]	64.5±29.1	1.2±1.3[#]	75.9±27.2	0.8±0.9[#]
Middle	109.7±36.1	0.9±1[#]	144.7±41.4[a]	1.2±1.3[#]	80.9±35.1	1.5±1.4[#]	73.9±30.2	0.8±0.7[#]
Distal	87.5±18.7	0.8±0.5[#]	129.6±46.7[a]	1.8±1.6[#]	88.4±34.2	1.3±1.1[#]	80.1±31.3	1.5±1.2[#]

#: denotes different from longitudinal direction, $p < 0.05$; a: differences from proximal site; b: differences from middle site. GM gastrocnemius medialis, GL gastrocnemius lateralis, SOL-med medial part of soleus, SOL-lat lateral part of soleus, L longitudinal, T transverse.

Table 2-2. Mean and standard deviations (s.d.) of the Young's modulus values for the tested specimens (MPa)

	GM-posterior		GM-anterior		SOL-med-posterior		SOL-med-anterior	
	L	T	L	T	L	T	L	T
Proximal	207.1±118.7	0.6±0.9#	198.2±118.3	1.1±1.2#	264.3±155.5	1.2±1#	211.6±166.1	0.7±0.9#
Middle	210.4±96	0.4±0.6#	196.1±89.2	0.8±0.9#	261.7±196.9	1.4±1.6#	199.1±113.1	0.8±0.9#
Distal	182.8±106.6	0.6±0.6#	207.5±103.2	0.5±0.5#	262±127.7	0.9±0.9#	177.6±120	0.8±0.5#
	GL-posterior		GL-anterior		SOL-lat-posterior		SOL-lat-anterior	
	L	T	L	T	L	T	L	T
Proximal	289.1±214.5	0.5±0.5#	283.9±168.9	1.1±1.1#	185.7±132.2	2.3±2.2#	164.1±124.6	0.8±0.9#
Middle	280±104.4	1±1.2#	323.3±151	1.4±1.4#	225.4±168.8	2±1.9#	197.9±181.2	0.7±0.5#
Distal	191.9±66.5	1.3±0.7#	304.6±157.1	1.9±1.9#	256.2±159.2	1.9±1.9#	173.8±75.6	1.3±1.4#

#: denotes different from longitudinal direction, $p < 0.05$; GM gastrocnemius medialis, GL gastrocnemius lateralis, SOL-med medial part of soleus, SOL-lat lateral part of soleus, L longitudinal, T transverse.

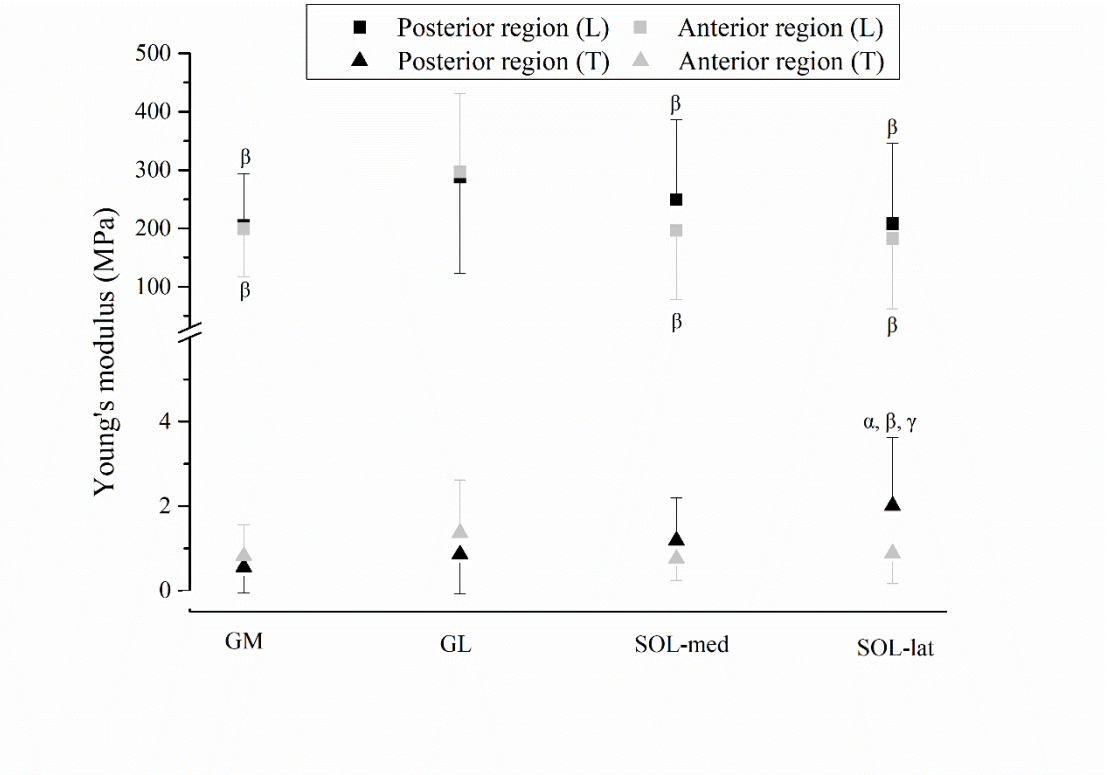

Fig. 2-5. Average (proximal/middle/distal sites, mean ± s.d.) Young's modulus in L (longitudinal) and T (transverse) directions of aponeuroses in posterior and anterior regions of the triceps surae. α: denotes different from GM, $p < 0.05$; β: denotes different from GL, $p < 0.05$; γ: denotes different from SOL-med, $p < 0.05$. GM gastrocnemius medialis, GL gastrocnemius lateralis, SOL-med medial part of soleus, SOL-lat lateral part of soleus.

Table 2-3. Mean and standard deviations (s.d.) of the hysteresis values for the tested specimens (%)

	GM-posterior		GM-anterior		SOL-med-posterior		SOL-med-anterior	
	L	T	L	T	L	T	L	T
Proximal	41.1±8.5	47.5±20.7	38±8.4	40.5±16.8	26.1±7.8	40.6±20.3[#]	31.3±7.1	45.2±15.1[#]
Middle	33.9±9.9	54±17.8[#]	45.2±8.8	40.2±9.6	33.7±11.5	38.7±18.7[#]	36.8±11.7	40.4±12.2[#]
Distal	28.2±8.7	53.8±15.8[#]	46.6±7[a]	48.6±18.3[a]	34.8±8.2	38.8±12.9[#]	33.7±8.7	44.5±21.6[#]
	GL-posterior		GL-anterior		SOL-lat-posterior		SOL-lat-anterior	
	L	T	L	T	L	T	L	T
Proximal	41.4±6.9	46.6±19.2[#]	29±8	50.3±21.3[#]	29.5±7.9	39.7±17.8	37.9±9.6	44.7±16.4[#]
Middle	36.5±8.2	37.8±16.4[#]	34.5±8.7	39.6±18.2[#]	35.3±9.9	32.4±9.7	38.1±11.3	48.5±16.4[#]
Distal	29±4.9[a]	41±9.4[a, #]	40.7±8.7	35.8±12.4[#]	35.6±10.2	39.1±17.4	34.6±10.3[b]	37.9±12[b, #]

#: denotes different from longitudinal direction, $p < 0.05$; a: differences from proximal site; b: differences from middle site. GM gastrocnemius medialis, GL gastrocnemius lateralis, SOL-med medial part of soleus, SOL-lat lateral part of soleus, L longitudinal, T transverse.

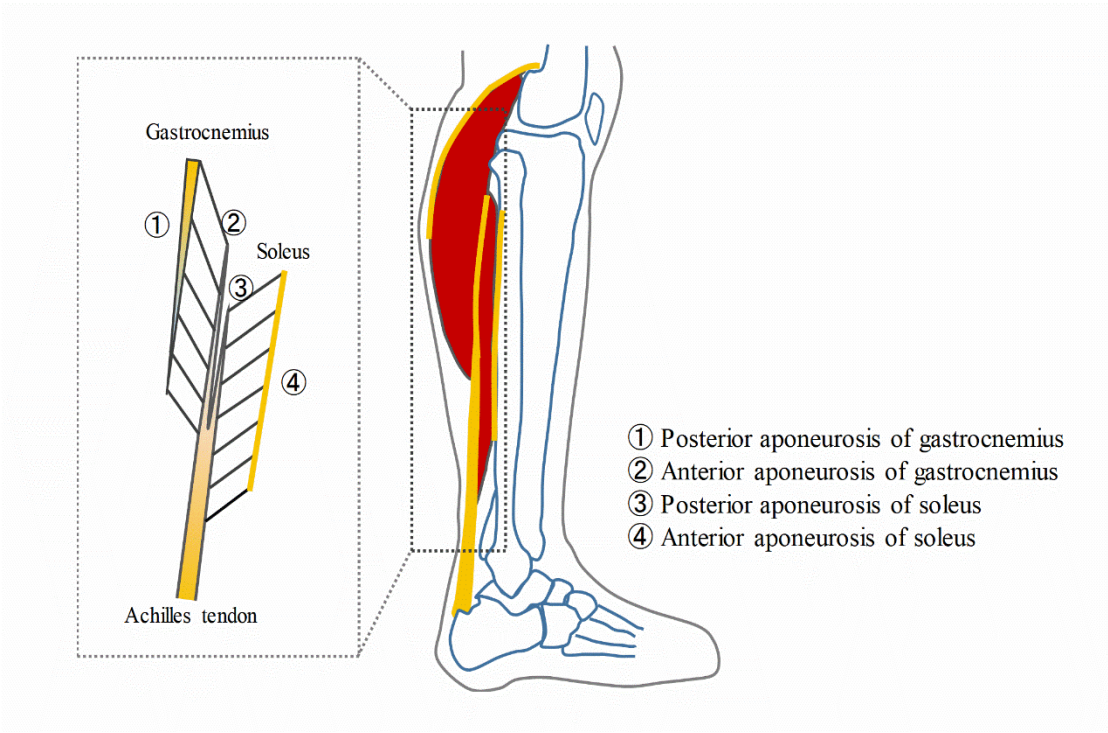

Fig. 2-6. Sagittal view of the triceps surae and schematic representation of aponeurosis thickness distribution. Orange color (with gradation) denotes tendinous tissue (i.e. tendon or aponeurosis).

CHAPTER 3 Inhomogeneous and anisotropic mechanical properties of the triceps surae muscles and aponeuroses *in vivo* during submaximal muscle contractions

3-1 Introduction

In chapter 2, the adjoining aponeuroses exist between gastrocnemii and soleus were found thinner but higher Young's modulus, which indicates different morphology and mechanical properties among aponeuroses of synergist muscles. In addition, the anisotropic elastic feature of the aponeuroses was more pronounced than *in vivo* observations, suggesting inherent material design of the aponeurosis that matches three-dimensional contractile behavior of muscle fibers during muscle contractions. The aponeurosis's length and width could be altered by the shape changes of muscle belly, which indicates mechanical loading of aponeuroses is more complex than that of tendons (Arellano et al., 2016; Scott and Loeb, 1995). Therefore, biaxial (longitudinal and transverse) stiffness changes of aponeurosis during muscle contraction need to be clarified. Kawakami et al. (1998) reported that different muscle architectures may have relation to differences in mechanical behaviors of muscles and aponeurosis. Consequently, information on changes of muscle architecture and muscle-aponeurosis stiffness becomes essential for the study of muscle-aponeurosis interactions during movement. Thus, the present study aims to 1) investigate the site- and direction-dependent differences of TS muscle and aponeuroses stiffness *in vivo*, during graded submaximal plantarflexion efforts and 2) examine the relationships between architecture changes and mechanical property changes of TS muscles and aponeuroses

in vivo.

3-2 Material and methods

3-2-1 Subjects

Twelve young male subjects (age: 27 ± 4 years, height: 171.8 ± 6.3 cm, body mass: 65.9 ± 11.9 kg, lower leg length: 39.3 ± 2.0 cm, body fat percentage: 18.0 ± 5.9%; means ± s.d.) volunteered for the current work. The subjects were non-active in any sports within 6 months prior to the test time. All subjects were informed about the study information and required to fill the informed consent before their participation. This study was approved by the Local Ethics Committee and conducted in accordance with the principles of the Declaration of Helsinki.

3-2-2 Experimental setup

A custom-made dynamometer (VTE, VINE, Japan) was used to measure the isometric plantar flexion torque. The signal from the dynamometer was processed by a strain amplifier (DPM-900, Kyowa, Japan). Then, it was acquired at 1000 Hz rate using a data acquisition system (PowerLab, ADInstruments, Australia) and recorded using a data acquisition software (LabChart 8.0, ADInstruments, Australia). B-mode and shear wave imaging could be obtained using ultrasound shear wave elastography (SWE, Version 6.4, Supersonic Imagine, Aix-en-Provence, France) with constant settings (pre-set, MSK; persistence, high; smoothing, 9). A foot pedal (SE2, Kinesis, USA) was used to synchronize videos recording (12Hz) of SWE and torque signal.

3-2-3 Torque and ultrasound shear wave imaging recordings

The subjects were asked to lay in the prone position with knee joint fully extended and ankle joint in neutral position. At first, the subjects were asked to keep relaxed and the passive torque was recorded. In the meanwhile, the transducer (L15-4, Aixplorer, Supersonic Imagine, Aix-en-Provence, France) of SWE was positioned longitudinally (along the muscle's line of action) on the proximal (30% level of lower leg length) and distal site (distal end of gastrocnemii) of the TS to measure shear wave imaging of proximal and distal sites of medial gastrocnemius (MG), lateral gastrocnemius (LG), medial side of soleus (SOL-med) and lateral side of soleus (SOL-lat). Furthermore, superficial aponeuroses of MG and LG (MPS and LPS) at the proximal site, adjoining aponeuroses (Fig. 3-1) between MG and SOL-med at proximal and distal sites (MPA and MDA) as well as adjoining aponeuroses between LG and SOL-lat at proximal and distal sites (LPA and LDA) were measured with the longitudinal transducer direction. Additionally, the transducer was changed to the transverse direction to measure the adjoining aponeuroses between gastrocnemii (MG and LG) and soleus at distal site (MDA-t and LDA-t) (Fig. 3-1). Videos of shear wave imaging were recorded twice over 5 s period. Subsequently, the subjects performed at least two maximal voluntary contractions (MVCs) of isometric plantar flexions after a warm-up (several submaximal contractions) in case that the difference between two MVCs was lower than 10%. During each MVC, the subjects were instructed to produce the maximal isometric force and hold at the maximal level for 3s. Thereafter, submaximal contractions at 20%, 40%

and 60% of MVC were performed. Besides, the subjects were asked to maintain at least 5 s period, during which, the shear wave imaging videos of the same muscle and aponeurosis locations as described in the above section were recorded. The order of transducer locations and muscle contraction levels was designed with randomization and counterbalance. After the completion of first cycle of submaximal contractions (20%, 40%, 60%), the second cycle of submaximal contractions was repeated to calculate the test-retest reliability (Fig. 3-2). All the ultrasound measurements were performed by the same tester, and the ultrasound transducer was maintained on the skin with minimal pressure. It should be mentioned that strictly, what we measured on aponeurosis are the surface acoustic wave signals, which can reflect the stiffness of the sound wave transmission direction, and they have been identified to have the same meaning as shear wave, therefore, we defined our measurements as SWV (Saavedra et al., 2017; Shiotani et al., 2019).

3-2-4 Data analysis

3-2-4-1 Plantar flexion torque

The signal of torque data was low-pass filtered with a cutoff frequency of 10 Hz. Initially, the MVC value was calculated from the average value of 2 s duration of highest torque value. Afterwards, the submaximal torque value was represented by the mean value of the two repeated measurements, while the value of each measurement was averaged from 3 s duration at each contraction level.

3-2-4-2 Shear wave velocity (SWV)

As the SWE videos were synchronized with torque signal using the foot pedal pulse, therefore, the start time of submaximal contraction was calculated by the time difference between foot pedal pulse and the start point of 3 s torque calculation period. Subsequently, the start image frame was found, and another 2 images were picked up every 12 frames (Fig. 3-3). The SWV of muscle or aponeurosis were measured using an adjustable region of interest (ROI, trace function) in the SWE machine. SWV of muscle or aponeurosis was represented by the mean value of the two repeated measurements, while the value of each measurement was averaged from 3 images of each second.

3-2-4-3 Pennation angle

Three images during at rest and submaximal contractions were obtained the same as those for SWV analysis, as described in the above section. For each muscle within one image, two visible muscle fascicles were used to calculate the pennation angles. Then, the averaged value of two pennation angles was used as pennation angle of each muscle in one image (Fukunaga et al., 1997a; Kawakami et al., 1998) (Fig. 3-4a).

3-2-4-4 Tendon length change index (*cosα – cosα'*)

In this study, we used the index of *cosα – cosα'* to represent the tendon length change of the muscle-tendon unit from at rest to submaximal contractions (20%, 40%, and 60% of MVC) (Chino et al., 2008; Purslow, 2003). The basis of using it was as

follows:

$$FL \cdot cos\alpha - FL' \cdot cos\alpha' = \Delta TL$$

$$FL \cdot sin\alpha = MT = FL' \cdot sin\alpha'$$

$$FL \cdot sin\alpha = FL' \cdot sin\alpha'$$

$$\frac{FL}{FL'} = \frac{sin\alpha}{sin\alpha'} \quad \rightarrow \quad FL' = \frac{sin\alpha}{sin\alpha'} \cdot FL$$

$$FL \cdot cos\alpha - \frac{sin\alpha}{sin\alpha'} \cdot FL \cdot cos\alpha' = \Delta TL$$

$$cos\alpha - \frac{sin\alpha}{sin\alpha'} \cdot cos\alpha' = \frac{\Delta TL}{FL}$$

Where *FL* is the fascicle length at rest, *FL'* is the fascicle length during contraction, *α* is the pennation angle at rest, *α'* is the pennation angle during contraction, *ΔTL* is the tendon length change, *MT* is the muscle thickness (Fig. 3-4b).

3-2-5 Statistics

All the data are shown as means ± standard deviation (s.d.). At first, we assessed the test-retest reliability of the SWVs of TS muscles and aponeuroses using the intraclass correlation coefficient (ICC), standard error of measurement (SEM) and coefficient of variation (CV) (Hopkins, 2000).

To test the site-, muscle- and level-dependent differences in SWVs and pennation angle of the TS, a three-way analysis of variance (ANOVA) [sites (proximal and distal), muscles (MG, LG, SOL-med, SOL-lat), levels (at rest, 20%, 40%, 60% of MVC)] was performed. If significant interactions and main effects were found, a one-way ANOVA with post hoc tests (Bonferroni) was used to compare the differences among muscles or contraction levels and a paired t-test was also used to compare the differences

between sites.

To compare the site-, side- and level-dependent differences in SWVs of TS adjoining aponeuroses, a three-way ANOVA [sites (proximal and distal), sides (medial and lateral) and levels (at rest, 20%, 40%, 60% of MVC)] was used. In addition, to determine the direction-dependent differences in SWVs of the adjoining aponeuroses, a three-way ANOVA [directions (longitudinal and transverse), sides (medial and lateral) and levels (at rest, 20%, 40%, 60% of MVC)] was also used. If significant interactions and main effects were found, a one-way ANOVA with post hoc tests (Bonferroni) could be used to compare the differences among contraction levels and a paired t-test was used to compare the differences between sites, sides or directions.

The average SWVs (in m/s) of MDA and LDA in the longitudinal and transverse directions during linear region (no significant increase) were calculated as aponeuroses stiffness and were compared by using a two-way ANOVA [directions (longitudinal and transverse) and sides (medial and lateral)]. If significant interactions and main effects were found, a paired t-test was also used to compare the differences between directions or sides.

Finally, the Pearson product-moment correlation coefficient was used to test the relationship between relative changes of tendon length and SWVs of TS muscles and aponeuroses.

All the statistical analyses were performed using SPSS Statistics 24.0 (IBM SPSS Statistics, SPSS Inc., Chicago, USA) and Origin 9.0 (OriginLab, Northampton, MA, USA). The significance level was set at $p < 0.05$.

3-3 Results

3-3-1 Shear wave velocities of triceps surae muscles and aponeuroses

Table 1 showed low SEM values (0.05 – 0.2 m/s) and high ICC values (0.84 – 1.00) for TS muscles and aponeuroses at rest, indicating the high reproducibility of the SWVs of TS muscles and aponeuroses at rest. However, lower ICC values (lowest: 0.34) could be shown in some cases during submaximal contractions.

There existed no significant site × muscle × level interaction on SWVs of muscles, while we observed significant site × muscle, site × level and muscle × level interactions ($p < 0.001$), and the main effects of site, muscle and level remained significant ($p < 0.001$). Only the SWVs of LG (3.2 – 9.1m/s) and SOL-lat (2.6 – 7m/s) at proximal site increased significantly from at rest to 60% of MVC levels. The SWV of soleus (4 – 7m/s) showed significantly lower than that of gastrocnemii (5.2 – 9.1m/s) during submaximal contractions ($p < 0.05$). In addition, the SWV of proximal site was higher than distal site for MG and soleus during submaximal contractions ($p < 0.05$) (Table 3-2).

LPS showed significantly graded increase from at rest to 60% as LG and SOL-lat ($p < 0.05$). For the SWVs of adjoining aponeuroses, the values of distal site (5.2 – 7.8 m/s) were significantly lower than that of the proximal site (6.7 – 9.7, $p < 0.05$) during submaximal contractions. SWV of LPA increased significantly from at rest to 40% of MVC, while MPA and LDA increased significantly from at rest to 20% of MVC ($p < 0.05$) (Fig. 3-5a). Significant differences existing between aponeuroses SWV of

longitudinal and transverse directions in the lateral side could be observed during at rest and submaximal contractions ($p < 0.05$). However, in the medial side, there was no significant difference between longitudinal and transverse directions at 40% and 60% of MVC levels (Fig. 3-5a). During the linear region, significant differences between longitudinal and transverse SWVs were shown, and the longitudinal SWV of LDA was significantly higher than that of MDA ($p < 0.05$, Fig. 3-5b).

3-3-2 Pennation angle of triceps surae muscles

There was no significant site × muscle × level interaction on pennation angle of the TS, while we observed significant site × muscle and level × muscle interactions ($p < 0.01$). The main effects of muscles and levels were significant ($p < 0.001$). For the pennation angle of both MG and LG, significant changes occurred at 40% of MVC level. However, for the pennation angle of SOL-med and SOL-lat, significant changes happened at 20% of MVC level. The pennation angle of soleus was higher in comparison with gastrocnemii during submaximal contractions ($p < 0.05$, Table 3-3).

Only the relative changes of SWVs of gastrocnemii and superficial aponeuroses were significantly correlated with the relative tendon length changes from at rest to submaximal contractions ($r = 0.43 – 0.63$, $p < 0.01$, Fig. 3-6a, b).

3-4 Discussion

The result showed inhomogeneous and anisotropic mechanical properties of the TS muscles and aponeuroses during submaximal muscle contractions. Clear non-linear

relationships between the stiffness of TS muscle-aponeurosis and muscle contraction levels except for proximal LG and SOL-lat muscle bellies and the superficial aponeuroses of LG were found.

For the passive stiffness of the TS, the distal site (near to the muscle-tendon junction point) was stiffer than proximal site, whereas during submaximal contractions, muscles in the distal site became softer than the proximal site. Consequently, TS muscles in the proximal site stiffen more accompany with the increasing level of plantar flexion. As documented by previous studies, there is inhomogeneous (proximal-distal differences) activation and adaption within the quadriceps femoris (QF) (Blazevich et al., 2006; Ema et al., 2013; Maeo et al., 2017) during muscle contraction and/or after exercise training. Additionally, studies (Giordano and Segal, 2006; Segal and Song, 2005) on the site-dependent activation of TS found that the proximal site of gastrocnemii and soleus activated higher than the distal site during calf-raising exercises or submaximal plantarflexions. Thus, higher stiffness of the TS at proximal site in the present study may be related to higher level of activation of muscles, but the reason for this different spatial activation within a muscle is still not clear, which need to be further investigated.

Besides, similar results of site-dependent changes in aponeuroses stiffness could also be shown in the present study (Fig. 3-5a). Previously, the aponeuroses were reported to play an important role in extra-muscular myofascial force transmission (Huijing and Baan, 2001; Huijing et al., 2007; Maas and Sandercock, 2010) between adjacent muscles. During muscle contraction, an *in vivo* study (Lieber et al., 2000) on

the frog semitendinosus demonstrated that muscle activation can increase the aponeuroses stiffness, so the higher activation of the TS at the proximal site influenced the adjoining aponeuroses stiffness. In addition to site-dependent differences, we also compared directional differences of the adjoining aponeuroses stiffness during submaximal contractions. As shown in Fig. 3-5a, the stiffness in the longitudinal direction was higher than that in the transverse direction from at rest to submaximal contractions, especially the aponeuroses between LG and soleus. This anisotropic difference between longitudinal and transverse directions showed larger in the lateral side than the medial side. A previous study reported that the transverse aponeurosis stiffness of MG increased in rats (Holt et al., 2016), which was consistent with our findings of differences on medial-lateral anisotropy. Azizi and Roberts (2009) reported that the aponeuroses can be stretched 4 times greater in the transverse direction than the longitudinal direction during active force production, showing consistence with findings in the present study. Different from the free tendon, aponeuroses increase both in length and width under biaxial load to modulate the muscle shape changes (Arellano et al., 2016). However, the stiffness of aponeuroses (LDA and LDA-t) both increased and then kept at a constant level during submaximal contractions, while stiffness of MDA did not make any change. Different behaviors of aponeuroses between medial and lateral side during force production waited to be explored.

Unexpectedly, significant non-linear relationships between SWVs of TS muscles and aponeuroses and levels of contractions were found except for LG and SOL-lat muscle bellies and LPS at proximal site. An in vitro study (Ettema and Huijing, 1994)

on gastrocnemius medialis (GM) muscle-tendon unit of the rat found a linear model for the force-stiffness relationship during isometric contractions. Additionally, previous *in vivo* studies proved that muscle shear modulus is linearly related to muscle torque not only during moderate-level (0-60% of MVC) isometric contractions (Bouillard et al., 2012; Bouillard et al., 2011) but also during higher levels (0-100% of MVC) (Ateş et al., 2015). In our findings, even the synergists (LG, MG and SOL) behave differently, with the LG and SOL-lat showed graded increase of SWV while MG and SOL-med did not. For MG and SOL-med, rather than a linear relationship with contraction levels, the muscle stiffness kept increasing until reaching a certain contraction level and the reason may come from the influence from adjacent aponeuroses. A previous *in vivo* study (Iwanuma et al., 2011) documented that the strain of aponeurosis close to the Achilles tendon presents no differences at 30% MVC and 60% MVC in the longitudinal direction (1.1 and 1.6%), which was similar with our results, and this characteristics happened not only at distal site but also at proximal site for the TS aponeuroses. Another study (Arampatzis et al., 2007) found that the mechanical properties of the TS aponeurosis do not show a graded response to the intensity of sports activity, which just support our findings of aponeurosis behavior. Rehorn and Blemker (2010) reported that the muscle along-fiber stretch distribution can be influenced by morphological properties of the aponeurosis during stretching, suggesting the existence of muscle-aponeurosis interaction within the muscle-tendon unit (MTU). As a result, due to the muscle-aponeurosis interaction during active muscle contraction, the neighboring muscles and aponeuroses showed similar changes (medial: non-linear, lateral: linear)

of mechanical properties in the present study.

Our results of muscle architecture obtained *in vivo* suggest that the TS muscle architecture changes as a function of force development during isometric plantar flexion, yet the significant increase of pennation angle was only within a range of submaximal contraction levels. A previous study (Narici et al., 1996) reported that MG pennation angle increased (15.7-33.7 deg) from at rest to MVC, which is similar to the results of the present study (from at rest to 60% MVC: 17.3-24.9 deg). Besides, we only asked the participants to perform from at rest to 60% MVC to match the common activity levels in life. The following step for higher level of contractions can make us better understand the effect of intensive training on muscle architecture. Regarding to the relationships between SWV of TS muscles and aponeuroses and the relative length changes, only the SWV of superficial aponeuroses of gastrocnemii significantly increased in response to the relative tendon length changes during submaximal contractions. This indicate the superficial aponeuroses are more compliant than the adjoining aponeuroses in the longitudinal direction to accommodate the expansion of the contracting muscle belly (Purslow, 2003) (Fig. 3-7).

3-5 Conclusion

The results further indicate that the TS muscles and aponeuroses showed inhomogeneous and anisotropic mechanical properties during submaximal muscle contractions, and the stiffening effect of muscle belly possibly make influence on the mechanical properties of aponeuroses during muscle contractions.

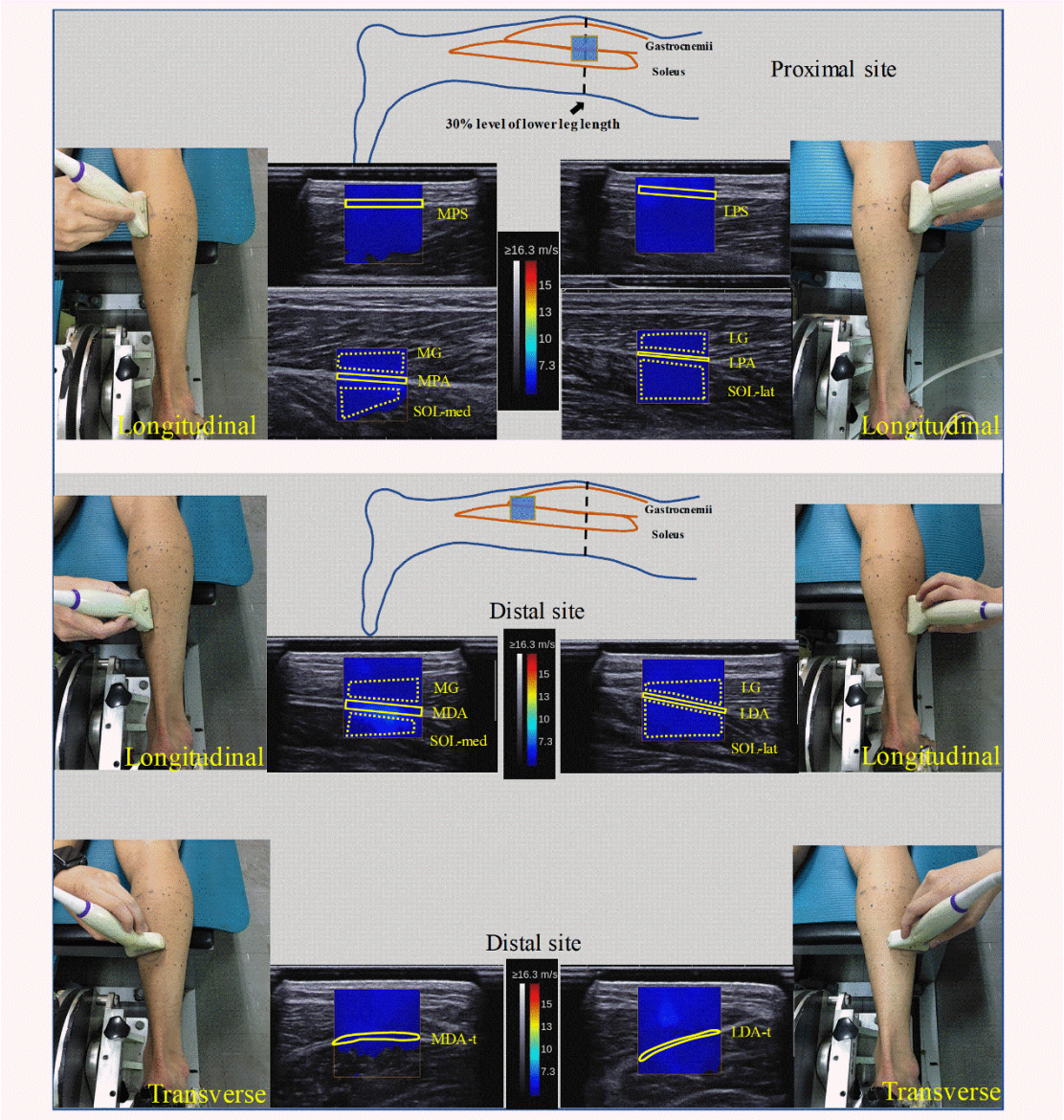

Fig. 3-1 Locations of shear wave elastography transducer and typical maps of shear wave velocities of triceps surae muscles and aponeuroses. The irregular yellow shapes represent regions of interest (ROIs) to measure the shear wave velocity values of muscles and aponeuroses.

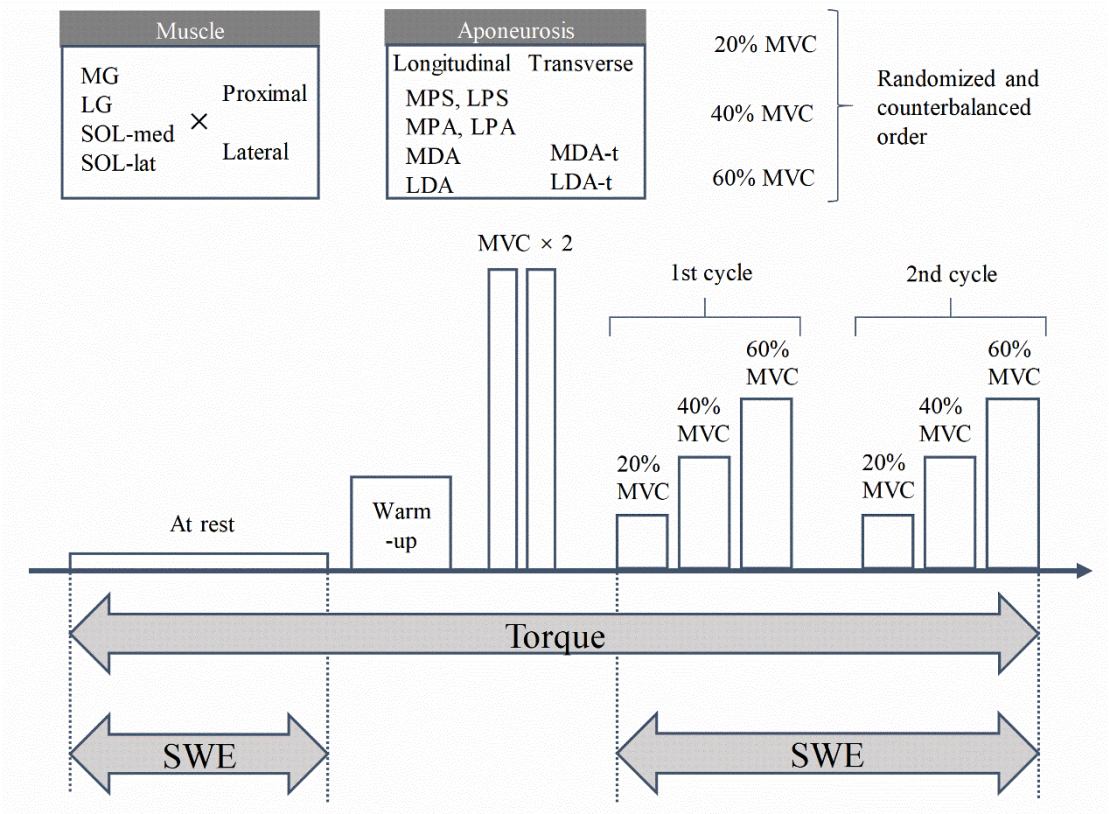

Fig. 3-2 Experimental protocol design. Participants first lay prone and stay at rest, then performed 2 maximal voluntary contractions (MVC) after warm-up, next, 2 cycles of submaximal contractions (20%, 40%, 60% of MVC) were conducted. The torque was collected during the whole process, while the ultrasound shear wave elastography (SWE) was used to measure triceps surae muscles and aponeuroses during at rest and submaximal contractions period.

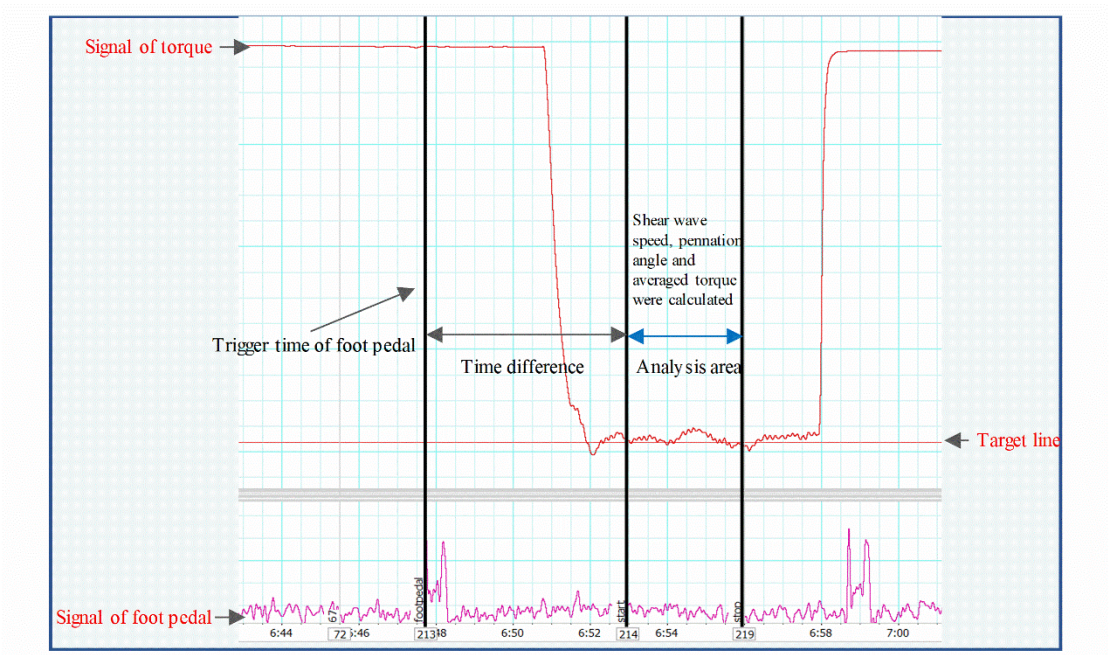

Fig. 3-3 Typical data analysis process to synchronize torque signal and ultrasound shear wave imaging.

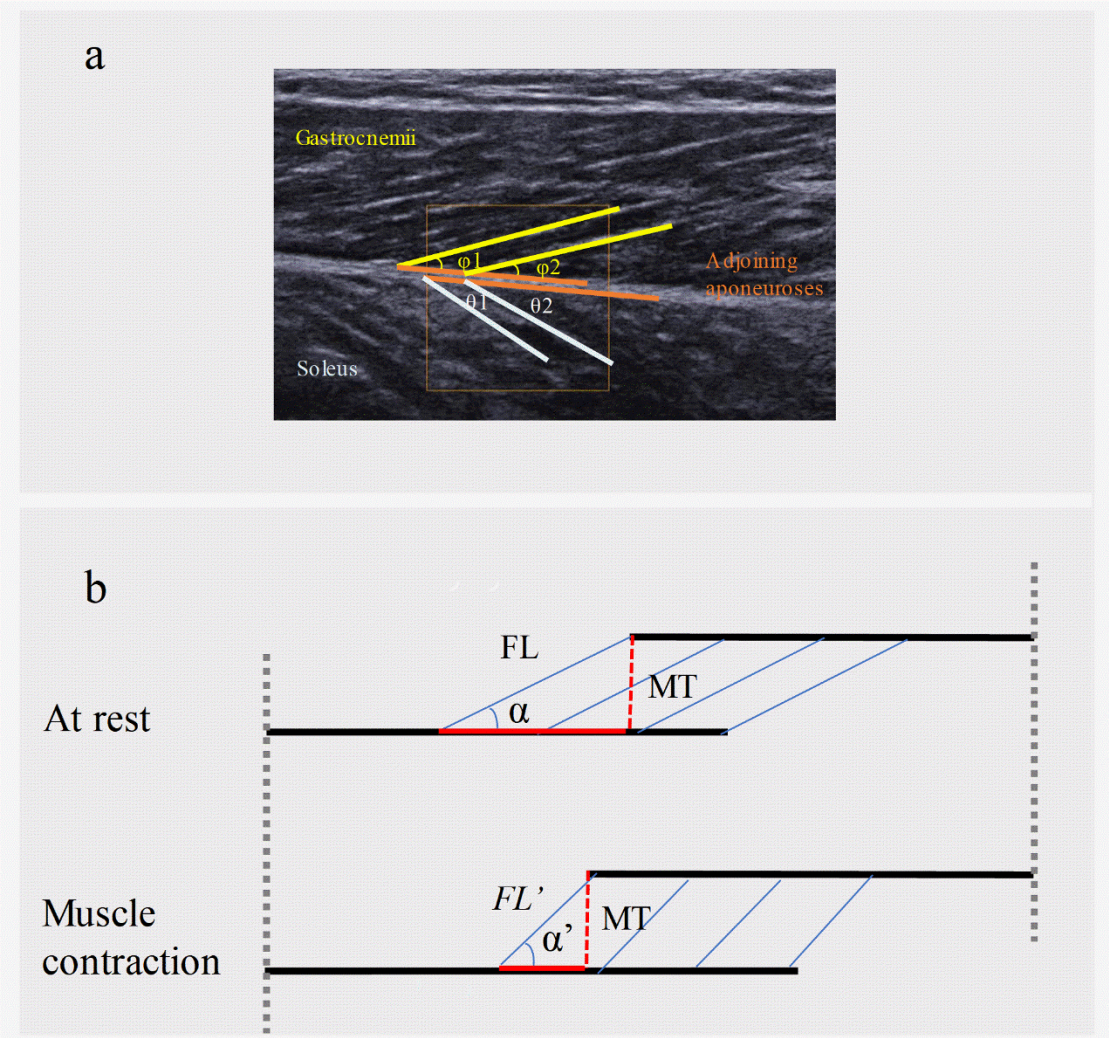

Fig. 3-4 Typical ultrasound images of gastrocnemii and soleus (a) and schematic diagram showing the relative tendon length change arising from a change in penneation angle (b). The yellow lines represent gastrocnemii fascicles, the orange lines represent the adjoining aponeuroses between gastrocnemii and soleus, the white lines represent soleus fascicles. The pennation angle was averaged for gastrocnemii (φ1 and φ2) and soleus (θ1 and θ2).

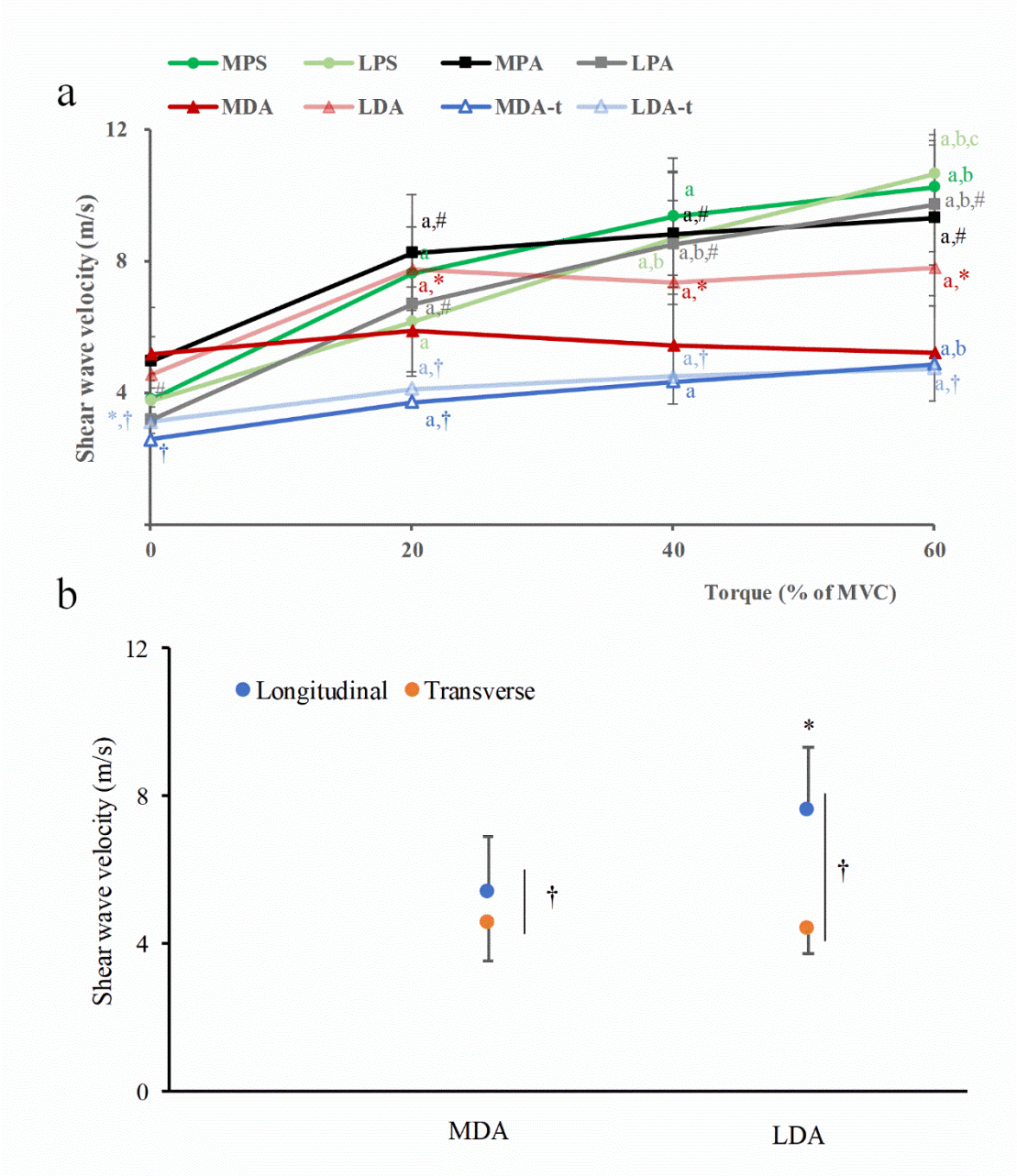

Fig. 3-5 The shear wave velocities (mean ± s.d.) of triceps surae aponeuroses between different sites and directions plotted with the different relative isometric contraction levels (% MVC torque) (a) and the averaged shear wave velocity of the adjoining aponeuroses in the linear region between longitudinal and transverse directions (b). a, vs. at rest; b, vs. 20%; c, vs. 40%; #, vs. proximal site; *, vs. medial side; †, vs. longitudinal direction

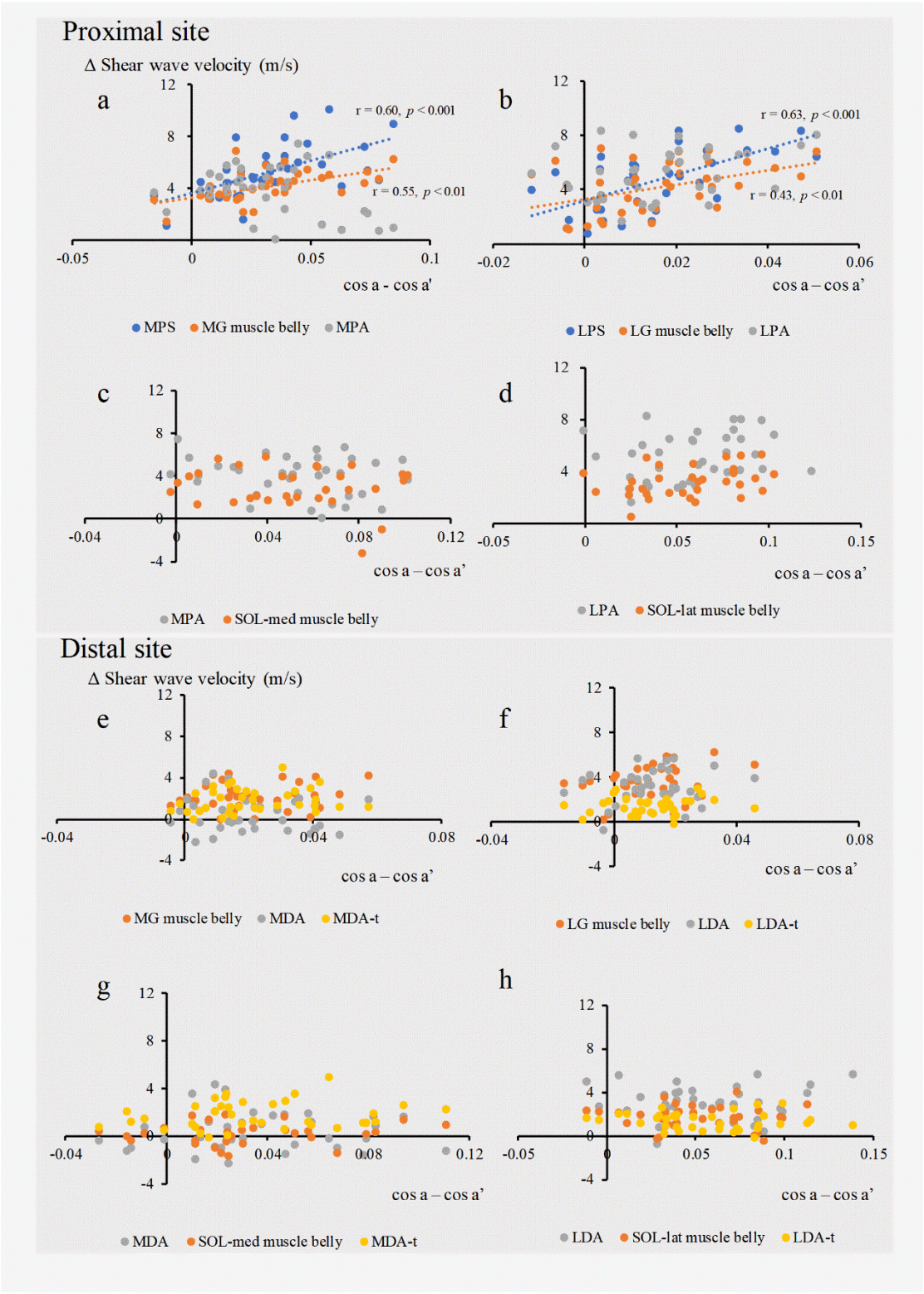

Fig. 3-6 Shear wave velocity / relative isometric plantar flexion torque (% of MVC) relationship for triceps surae muscles and aponeuroses.

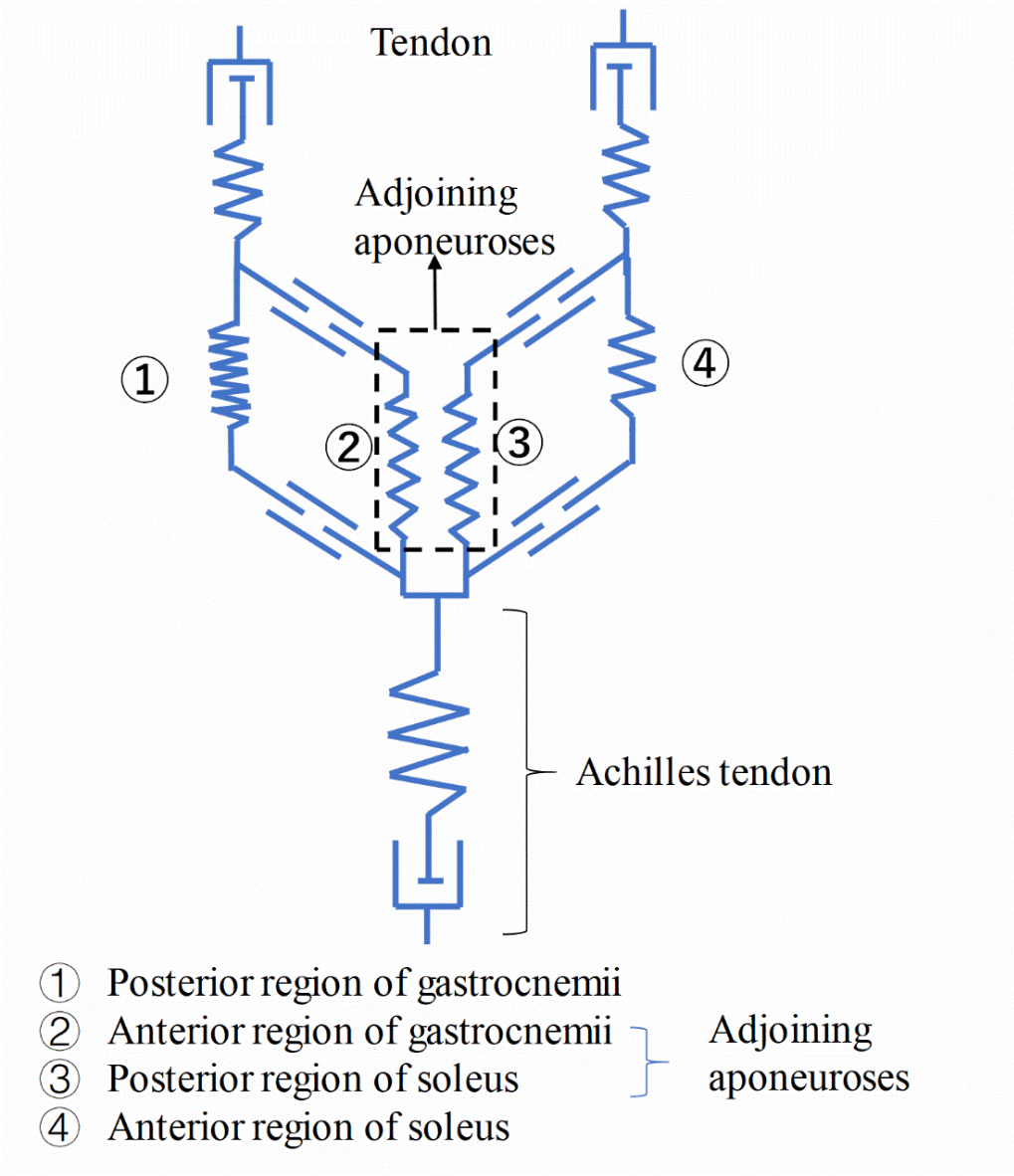

Fig. 3-7 Simulated model of triceps surae muscle-aponeuroses-tendon unit.

Table. 3-1 Reproducibility for shear wave velocities of triceps surae muscles and aponeuroses at different contraction levels

Direction	Site		At rest			20%			40%			60%		
			CV (%)	SEM (m/s)	ICC	CV (%)	SEM (m/s)	ICC	CV (%)	SEM (m/s)	ICC	CV (%)	SEM (m/s)	ICC
Longitudinal	Proximal	MPS	1.57	0.05	1.00	11.85	0.83	0.71	7.16	0.63	0.88	4.33	0.42	0.95
		MG	2.42	0.06	0.98	10.62	0.7	0.48	7.06	0.68	0.47	5.22	0.38	0.84
		MPA	4.3	0.18	0.95	4.63	0.33	0.96	6.24	0.44	0.94	6.12	0.44	0.97
		SOL-med	3.23	0.1	0.97	8.55	0.52	0.8	10.32	0.63	0.87	7.2	0.48	0.82
Longitudinal	Proximal	LPS	1.93	0.06	0.99	11.67	0.86	0.75	8.72	0.68	0.89	9.26	0.98	0.51
		LG	2.24	0.07	0.98	9.7	0.73	0.73	10.62	0.77	0.68	5.99	0.65	0.37
		LPA	2.72	0.08	0.96	8.83	0.6	0.7	5.28	0.37	0.92	6.97	0.57	0.91
		SOL-lat	2.89	0.07	0.96	6.97	0.29	0.86	6.98	0.43	0.62	8.02	0.61	0.63
Longitudinal	Distal	MG	1.81	0.06	0.99	5.26	0.31	0.86	4.88	0.25	0.95	7.69	0.42	0.83
		MDA	3.92	0.18	0.98	15.23	0.78	0.73	14.72	0.68	0.87	11.88	0.55	0.86
		SOL-med	3.74	0.14	0.96	17.82	0.71	0.41	14.03	0.6	0.68	14.93	0.63	0.74
Transverse	Distal	MDA-t	3.99	0.08	0.98	11.98	0.52	0.68	18.17	0.79	0.34	13.62	0.58	0.82
Longitudinal	Distal	LG	3.28	0.15	0.97	8.72	0.54	0.9	6.53	0.49	0.93	9.42	0.86	0.75
		LDA	2.72	0.14	0.97	7.66	0.53	0.9	8.61	0.55	0.93	8.07	0.66	0.84
		SOL-lat	5.23	0.19	0.84	8.21	0.47	0.75	14.6	0.9	0.42	11.24	0.65	0.65
Transverse	Distal	LDA-t	7.37	0.2	0.93	10.16	0.45	0.63	11.4	0.45	0.71	11.21	0.53	0.57

CV, coefficient of variation; SEM, standard error of measurement; ICC, Intraclass correlation coefficient

Table. 3-2 Shear wave velocities (mean ± s.d.) of the triceps surae at rest and during submaximal contraction levels

Muscle	Contraction level	Shear wave velocity (m/s)			
		Proximal		Distal	
MG	at rest	3.3±0.5		3.7±0.8	
	20%	6.4±0.8	a	5.2±0.8	a, #
	40%	7.6±0.8	a, b	6±1.1	a, #
	60%	8.3±0.9	a, b	6.3±1	a, b, #
LG	at rest	3.2±0.4		4.3±0.8	#
	20%	5.4±1.3	a	7.1±1.6	a, I, #
	40%	7.4±1.2	a, b	7.6±1.9	a, I
	60%	9.1±0.6	a, b, c	8.7±1.5	a, I
SOL-med	at rest	3.1±0.5		3.8±0.8	#
	20%	5.3±1.1	a	4±0.7	II
	40%	6±1.9	a, I, II	4±1	I, II, #
	60%	7±1.1	a, b, I, II	4±1.1	I, II, #
SOL-lat	at rest	2.6±0.4	I, II	3.7±0.4	#
	20%	5±0.7	a, I	5.4±0.9	a, II, III
	40%	5.7±0.7	a, I, II	5±1	a, II
	60%	7±0.8	a, b, c, I, II	5.7±1	a, II, III, #

Note: a, vs. at rest; b, vs. 20%; c, vs. 40%; I, vs. MG; II , vs. LG; III, vs. SOL-med; #, vs. proximal site; $p < 0.05$

Table. 3-3 Pennation angle (mean ± s.d.) of the triceps surae at rest and during submaximal contraction levels

	Contraction level	Pennation angle (°)			
		Proximal		Distal	
MG	at rest	18.4±2		17.3±2.3	
	20%	21.3±2.5		19.1±2.5	
	40%	23.8±3.4	a	21.3±2.8	a
	60%	24.9±3.7	a, b	22.2±3.2	a, b
LG	at rest	15.6±2.2		15.1±2.1	
	20%	16.6±2.3	I	16.2±1.9	
	40%	18.9±1.2	a, I	17.7±2.1	a
	60%	20.6±2.2	a, b, I	18.6±2.5	a, b
SOL-med	at rest	21.1±4.7	II	25.7±3.8	I, II
	20%	26.4±4.4	I, II	28.3±2.9	I, II
	40%	29.7±4.9	a, I, II	30.7±2.1	a, I, II
	60%	29.1±4.8	a, I, II	31.5±2.6	a, I, II
SOL-lat	at rest	21.2±3	II	22.7±3	I, II
	20%	27.1±3.6	a, I, II	28.1±2.8	a, I, II
	40%	29.2±3.6	a, I, II	30.3±3.5	a, I, II
	60%	30.9±3.2	a, I, II	31.6±2.8	a, I, II

Note: a, vs. at rest; b, vs. 20%; I, vs. MG; II , vs. LG; $p < 0.05$

CHAPTER 4 Inhomogeneous and anisotropic mechanical properties of the triceps surae aponeuroses in older adults: correlations with muscle strength and walking performance

4-1 Introduction

The main function of TS muscle-tendon unit is plantar flexion, which is closely related to human bipedal walking performance. Since the changes of aponeurosis mechanical properties during different levels of plantar flexion have been investigated in chapter 3, it becomes necessary to clarify the relationships between aponeurosis mechanical properties and muscle strength and walking performance. Walking performance is of major importance to human physical activity, especially for the elderly (Valenti et al., 2016). Previous studies (Bendall et al., 1989; Himann et al., 1988; Song and Geyer, 2018) reported a decline in walking speed over the aging process, which was associated with deteriorated quality of living in the elderly. The TS work as the major agonist for stabilizing the body while thrusting it forward (Bassey et al., 1988) during human walking. In addition, spring-like behavior of tendinous tissues (i.e., tendon and aponeurosis) of these muscles also contributes to the maintenance of walking speed by storing and releasing elastic energy (Franz and Thelen, 2016; Fukunaga et al., 2001; Hof et al., 2002). The matching of muscle fibers as force generators and tendinous tissues as elastic springs can influence walking performance (Stenroth et al., 2017). However, it is unknown whether enlargement of inter-individual variability of walking ability in the elderly is attributable to the changes in muscle strength or tendinous tissue, or both. In chapter 3, different behavior between medial

and lateral side of TS muscles and aponeuroses were found, and aponeuroses stiffness showed inhomogeneous and anisotropic during submaximal muscle contractions. Variations and direction-dependent differences (anisotropy) of mechanical properties of aponeuroses have been confirmed in chapter 2, but anisotropic features of aponeurosis dimensions and mechanical property have not been confirmed *in vivo*, especially in the elderly. Besides, the extent to which free tendon and aponeuroses mechanical properties contribute to walking performance in the elderly is not clear to date. In the present study, we sought to investigate the site- and direction-dependent variations of TS aponeuroses stiffness *in vivo* using SWE, and examined correlations between aponeuroses' stiffness and muscle strength and walking performance in the elderly.

4-2 Material and methods

4-2-1 Subjects

Seventy-nine healthy older adults (38 males and 41 females, age 73 ± 5 years, height 158.8 ± 9.0 cm, body mass 58.1 ± 9.5 kg; mean ± s.d.) participated in this study. All participants provided written-informed consent prior to the study. This study was approved by the Institutional Research Ethics Committee and was carried out in accordance with the Declaration of Helsinki.

4-2-2 Elastography measurements

The participants lay prone on an examination table with the feet off the edge of the

table, keeping fully relaxed in a neutral position (i.e., knee fully extended, ankle at 90° with neutral rotation). The right lower leg was chosen for the measurement. The SSI measurement of TS aponeuroses was performed using an Aixplorer ultrasound scanner (Version 6.4, Supersonic Imagine, Aix-en-Provence, France) with constant settings (pre-set, MSK; persistence, high; smoothing, 9). A linear transducer (L15-4, Aixplorer, Supersonic Imagine, Aix-en-Provence, France) was used to locate TS aponeuroses from the proximal (corresponding to the level of 30% of lower leg length) and distal (the distal end of gastrocnemii) sites. On the proximal site, superficial aponeurosis of MG and LG (MPS and LPS) and adjoining aponeuroses of gastrocnemii and soleus (MPA and LPA) were collected. On the distal site, adjoining aponeuroses of gastrocnemii and soleus (MDA and LDA) were collected (Fig. 4-1). The transducer was placed parallel (longitudinal) to the muscle's line of action to each site and at least 5s of shear wave data were collected for each scanning location. In addition, at the distal site of adjoining aponeuroses of medial gastrocnemius and soleus (MDA), the transducer was rotated (90°) from parallel to perpendicular (transverse) to the muscle's line of action to acquire a transverse view of the adjoining aponeuroses (MDA-t, Fig. 4-1). All ultrasound measurements were performed by an experienced examiner.

4-2-3 MRI measurement

T1-weighted gradient-echo transaxial cross-sectional images of the right lower leg were collected using a 1.5T magnetic resonance imaging (MRI) scanner (Signa EX-CITE, GE Medical Systems, USA). The scan parameters were as follows: echo time,

3.332 ms; repetition time, 7.816 ms; slice thickness, 4 mm; gap, 0mm; matrix size, 288 × 288; pixel bandwidth, 122Hz; field of view, 100 mm. Subjects were asked to lie on the magnet bore in a supine position with both legs fully extended and relaxed during the test. The MR images were exported to a computer, and an image at the 30% length of right lower leg level was selected to measure the cross-sectional area (CSA) of MG, LG and SOL with a software (ImageJ, National Institutes of Health, USA) (Saito et al., 2016). CSA of the TS was defined as the sum of CSA of MG, LG and SOL (Fig. 4-2).

4-2-4 Muscle strength and walking performance protocol

Isometric plantar flexion torque on the right leg was measured with a custom-made dynamometer (VTE, VINE, Japan) in a seated position, and the footplate was adjusted to make sure the knee was fully extended and the ankle at approximate neutral position. The thigh and ankle of each participant were secured with a broad strap and three practice trials were performed in accordance with careful instruction, and then at least two maximal voluntary contractions (MVC) of plantar flexion were conducted. In the case of ≥10% variation between the two MVC trials, he or she was asked to perform further trials interspersed with sufficient recovery until the two best values fell within the range of 10%. The best value of the two was then used for further analysis.

The walking trials were conducted on an over 10 m expanse of floor, on which two infrared velocimeters were set at 5 m distance to measure walking speed. Several meters were provided for participants to accelerate and decelerate before and after the 5 m test distance. The participants were asked to walk in normal (comfortable) and fast

(as fast as they could safely without running) speed twice, respectively.

4-2-5 Data processing

Plantar flexion torque was normalized to CSA of the TS for each subject. Shear wave data were exported from the machine, Young's modulus was analyzed with a customized code of Matlab (Mathworks, Natick, MA, USA) and the shear wave velocity was calculated from Young's modulus (equation 4-1).

$$\rho c^2 = \mu = E/2\,(1+\nu) \qquad (4\text{-}1)$$

Where μ is the shear modulus, ρ is the tissue density, c is the shear wave velocity, E is Young's modulus, ν is the Poisson's ratio, and the Poisson's ratio $\nu \approx 0.5$ for the connective tissue (Vergari et al., 2011). Strictly, SWV measurement of the fascial structures included the surface acoustic wave signals from the thin layer of the soft tissues, but in the present study we defined our measurements as SWV according to our preceding study (Shiotani et al., 2019).

4-2-6 Statistical analysis

All data are shown as means ± standard deviations (s.d.). An independent sample t-test was used to examine gender differences in the subject characteristics, that is, CSA of the TS, SWVs of TS aponeuroses, MVC of plantarflexion torque and walking speed.

Differences in SWVs of TS aponeuroses were examined with two-way analysis of variance (ANOVA) [sides (medial and lateral) × sites (superficial of gastrocnemii, proximal and distal sites of adjoining aponeuroses between gastrocnemii and soleus)].

A post-hoc test with Bonferroni corrections was performed where appropriate. Eta squared (η^2) or Partial eta squared (η_p^2) were calculated as an index of effect size (Levine and Hullett, 2002).

A paired t-test was used to test the differences in SWVs of aponeuroses between longitudinal and transverse directions, and *Cohen's d* was calculated as an index of effect size.

Pearson product-moment correlation was used to examine the relationships of SWVs between longitudinal and transverse directions, walking speed and CSAs of MG, LG and SOL, walking speed and plantar flexion torque, SWVs of TS aponeuroses and CSAs of MG, LG and SOL, normalized plantar flexion torque and SWVs of aponeuroses, walking speed and SWVs of aponeuroses. All the statistical analyses were performed using SPSS Statistics 24.0 (IBM SPSS Statistics, SPSS Inc., Chicago, USA) and Origin 9.0 (OriginLab, Northampton, MA, USA). The statistical significance level was set at $p < 0.05$.

4-3 Results

There were no significant differences in age, SWVs of adjoining aponeuroses and normal walking speed between elderly male and female individuals, while the males were taller, heavier, leaner, had larger TS and greater plantar flexion strength, and walked faster during fast walking than the females ($p < 0.05$, Table. 4-1).

Significant side × site interaction was observed ($p = 0.021$, $\eta_p^2 = 0.016$: small), and main effects of side ($p < 0.001$, $\eta_p^2 = 0.328$: large) and site ($p < 0.001$, $\eta_p^2 = 0.187$:

medium) were both significant for the SWVs of aponeuroses (Fig. 4-3). The values were significantly higher in the medial side (4.8 – 6.4 m/s) when compared to the lateral side (3.3 – 4.6 m/s, $p < 0.05$), and SWVs of adjoining aponeuroses were significantly higher than those of gastrocnemii superficial aponeuroses (Fig. 4-3).

Aponeurosis passive SWV was highly variable in the longitudinal (CV, 27.8%) and transverse directions (CV, 33.9%). SWV in the transverse direction (3.4 ± 1.2 m/s) was 1.9-fold lower than the longitudinal direction (6.4 ± 1.8 m/s, $p < 0.001$, $d = 1.73$: large, Fig. 4-4a). There was significant relationship between longitudinal SWV and transverse SWV in both males ($r = 0.36$, $p < 0.05$) and females ($r = 0.39$, $p < 0.05$, Fig. 4-4b).

There was no significant relationship between aponeurosis SWV and CSA of MG, LG and SOL either in males or females, or in any sites. CSA of LG in males and plantar flexion torque were significantly correlated to fast walking speed ($r = 0.33$ and 0.27, $p < 0.05$, Fig. 4-5b, d). SWVs of the adjoining aponeuroses between gastrocnemii and soleus were significantly correlated with normalized plantar flexion torque ($r = 0.26$-0.29, $p < 0.05$, Table. 4-2), while SWV of the adjoining aponeurosis between MG and soleus was significantly correlated with normal and fast walking speed ($r = 0.25$-0.26, $p < 0.05$), especially in females ($r = 0.33$-0.37, $p < 0.05$, Table. 4-2).

4-4 Discussion

The novel finding was that we confirmed the anisotropic mechanical properties of aponeurosis in the elderly *in vivo*, with considerable inter-individual variability of

aponeurosis stiffness. Nonetheless, the inter-individual variability of TS aponeuroses stiffness was associated with the inter-individual variability of muscle strength and walking performance in the elderly.

The TS muscle-tendon unit plays a considerable role in propelling forces to human locomotion, i.e. walking and running (Hof et al., 2002). Changes of muscle mass were shown to be related to muscle strength loss and functional physical performance in older adults (Hughes et al., 2001). As a serial connection part between muscle and tendon (Blitz and Eliot, 2007), the aponeurosis can act as a mechanical interface between muscle and tendon. The present study showed highly variable SWV of the TS aponeuroses, and the stiffness of adjoining aponeuroses between the gastrocnemii and soleus was found to be positively correlated with walking speed, especially in females. This finding strongly suggests that the aponeurosis elasticity can be a limiting factor to walking performance in the elderly. Together with the result of the relationship between muscle CSA and walking speed, it may be assumed that reduction in muscle size / strength (mostly in males) and softening of the aponeuroses (mostly in females) of the TS muscle-tendon unit lead to slowing of walking speed. No significant correlation between muscle size and aponeurosis SWV in any of the TS suggests no direct association of muscle atrophy and aponeurosis elasticity, but this notion needs further studies on larger samples including young populations.

Site-dependent differences were observed in the SWVs of adjoining aponeuroses between gastrocnemius and soleus and the superficial aponeurosis of gastrocnemius in the elderly, which is consistent with findings of mechanical properties of TS

aponeuroses taken from elderly cadavers (Shan et al., 2019). Blitz and Eliot (2007) reported that there is tendinous connection between the adjoining aponeuroses, which may be the reason of higher SWVs of the adjoining aponeuroses. A weak correlation between tendon thickness, depth and SWV was documented (DeWall et al., 2014), and Shan and others (2019) found the different thickness distribution of TS aponeuroses between different regions, this could also be a factor for the differences between superficial and deep aponeurosis. As the attachments of both gastrocnemius and soleus fibers, the adjoining aponeuroses showed higher SWV in the distal site than in the proximal site. The adjoining aponeuroses may undergo unique localized muscle-aponeurosis interactions from both gastrocnemii and soleus. In addition to the differences between proximal and distal sites, we found that the SWV of the medial side was higher than that of the lateral side of aponeuroses, which was consistent with a previous study (DeWall et al., 2014) on the Achilles tendon and aponeuroses. They explained that the differences may arise from greater intrinsic tissue stiffness or higher passive tension in the medial side. In the TS, MG was characterized by larger physiological CSA and higher fascicle angles with shorter fascicle lengths than LG (Kawakami et al., 1998). As an attachment base of muscle fibers, the aponeurosis might adapt to different medial-lateral fascicular architecture, leading to different elastic properties.

Consistent with our hypothesis, our results showed that the SWVs of aponeuroses was biaxially anisotropic *in vivo*, which was similar to previous results (Azizi et al., 2009; Shan et al., 2019). Higher SWVs of the adjoining MG and soleus aponeuroses in

the longitudinal direction, would allow them to act more efficiently as springs within the muscle-tendon unit, whilst higher compliance in the transverse direction, possibly accommodates the expansion of the contracting muscle belly. The aponeurosis stiffness in the transverse direction was not related to either walking performance or triceps surae CSA, unlike the aponeurosis stiffness in the longitudinal direction. It seems that the aponeurosis stiffness anisotropy is not muscle size- or function-dependent. However, changes in stiffness of longitudinal and transverse directions with contraction have been observed (Azizi and Roberts, 2009), and this can affect strength development and/or walking performance, which warrants further investigation.

4-5 Conclusions

The mechanical properties of TS aponeuroses demonstrate spatial variations and anisotropy *in vivo*, and the anisotropy is not muscle size dependent. The mechanical properties of adjoining aponeuroses were correlated with walking performance in the elderly together with the TS's force generating capacity.

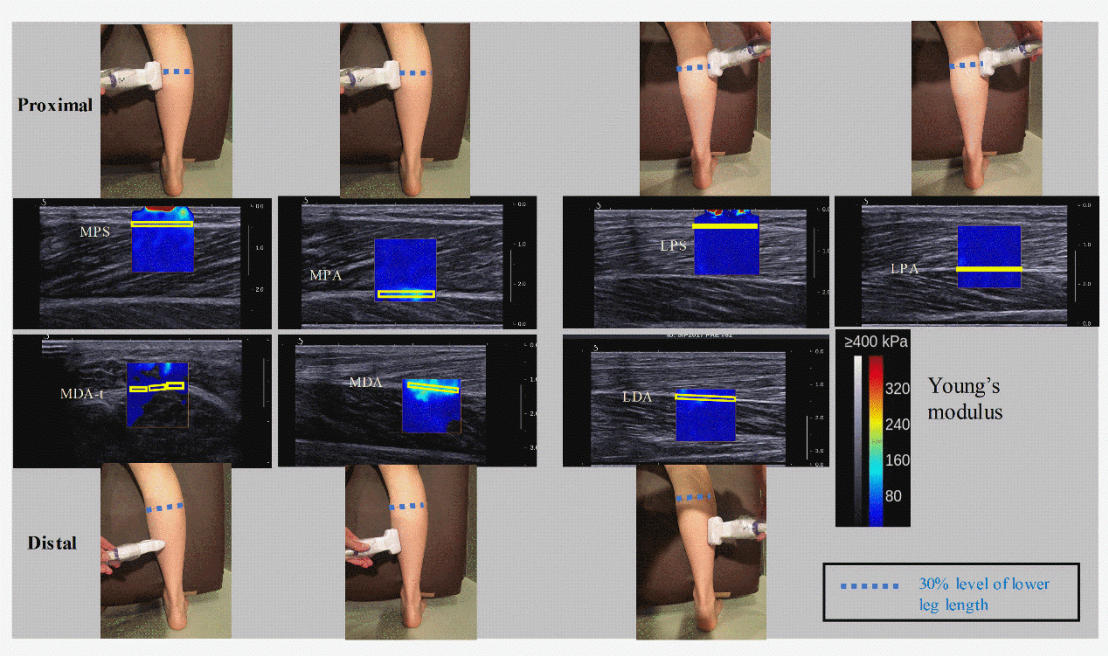

Fig. 4-1 Participants were asked to lie on the examination table with the feet off the edge keeping fully relaxed in a neutral position. Young's modulus data was measured in aponeuroses [superficial aponeuroses of MG and LG at proximal site (MPS and LPS), adjoining aponeuroses of gastrocnemius and soleus at proximal site (MPA and LPA), adjoining aponeuroses of gastrocnemius and soleus at distal site (MDA and LDA), and transverse direction of MDA (MDA-t)]. Regions of interest (ROIs) were determined as the yellow outlines.

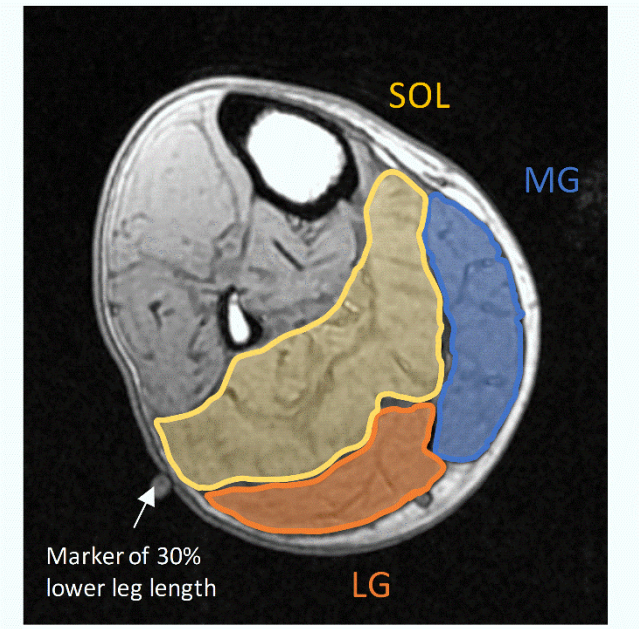

Fig. 4-2 MRI of the lower leg muscle cross-sectional area (CSA) at proximal 30% of lower leg length level showing the process of tracing of medial gastrocnemius (MG), lateral gastrocnemius (LG) and soleus (SOL) muscles.

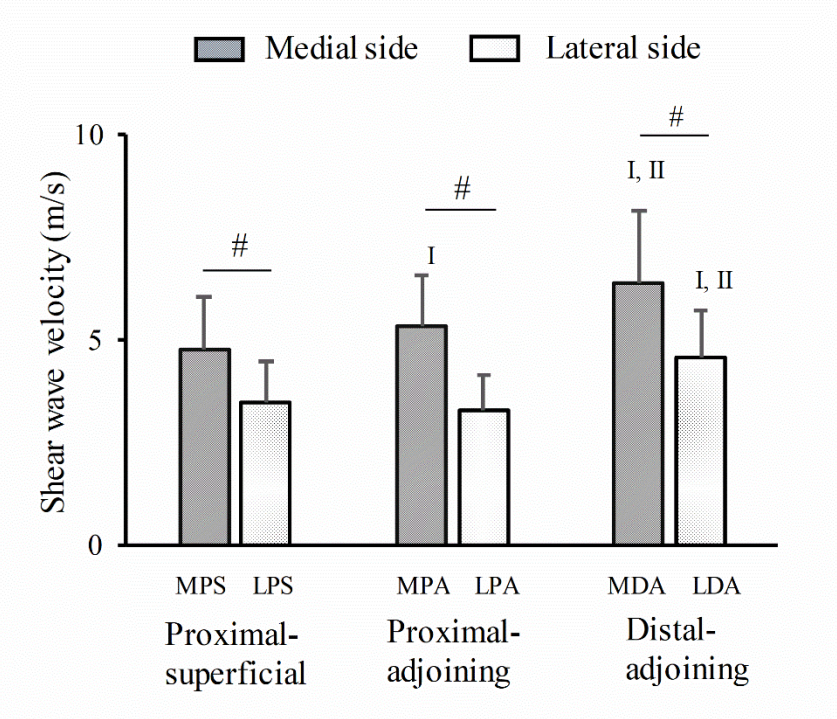

Fig. 4-3 Average (± s.d.) shear wave velocity of triceps surae aponeuroses at rest.

#, different between medial and lateral side; I, different from superficial aponeurosis ($p < 0.05$); II, different from proximal adjoining aponeurosis ($p < 0.05$).

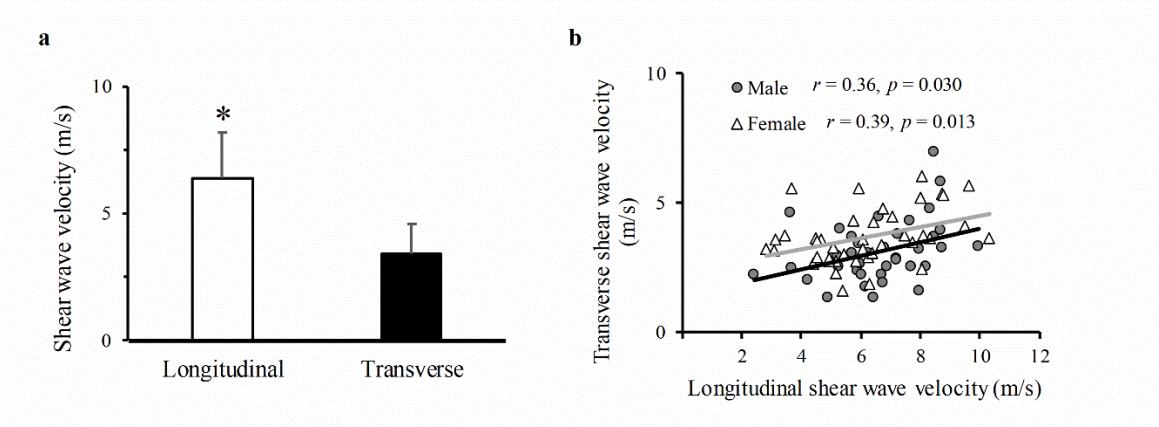

Fig. 4-4 Shear wave velocity of adjoining aponeuroses between MG and soleus along longitudinal and transverse directions (a), and the correlation of shear wave velocity between longitudinal and transverse directions (b). *, vs. transverse direction, $p < 0.01$.

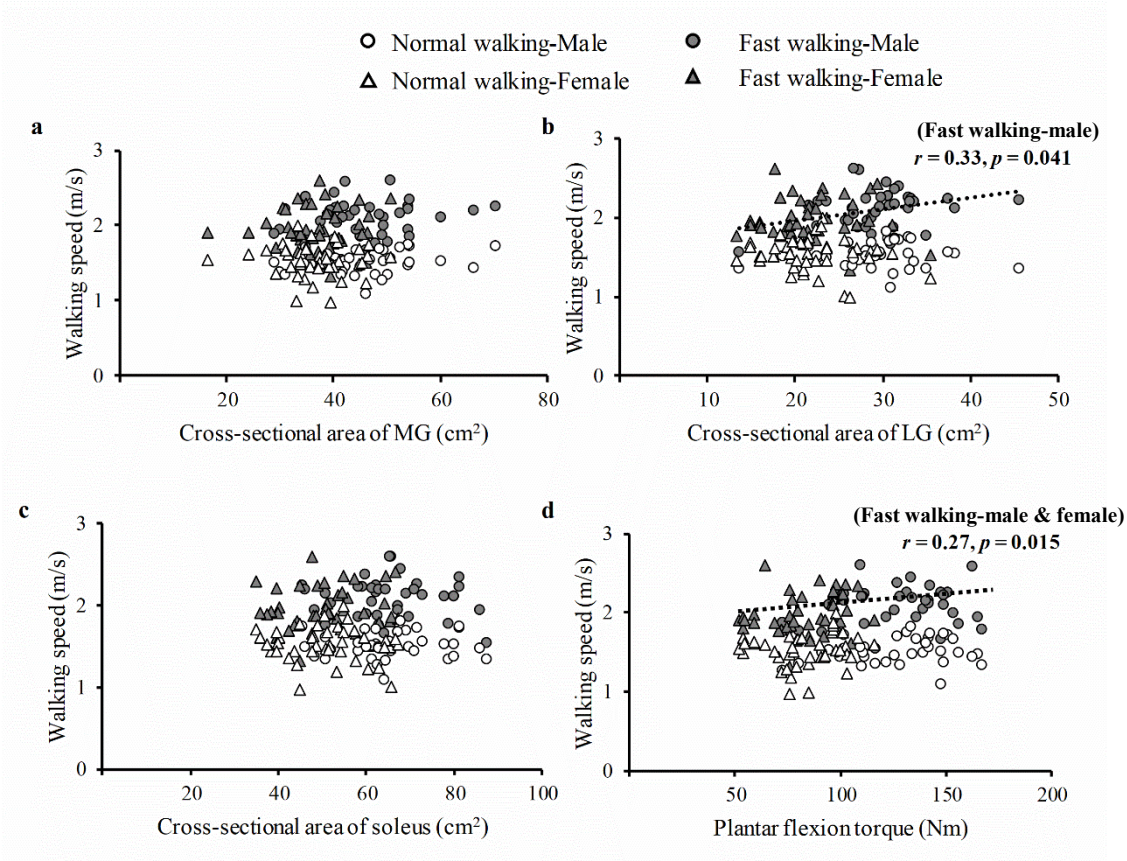

Fig. 4-5 The correlations between walking speed and cross-sectional area (CSA) of medial gastrocnemius (a), lateral gastrocnemius (b), soleus (c) and plantar flexion torque (d).

Table 4-1. Subject characteristics (mean ± s.d.)

	Male (n = 38)	Female (n = 41)	Total (n = 79)
Age (years)	72.8 ± 4.8	73.0 ± 6.0	72.9 ± 5.4
Height (cm)	166.4 ± 4.8	151.7 ± 5.4 [a]	158.8 ± 9.0
Body mass (kg)	64.3 ± 6.7	52.3 ± 8.0 [a]	58.1 ± 9.5
Body fat (%)	20.0 ± 6.1	29.6 ± 8.0 [a]	25.0 ± 8.6
Cross-sectional area of the triceps surae (cm^2)			
MG	45.8 ± 9.1	36.8 ± 6.5 [a]	41.1 ± 9.0
LG	29.2 ± 5.6	21.8 ± 4.8 [a]	25.4 ± 6.3
SOL	65.5 ± 10.8	51.0 ± 9.2 [a]	58.0 ± 12.3
Shear wave velocities of triceps surae aponeuroses (m/s)			
MPS	5.1 ± 1.3	4.5 ± 1.2 [a]	4.8 ± 1.3
MPA	5.6 ± 1.3	5.2 ± 1.1	5.4 ± 1.2
MDA	6.6 ± 1.6	6.2 ± 1.9	6.4 ± 1.8
MDA-t	3.1 ± 1.2	3.7 ± 1.1 [a]	3.4 ± 1.8
LPS	3.5 ± 0.9	3.5 ± 1.0	3.5 ± 1.0
LPA	3.4 ± 1.0	3.3 ± 0.7	3.3 ± 0.8
LDA	4.8 ± 1.2	4.4 ± 1.1	4.6 ± 1.1
MVC of Plantar flexion torque (Nm)	127.2 ± 24.2	83.6 ± 16.8 [a]	104.3 ± 30.0
Walking speed (m/s)			
Normal	1.52 ± 0.16	1.53 ± 0.21	1.52 ± 0.19
Fast	2.10 ± 0.24	1.97 ± 0.27 [a]	2.03 ± 0.26

Note: MG = medial gastrocnemius, LG = lateral gastrocnemius, SOL = soleus, MPS = medial proximal superficial aponeurosis, MPA = medial proximal adjoining aponeuroses, MDA = medial distal adjoining aponeuroses, MDA-t = medial distal adjoining aponeuroses in the transverse direction, LPS = lateral proximal superficial aponeurosis, LPA = lateral proximal adjoining aponeuroses, LDA = lateral distal adjoining aponeuroses, MVC = maximal voluntary contraction.

[a]: significantly different from male, $p < 0.05$

Table 4-2. Pearson correlation coefficients (*r*) for the relation of normalized plantar flexion torque, normal walking speed and fast walking speed with the shear wave velocities of triceps surae aponeuroses in older adults.

		Normalized plantar flexion torque (Nm/cm2)						Normal walking speed (m/s)						Fast walking speed (m/s)					
		Male (*n*=38)		Female (*n*=41)		Total (*n*=79)		Male (*n*=38)		Female (*n*=41)		Total (*n*=79)		Male (*n*=38)		Female (*n*=41)		Total (*n*=79)	
		r	*p*	*r*	*p*	*r*	*p*	*r*	*p*	*r*	*p*	*r*	*p*	*r*	*p*	*r*	*p*	*r*	*p*
Shear wave velocities of triceps surae aponeuroses (m/s)	MPS	0.31	0.066	-0.09	0.579	0.21	0.067	0.13	0.453	0.13	0.411	0.12	0.296	0.25	0.125	0.23	0.151	0.28*	0.012
	MPA	0.27	0.108	0.23	0.158	0.29*	0.009	-0.13	0.451	0.03	0.866	-0.05	0.691	-0.09	0.600	0.10	0.525	0.05	0.685
	MDA	0.18	0.299	0.02	0.91	0.14	0.23	0.14	0.404	0.33*	0.032	0.26*	0.022	0.02	0.894	0.37*	0.017	0.25*	0.028
	MDA-t	0.16	0.342	0.01	0.929	-0.02	0.879	0.22	0.192	0.09	0.561	0.15	0.203	0.32	0.055	0.27	0.093	0.21	0.059
	LPS	0.31	0.059	-0.15	0.35	0.07	0.54	0.27	0.105	-0.13	0.424	0.02	0.841	0.21	0.213	-0.02	0.906	0.07	0.528
	LPA	0.35*	0.031	0.05	0.768	0.26*	0.024	0.24	0.152	-0.12	0.47	0.05	0.638	0.19	0.255	-0.01	0.936	0.11	0.323
	LDA	0.30	0.085	0.1	0.557	0.26*	0.025	0.09	0.587	-0.1	0.543	-0.02	0.874	-0.08	0.643	-0.04	0.793	-0.018	0.88

Note: MPS = medial proximal superficial aponeurosis, MPA = medial proximal adjoining aponeuroses, MDA = medial distal adjoining aponeuroses, MDA-t = medial distal adjoining aponeuroses in the transverse direction, LPS = lateral proximal superficial aponeurosis, LPA = lateral proximal adjoining aponeuroses, LDA = lateral distal adjoining aponeuroses.

*: Correlation is significant at the 0.05 level (2-tailed).

CHAPTER 5 General discussion

5-1 Main findings of each chapter

The main findings of each chapter are as follows.

Chapter 2

1. In each region of the TS aponeuroses, except for the anterior regions of soleus, the thickness distributed inhomogeneously from the proximal to distal sites.
2. Site-dependent differences of stiffness within the gastrocnemius aponeurosis were shown. On the other hand, the Young's modulus did not show site-dependent differences in any regions, although there were tendencies in the values being smaller around terminations of both anterior and posterior aponeuroses of the gastrocnemius.
3. Compared to other regions of gastrocnemii and soleus, thinner thickness but higher Young's modulus in the anterior region of GL aponeurosis (longitudinal) and posterior region of SOL-lat aponeurosis (transverse) was found.
4. The medial-lateral differences in thickness and Young's modulus may reflect different muscle-aponeurosis interaction between synergist muscles (GM, GL and soleus), which affects the muscle force transmission to the tendon differently, and contributes differently to the limb movement control between medial and lateral side.
5. The stiffness and Young's modulus in the transverse direction were much smaller (<1%) than the values in the longitudinal direction, regardless of regions.

6. The energy dissipation along longitudinal and transverse directions was different, with the former being smaller than the latter.

Chapter 3

1. For the passive stiffness of the TS, the distal site (near to the muscle-tendon junction point) was stiffer than proximal site, whereas during submaximal contractions, muscles in the distal site became softer than the proximal site.
2. The stiffness in the longitudinal direction was higher than that in the transverse direction from at rest to submaximal contractions, especially the aponeuroses between LG and soleus.
3. Significant non-linear relationships between SWVs of TS muscles and aponeuroses and levels of contractions were found except for LG and SOL-lat muscle bellies and LPS at proximal site.

Chapter 4

1. The present study showed highly variable SWV of the TS aponeuroses, and the stiffness of adjoining aponeuroses between the gastrocnemii and soleus was found to be positively correlated with walking speed, especially in females.
2. Site-dependent differences were observed in the SWVs of adjoining aponeuroses between gastrocnemius and soleus and the superficial aponeurosis of gastrocnemius in the elderly.
3. The results showed that the SWVs of aponeuroses was biaxially anisotropic *in vivo*,

and SWVs of the adjoining MG and soleus aponeuroses in the longitudinal direction were higher than that of the adjoining LG and soleus aponeuroses.

5-2 Generalization of the findings: site- and direction-dependence

Within the human muscle-tendon unit, a large part of the tendinous tissues is aponeuroses which located on the surface regions of muscle. And the aponeurosis's shape is much more complicated than the free tendon. This thesis proved the inhomogeneous and anisotropic features in the morphology and mechanical properties of the human TS aponeuroses by both cadaveric and *in vivo* studies.

In chapter 2, thinner thickness and higher Young's modulus was found in the adjoining aponeuroses (anterior region of LG and posterior region of soleus), which is different with the superficial (posterior) region of LG. However, such findings were not found in any other region of MG and SOL-med, which indicate the medial-lateral differences of aponeurosis morphology and mechanical property may affect the muscle-aponeurosis interaction between synergist muscles. According to the findings of chapter 3, the superficial region of aponeuroses in the lateral side showed significant increase of stiffness while the adjoining aponeuroses stiffness kept constant from 20% to 60% MVC level. It indicates that the superficial regions of gastrocnemii aponeuroses are more compliant to modulate the shape changes while the adjoining aponeuroses are stiffer and can transmit the forces from muscle fibers to the tendon more efficiently during contraction. Besides to the site-dependent differences among different regions of gastrocnemii and soleus, *in vivo* studies found the site-dependent differences from

proximal to distal site of the adjoining aponeuroses SWVs for both younger and older adults. Since the thickness from proximal to distal site is found to get thicker in cadaveric study (Shan et al., 2019), this thickness distribution could be a factor for the differences of SWV *in vivo* (DeWall et al., 2014).

Cadaveric study found no site-dependent differences (proximal to distal) in Young's modulus of the aponeuroses, but the SWV showed significant site-dependent differences for the adjoining aponeuroses. Previous study found that the SWV is correlated with the tissue elastic modulus (Royer et al., 2011), which suggest the difference of inherent aponeuroses elasticity, while the inter-individual variabilities of the cadaver aponeuroses were possibly too large. Muramatsu et al. (2001) reported that there was no significant difference in strain between the proximal and distal aponeuroses during submaximal muscle contractions (10% to 90% of MVC). On the other hand, another study reported that the elongation of the aponeurosis is heterogeneously distributed along its length (Zuurbier et al., 1994), which is consistent with the results in chapter 3: it showed significant differences between proximal and distal site during 20% to 60% of MVC contractions. Since the aponeurosis bears biaxial loading during muscle contraction, even though the elongations of aponeuroses along the longitudinal direction were similar, the deformation of aponeuroses shape may be different in the other direction between proximal and distal sites.

The calf strain, especially the medial gastrocnemius strain occurs most commonly among both athletes and non-athletes (Hsu et al., 2018). Previous study reported that medial gastrocnemius is injured more commonly than lateral gastrocnemius, the reason

is proved to be higher muscle activity in the medial side (Cibulka et al., 2017). This is related to the medial-lateral differences of aponeurosis mechanical properties of this thesis. As the strain happens when the muscle belly is stretched maximally, stiffer aponeurosis in the medial side make the medial gastrocnemius not more compliant than the lateral side, which leads to MG strain happen more frequently. This notion should be clarified in the further clinic-related studies.

Regarding to the direction-dependent differences, the human aponeuroses have been further proved to be anisotropic by this thesis. The findings of chapter 2 are consistent with the features of animal aponeurosis (Azizi and Roberts, 2009), and the *in vivo* findings of chapter 3 and 4 are consistent with the results of human fascia (Otsuka et al., 2019) and aponeurosis (Iwanuma et al., 2011). The aponeuroses are more compliant in the transverse direction to accommodate the expansion of the contracting muscle belly, while higher Young's modulus and/or SWV in the longitudinal direction may help to act as a mechanical spring within the muscle-tendon unit. This anisotropy feature allows aponeurosis bear biaxial loading comparing to uniaxial loading of the free tendon during contraction. As the aponeurosis helps to transmit the forces from muscle fibers to the free tendon, this transmission could be affected by anisotropy of aponeurosis during contraction.

5-3 Applicability of the findings

5-3-1 Implications for muscle-aponeurosis interaction during contraction

A previous study stated that the elastic mechanism (e.g. energy conservation vs.

power amplification) of biological springy tissues (such as tendinous tissue) is important for the effective function of muscle-tendon complex to enhance movement (Roberts and Azizi, 2011), since such a mechanism will allow the locomotor system to operate by not only the muscle motors but by the interactions between muscle motors and elastic tendon springs. A previous study (Azizi and Roberts, 2009) showed the variation in the mechanical properties of aponeurosis with biaxial loading during active force production, and another *in vivo* study (Iwanuma et al., 2011) found no significant changes of aponeurosis strains in the longitudinal direction between 30% and 60% MVC, while the free tendon was deformed. And the results of chapter 3 showed that the aponeuroses stiffness showed no significant increase from 20% to 60% MVC, which was consistent with previous study. In addition, for the differences between longitudinal and transverse direction, our cadaveric study showed the Young's modulus in the longitudinal direction was about 100 times higher than in the transverse direction. However, *in vivo* study of Iwanuma et al. (2011) showed much lower differences (10 times) between longitudinal and transverse strain, as well as the results of SWV between longitudinal and transverse direction in chapter 4. Since the specimens measured in the cadaveric study were in isolated condition, which was different with *in vivo* conditions. Therefore, the differences between findings of cadaveric study and *in vivo* studies may be due to the influence from contracting muscle fibers to attached aponeurosis. As described earlier, the elasticity of the aponeurosis, and hence the use of elastic energy thereof, may depend on the muscle contraction levels. The mechanical properties of the aponeurosis could allow for the muscle belly deformation at low force

levels, while limiting muscle fibers' further deviation longitudinally at higher force levels so that the free tendon can behave like a spring during movements. Future work on *in vivo* study should consider how the inter-muscle and inter-direction differences of TS aponeuroses elasticity depend on muscle contraction levels.

5-3-2 Implications for motor performance

Human motor performance is quite vital aspect of diverse daily activities, such as walking, running and jumping. Within the TS muscle-tendon unit, both TS and the Achilles tendon were proved to contribute to the walking performance (Francis et al., 2013; Franz et al., 2015; Franz and Thelen, 2016; Fukunaga et al., 2001). The studies showed that the TS maintains a near-constant length to generate minimal power with minimal energetic cost during walking, while the Achilles tendon works to improve the energy efficiency by performing a stretch-recoil cycle to generate elastic strain energy during walking (Fukunaga et al., 2001; Lichtwark et al., 2007). However, the contribution of aponeurosis to walking performance still remains obscure. In chapter 4 of this thesis, we found the significant correlations between the stiffness of adjoining aponeuroses and walking performance in the elderly (Table 4-2), which suggests that the aponeuroses stiffness can be a limiting factor to walking performance in the elderly. Stenroth (2016) reported that the TS in the elderly operated within a narrower range of muscle fascicle length changes while a greater proportion of tendinous tissue length changed during preferred walking speed, the elderly preferentially minimize energy cost of TS during walking, which indicates that tendinous tissue elasticity contributes

more to the walking speed in the elderly. Therefore, for the serial elastic component, both tendon and aponeurosis connect to muscle fibers, providing spring-like actions that can influence muscle contraction and motor function, and their key parameter such as stiffness could be modulated during movement. Previous study reported that the tendon stiffness significantly increased after long-term exercise (Buchanan and Marsh, 2001), which indicate that the stiffness could be modulated to adapt to the effective operation of muscle-tendon unit. This variations in tendon stiffness also appears to occur in the aponeurosis, which serially connected to the free tendon and provide a wide attachment surface for muscle fibers. Some previous studies reported that the stiffness of the aponeurosis behaves differently between active contraction and passive loading condition (Azizi and Roberts, 2009; Lieber et al., 2000; Zuurbier et al., 1994) (Fig. 5-1). As the findings of this thesis, the anisotropic mechanical property of aponeurosis bears biaxial loading during contraction, and the softer feature in the transverse direction may influence the stiffness in the longitudinal direction. However, the modulation of aponeurosis mechanical property in the longitudinal and transverse directions during movement, and the extent to which the mechanical properties of tendon and aponeurosis contribute to motor performance need to be further investigated.

5-4 Limitations

The limitations of our study should be noted. Firstly, all the specimens were dissected from formalin-fixed cadavers in chapter 2. Previous studies (Marieswaran et al., 2018; Zhang et al., 2016a) found that formalin fixation decreased stiffness and

Young's modulus of human femur-ACL-tibial complex significantly compared to the fresh tissues (as for stiffness, fresh: 166.45 ± 36.03 N/mm, formalin-fixed: 71.68 ± 5.05 N/mm; as for Young's modulus, fresh: 71.5 ± 18.67 N/mm, formalin-fixed: 31.77 ± 2.52 N/mm) and formalin-fixed bones showed a significantly lower Young's modulus (-12%) compared to the fresh tissues. On the other hand, the cadavers in the current study were donated from elderly individuals. An existing study (Lewis and Shaw, 1997) proved that the donor age can affect mechanical properties of human Achilles tendon, and many studies (Magnusson et al., 2008; Narici et al., 2005; Onambele et al., 2006) have found higher tendinous compliance in elderly individuals. Therefore, the conclusion of the present study may be limited to the characteristics of the muscle-tendon unit in the elderly. Anisotropic mechanical behavior of the soft tissues may also be affected by fixation although there has been no such report to date. Therefore, we conducted additional data collection (Shan et al., 2019) to examine the effect of formalin on the mechanical properties of aponeuroses by using urea that has been reported to neutralize formaldehyde within cadaveric tissues without affecting cadaveric and histological quality (Ninh et al., 2018). The results (Fig. 5-3) showed that the Young's modulus was slightly but significantly increased (pre: 143.1 ± 77.3 MPa, post: 157.3 ± 79.8 MPa) only in the longitudinal direction after the urea treatment, while there was no significant change for the transverse direction or longitudinal/transverse ratio (Table 5-1). This suggests that the anisotropic mechanical behavior would already have existed before formalin fixation. Additionally, we used 50% alcohol (an agent that dehydrates tissue) instead of normal saline solution to keep the specimens, and to check

whether this dehydrating agent potentially impacts our results or not, an additional experiment was carried out. The results (Fig.5-2 and 5-3) showed that the moisture content of TS aponeuroses was not changed significantly, and there were no significant changes in the Young's modulus either in the longitudinal or transverse direction after 50% alcohol treatment for 5 hours. Although we tested each specimen twice in two directions with a randomized counterbalanced order, it may still have influenced the properties between longitudinal and transverse directions. Our additional experiments with one specimen for only one direction showed similar results (Fig. 5-3), but this can be taken into consideration for the future studies. The present results will open the possibility of understanding how aponeuroses mechanical properties are related with the muscle-aponeurosis-tendon behavior and/or interactions between the gastrocnemii and soleus during contractions *in vivo*.

Some limitations also need to be considered for *in vivo* studies using SWE. Although SWE has been proved to be a non-invasive and reproducible methods to characterize tissue stiffness, the shear wave imaging technique used in the present study sometimes showed artifact in the deep site of muscle and/or aponeuroses when the transducer was placed in the transverse direction. Besides, SWE has been proved to be a valid tool for measuring shear modulus of pennate muscle along the muscle's fascicle direction (Miyamoto et al., 2015), which may account for low values of ICC for aponeurosis stiffness in the transverse direction during submaximal contractions in the current work. In chapter 3 and 4, the SWV of TS muscles and gastrocnemius were measured not only at rest but also during submaximal muscle contractions. A previous

study documented that the SWE can be useful for interring muscle stiffness across a wide range of contraction intensity (Yoshitake et al., 2014), however, we observed the saturations of aponeurosis tissue appeared during higher intensities (>75% MVC), there is still limitations for SWE to measure the tendinous tissues during higher intensities of muscle contractions. Another limitation of the study in chapter 3 is that we did not evaluate the myoelectric activity to ensure the muscle activities during different level of contractions. Since we applied the probe in both proximal and distal sites of the TS, appropriate sites for EMG electrodes cannot be located, which should be considered in further studies. Finally, elderly cadavers were used to measure the intrinsic morphological and mechanical properties of aponeurosis, and older adults were recruited for the investigation of correlation between aponeurosis stiffness at rest and walking performance, however, the aponeurosis stiffness changes during muscle contractions were studied only from younger males. Since the subjects should be asked to perform many trials of muscle contractions, it's hard to apply for the elderly adults, so we only measured the aponeurosis stiffness at rest for the elderly in chapter 4. This may be limitation since age-related changes may affect the mechanical properties of muscle-tendon unit (Danos et al., 2016; Svensson et al., 2016).

5-5 Conclusion of the thesis

In vivo as well as ex situ evidence showed the human aponeuroses with inhomogeneous and anisotropic morphological and mechanical properties, suggesting inherent material design of the aponeurosis that matches three-dimensional contractile

behavior of muscle fibers. The muscle-aponeurosis interaction varies depend on different directions and muscle contraction levels, which is essential for human motor performance.

5-6 Future directions

In the future it should be clarified that aging- and exercise-related morphological and mechanical properties of the TS muscle-tendon unit and investigate muscle-aponeurosis-tendon interaction during different type of muscle contractions and different during different motor performance. Combing with kinematics of joint movement and muscle activities, using musculoskeletal modeling to improve understanding the mechanism of muscle-tendon interaction during human movement.

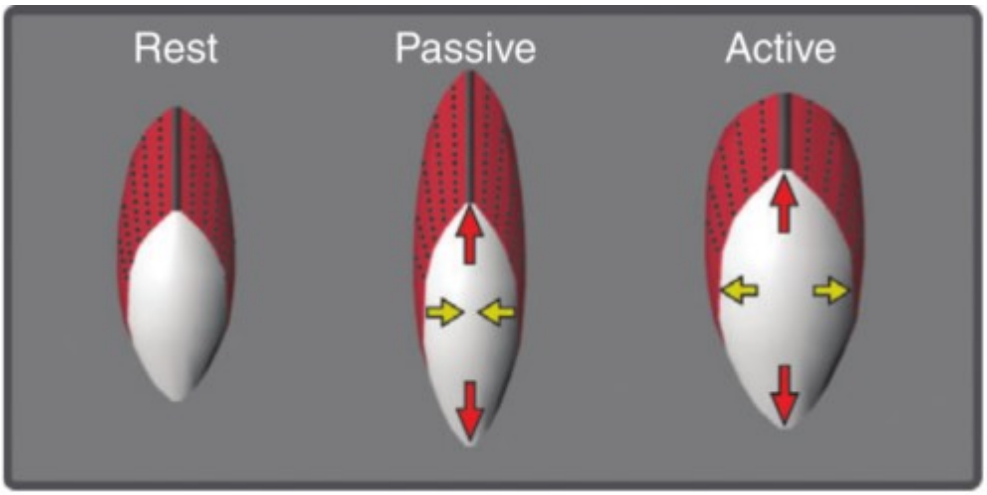

Fig. 5-1 A schematic of aponeurosis behavior during active and passive force production. (Robert and Azizi, 2011)

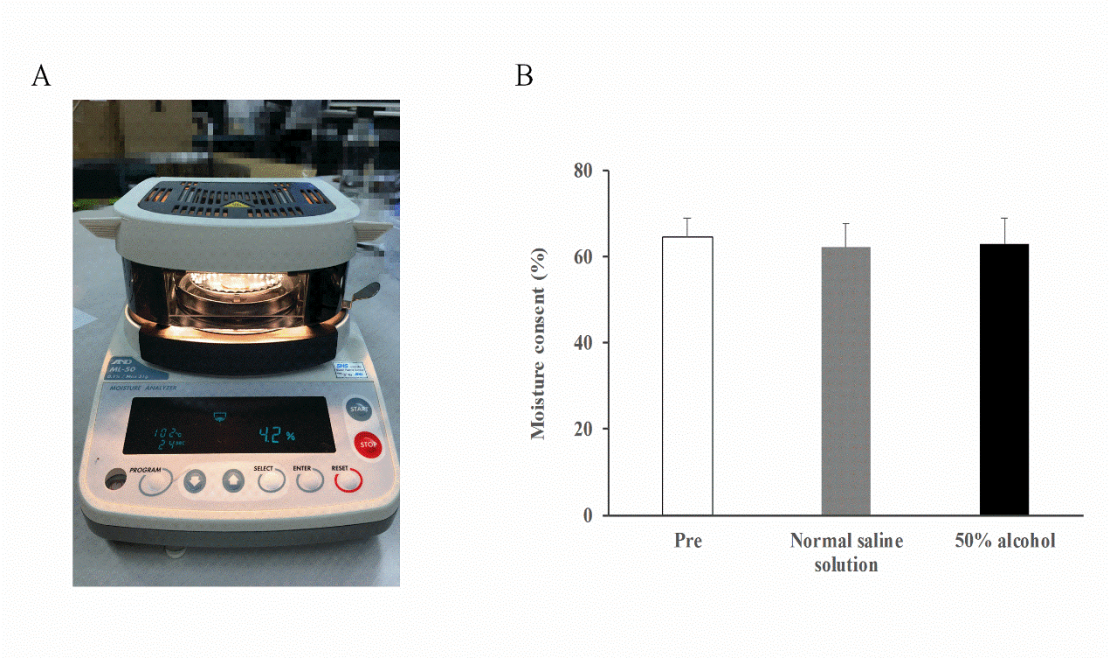

Fig. 5-2 Moisture content test on aponeuroses samples from a cadaver. (A) A moisture analyzer with a testing specimen. (B) Average (mean ± s.d.) moisture content of triceps surae aponeuroses before placing any solution (Pre), after normal saline solution for 5hr and after 50% alcohol solution for 5hr.

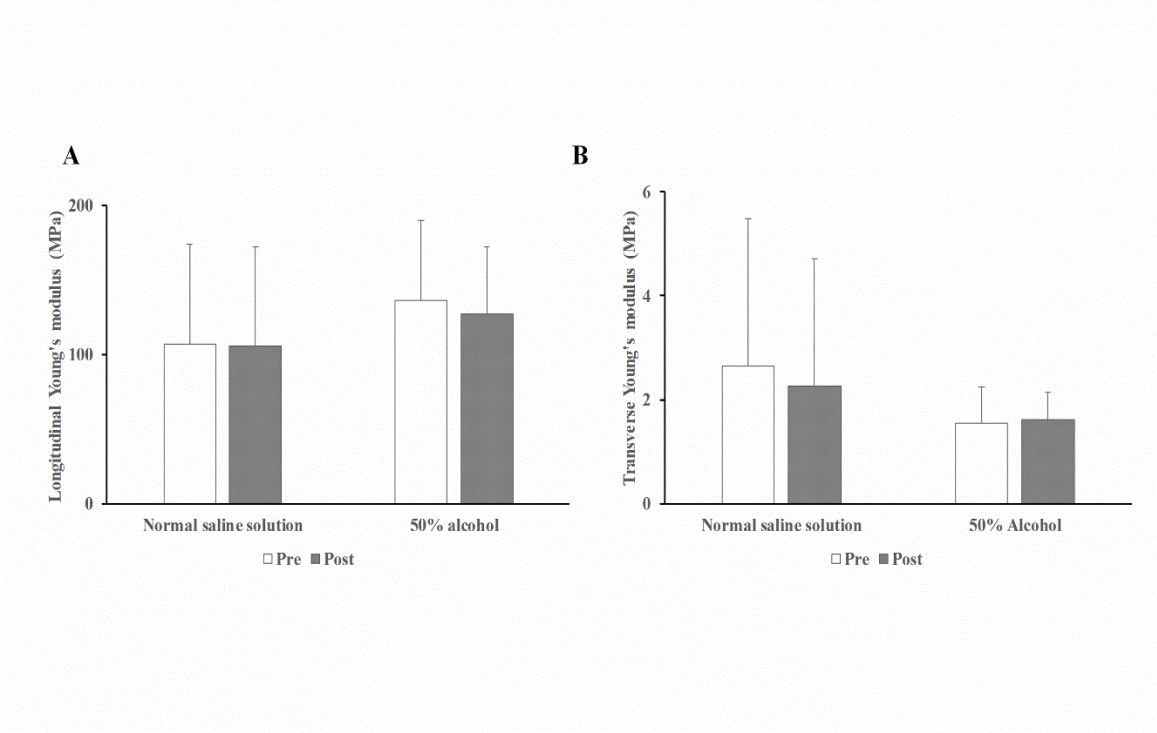

Fig. 5-3 Mechanical properties of triceps surae aponeuroses with different solution method. Average (mean ± s.d.) Young's modulus of triceps surae aponeuroses in the longitudinal (A) and transverse (B) directions before (Pre) and after (Post) normal saline, 50% alcohol and 18% urea treatment. *: denotes different from pre, $p < 0.05$.

Table 5-1. Longitudinal/transverse ratio of Young's modulus before and after 18% urea treatment

	Pre	Post
Urea	111.7 ± 54.1	113.2 ± 65.4

References

Arampatzis, A., Karamanidis, K., Morey-Klapsing, G., De Monte, G., Stafilidis, S., 2007. Mechanical properties of the triceps surae tendon and aponeurosis in relation to intensity of sport activity. J Biomech 40, 1946-1952.

Arampatzis, A., Karamanidis, K., Stafilidis, S., Morey-Klapsing, G., DeMonte, G., Bruggemann, G.P., 2006. Effect of different ankle- and knee-joint positions on gastrocnemius medialis fascicle length and EMG activity during isometric plantar flexion. J Biomech 39, 1891-1902.

Arellano, C.J., Gidmark, N.J., Konow, N., Azizi, E., Roberts, T.J., 2016. Determinants of aponeurosis shape change during muscle contraction. J Biomech 49, 1812-1817.

Arnold, E.M., Hamner, S.R., Seth, A., Millard, M., Delp, S.L., 2013. How muscle fiber lengths and velocities affect muscle force generation as humans walk and run at different speeds. The Journal of experimental biology 216, 2150-2160.

Ateş, F., Andrade, R.J., Freitas, S.R., Hug, F., Lacourpaille, L., Gross, R., Yucesoy, C.A., Nordez, A., 2018. Passive stiffness of monoarticular lower leg muscles is influenced by knee joint angle. Eur J Appl Physiol.

Ateş, F., Hug, F., Bouillard, K., Jubeau, M., Frappart, T., Couade, M., Bercoff, J., Nordez, A., 2015. Muscle shear elastic modulus is linearly related to muscle torque over the entire range of isometric contraction intensity. J Electromyogr Kinesiol 25, 703-708.

Azizi, E., Halenda, G.M., Roberts, T.J., 2009. Mechanical properties of the gastrocnemius aponeurosis in wild turkeys. Integr Comp Biol 49, 51-58.

Azizi, E., Roberts, T.J., 2009. Biaxial strain and variable stiffness in aponeuroses. J

Physiol 587, 4309-4318.

Backer, H.C., Wong, T.T., Vosseller, J.T., 2019. MRI Assessment of Degeneration of the Tendon in Achilles Tendon Ruptures. Foot Ankle Int, 1071100719845016.

Bassey, E.J., Bendall, M.J., Pearson, M., 1988. Muscle strength in the triceps surae and objectively measured customary walking activity in men and women over 65 years of age. Clinical Science 74, 85-89.

Baumer, T.G., Davis, L., Dischler, J., Siegal, D.S., van Holsbeeck, M., Moutzouros, V., Bey, M.J., 2017. Shear wave elastography of the supraspinatus muscle and tendon: Repeatability and preliminary findings. J Biomech 53, 201-204.

Bendall, M.J., Bassey, E.J., Pearson, M.B., 1989. Factors affecting walking speed of elderly people. Age Ageing 18, 327-332.

Benjamin, M., Kaiser, E., Milz, S., 2008. Structure-function relationships in tendons: a review. J Anat 212, 211-228.

Bercoff, J., Tanter, M., Fink, M., 2004. Supersonic shear imaging: a new technique for soft tissue elasticity mapping. IEEE Trans Ultrason Ferroelectr Freq Control 51, 396-409.

Blazevich, A.J., Gill, N.D., Zhou, S., 2006. Intra- and intermuscular variation in human quadriceps femoris architecture assessed in vivo. J Anat 209, 289-310.

Blitz, N.M., Eliot, D.J., 2007. Anatomical aspects of the gastrocnemius aponeurosis and its insertion: a cadaveric study. J Foot Ankle Surg 46, 101-108.

Blitz, N.M., Eliot, D.J., 2008. Anatomical aspects of the gastrocnemius aponeurosis and its muscular bound portion: a cadaveric study-part II. J Foot Ankle Surg 47, 533-

540.

Bojsen-Moller, J., Hansen, P., Aagaard, P., Svantesson, U., Kjaer, M., Magnusson, S.P., 2004a. Differential displacement of the human soleus and medial gastrocnemius aponeuroses during isometric plantar flexor contractions in vivo. J Appl Physiol 97, 1908-1914.

Bojsen-Moller, J., Hansen, P., Aagaard, P., Svantesson, U., Kjaer, M., Magnusson, S.P., 2004b. Differential displacement of the human soleus and medial gastrocnemius aponeuroses during isometric plantar flexor contractions in vivo. J Appl Physiol (1985) 97, 1908-1914.

Bojsen-Møller, J., Magnusson, S.P., 2019. Mechanical properties, physiological behavior and function of aponeurosis and tendon. J Appl Physiol 4.

Bouillard, K., Hug, F., Guevel, A., Nordez, A., 2012. Shear elastic modulus can be used to estimate an index of individual muscle force during a submaximal isometric fatiguing contraction. J Appl Physiol (1985) 113, 1353-1361.

Bouillard, K., Nordez, A., Hug, F.o., 2011. Estimation of individual muscle force using elastography. PLoS One 6, e29261.

Brandenburg, J.E., Eby, S.F., Song, P., Zhao, H., Brault, J.S., Chen, S., An, K.N., 2014. Ultrasound elastography: the new frontier in direct measurement of muscle stiffness. Arch Phys Med Rehabil 95, 2207-2219.

Branthwaite, H., Pandyan, A., Chockalingam, N., 2012. Function of the triceps surae muscle group in low and high arched feet: an exploratory study. Foot (Edinb) 22, 56-59.

Buchanan, C.I., Marsh, R.L., 2001. Effects of long-term exercise on the biomechanical properties of the Achilles tendon of guinea fowl. J Appl Physiol 90, 164-171.

Chino, K., Oda, T., Kurihara, T., Nagayoshi, T., Yoshikawa, K., Kanehisa, H., Fukunaga, T., Fukashiro, S., Kawakami, Y., 2008. In vivo fascicle behavior of synergistic muscles in concentric and eccentric plantar flexions in humans. J Electromyogr Kinesiol 18, 79-88.

Chow, R.S., Medri, M.K., Martin, D.C., Leekam, R.N., Agur, A.M., McKee, N.H., 2000. Sonographic studies of human soleus and gastrocnemius muscle architecture: gender variability. Eur J Appl Physiol 82, 236-244.

Cibulka M, Wenthe A, Boyle Z, Callier D, Schwerdt A, Jarman D, Strube MJ. Variation in medial and lateral gastrocnemius muscle activity with foot with foot position. Int J Sports Phys Ther. 2017 Apr;12(2):233-241.

Cortes, D.H., Suydam, S.M., Silbernagel, K.G., Buchanan, T.S., Elliott, D.M., 2015. Continuous Shear Wave Elastography: A New Method to Measure Viscoelastic Properties of Tendons in Vivo. Ultrasound Med Biol 41, 1518-1529.

Danos, N., Holt, N.C., Sawicki, G.S., Azizi, E., 2016. Modeling age-related changes in muscle-tendon dynamics during cyclical contractions in the rat gastrocnemius. J Appl Physiol (1985) 121, 1004-1012.

David Hsu, Ke-Vin Chang, 2018. Gastrocnemius Strain. StatPearls Publishing LLC.

DeWall, R.J., Slane, L.C., Lee, K.S., Thelen, D.G., 2014. Spatial variations in Achilles tendon shear wave speed. J Biomech 47, 2685-2692.

Eby, S.F., Song, P., Chen, S., Chen, Q., Greenleaf, J.F., An, K.N., 2013. Validation of

shear wave elastography in skeletal muscle. J Biomech 46, 2381-2387.

Ema, R., Wakahara, T., Miyamoto, N., Kanehisa, H., Kawakami, Y., 2013. Inhomogeneous architectural changes of the quadriceps femoris induced by resistance training. Eur J Appl Physiol 113, 2691-2703.

Ettema, G.J.C., Huijing, P.A., 1994. Skeletal muscle stiffness in static and dynamic contractions. J Biomech 27, 1361-1368.

Farris, D.J., Trewartha, G., McGuigan, M.P., 2011. Could intra-tendinous hyperthermia during running explain chronic injury of the human Achilles tendon? J Biomech 44, 822-826.

Faul, F., Erdfelder, E., Lang, A.-G., Buchner, A., 2007. G*Power 3: A flexible statistical power analysis program for the social, behavioral, and biomedical sciences. Behav Res Methods 39, 175-191.

Fiatarone, M.A., Marks, E.C., Ryan, N.D., Meredith, C.N., Lipsitz, L.A., Evans, W.J., 1990. High-intensity strength training in nonagenarians: effects on skeletal muscle. The Journal of the American Medical Association 263, 3029-3034.

Finni, T., 2006. Structural and functional features of human muscle-tendon unit. Scand J Med Sci Sports 16, 147-158.

Finni, T., Hodgson, J.A., Lai, A.M., Edgerton, V.R., Sinha, S., 2003. Nonuniform strain of human soleus aponeurosis-tendon complex during submaximal voluntary contractions in vivo. J Appl Physiol 95, 829-837.

Finni, T., Peltonen, J., Stenroth, L., Cronin, N.J., 2012. Viewpoint: On the hysteresis in the human Achilles tendon. J Appl Physiol 114, 515-517.

Foster-Burns, S.B., 1999. Sarcopenia and decreased muscle strength in the elderly woman: resistance training as a safe and effective intervention. J Women Aging 11, 75-85.

Foure, A., Cornu, C., Nordez, A., 2012. Is tendon stiffness correlated to the dissipation coefficient? Physiol Meas 33, N1-N9.

Foure, A., Nordez, A., Cornu, C., 2010. Plyometric training effects on Achilles tendon stiffness and dissipative properties. J Appl Physiol (1985) 109, 849-854.

Francis, C.A., Lenz, A.L., Lenhart, R.L., Thelen, D.G., 2013. The modulation of forward propulsion, vertical support, and center of pressure by the plantarflexors during human walking. Gait Posture 38, 993-997.

Franz, J.R., Slane, L.C., Rasske, K., Thelen, D.G., 2015. Non-uniform in vivo deformations of the human Achilles tendon during walking. Gait Posture 41, 192-197.

Franz, J.R., Thelen, D.G., 2016. Imaging and simulation of Achilles tendon dynamics: Implications for walking performance in the elderly. J Biomech 49, 1403-1410.

Friederich, J.A., Brand, R.A., 1990. Muscle fiber architecture in the human lower limb. J Biomech 23.

Fukunaga, T., Ichinose, Y., Ito, M., Kawakami, Y., Fukashiro, S., 1997a. Determination of fascicle length and pennation in a contracting human muscle in vivo. J Appl Physiol 82, 354-358.

Fukunaga, T., Kawakami, Y., Kubo, K., Kanehisa, H., 2002. Muscle and tendon interaction during human movements. Exerc Sport Sci Rev 30, 106-110.

Fukunaga, T., Kawakami, Y., Kuno, S., Funato, K., Fukashiro, S., 1997b. Muscle architecture and function in humans. J Biomech 30, 457-463.

Fukunaga, T., Kubo, K., Kawakami, Y., Fukashiro, S., Kanehisa, H., Maganaris, C.N., 2001. In vivo behaviour of human muscle tendon during walking. Proc Biol Sci 268, 229-233.

Giordano, S.B., Segal, R.L., 2006. Leg muscles differ in spatial activation patterns with differing levels of voluntary plantarflexion activity in humans. Cells Tissues Organs 184, 42-51.

Gray, H., Williams, P.L., Bannister, L.H., 1995. Gray's Anatomy. 38th ed. Churchill Livingstone.

Gras, L.L., Mitton, D., Viot, P., Laporte, S., 2012. Hyper-elastic properties of the human sternocleidomastoideus muscle in tension. J Mech Behav Biomed Mater 15, 131-140.

Haims, A.H., Schweitzer, M.E., Patel, R.S., Hecht, P., Wapner, K.L., 2000. MR imaging of the Achilles tendon: overlap of findings in symptomatic and asymptomatic individuals. International Skeletal Society 29, 640-645.

Hanna, J.B., Schmitt, D., 2011. Comparative triceps surae morphology in primates: a review. Anat Res Int 2011, 191509.

Hayashi, S., Homma, H., Naito, M., Oda, J., Nishiyama, T., Kawamoto, A., Kawata, S., Sato, N., Fukuhara, T., Taguchi, H., Mashiko, K., Azuhata, T., Ito, M., Kawai, K., Suzuki, T., Nishizawa, Y., Araki, J., Matsuno, N., Shirai, T., Qu, N., Hatayama, N., Hirai, S., Fukui, H., Ohseto, K., Yukioka, T., Itoh, M., 2014. Saturated salt

solution method: a useful cadaver embalming for surgical skills training. Medicine (Baltimore) 93, e196.

Herzog, J.A., Leonard, T.R., Jinha, A., Herzog, W., 2012. Hysteresis and efficiency in passive skeletal muscle myofibrils. Biophysical Journal 102, 360a.

Himann, J.E., Cunningham, D.A., Rechnitzer, P.A., Paterson, D.H., 1988. Age related changes in speed of walking. Med Sci Sports Exerc 20, 161-166.

Hof, A.L., Zandwijk, J.P.V., Bobbert, M.F., 2002. Mechanics of human triceps surae muscle in walking, running and jumping. Acta Physiol Scand 174, 17-30.

Holt, N.C., Danos, N., Roberts, T.J., Azizi, E., 2016. Stuck in gear: age-related loss of variable gearing in skeletal muscle. The Journal of experimental biology 219, 998-1003.

Honeine, J.L., Schieppati, M., Gagey, O., Do, M.C., 2013. The functional role of the triceps surae muscle during human locomotion. PLoS One 8, e52943.

Hopkins, W.G., 2000. Measures of Reliability in Sports Medicine and Science. Sports Med 30, 1-15.

Hughes, V.A., Frontera, W.R., Wood, M., Evans, W.J., Dallal, G.E., Roubenoff, R., Singh, M.A.F., 2001. Longitudinal Muscle Strength Changes in Older Adults: Influence of Muscle Mass, Physical Activity, and Health. The Journals of Gerontology: Series A 56, 209-217.

Huijing, P.A., 1999. Muscle as a collagen fiber reinforced composite: a review of force transmission in muscle and whole limb. J Biomech 32, 329-345.

Huijing, P.A., Baan, G.C., 2001. Myofascial force transmission causes interaction

between adjacent muscles and connective tissue: effects of blunt dissection and compartmental fasciotomy on length force characteristics of rat extensor digitorum longus muscle. Arch Physiol Biochem 109, 97-109.

Huijing, P.A., Baan, G.C., 2003. Myofascial force transmission: muscle relative position and length determine agonist and synergist muscle force. J Appl Physiol 94, 1092-1107.

Huijing, P.A., van de Langenberg, R.W., Meesters, J.J., Baan, G.C., 2007. Extramuscular myofascial force transmission also occurs between synergistic muscles and antagonistic muscles. J Electromyogr Kinesiol 17, 680-689.

Hwang, S.W., Nam, Y.S., Hwang, K., Han, S.H., 2012. Thickness and tension of the gluteal aponeurosis and the implications for subfascial gluteal augmentation. J Anat 221, 69-72.

Innocenti, B., Larrieu, J.-C., Lambert, P., Pianigiani, S., 2017. Automatic characterization of soft tissues material properties during mechanical tests. Muscles, Ligaments and Tendons Journal 7, 529-537.

Ishikawa, M., Komi, P.V., Grey, M.J., Lepola, V., Bruggemann, G.P., 2005. Muscle-tendon interaction and elastic energy usage in human walking. J Appl Physiol 99, 603-608.

Ito, M., Kawakami, Y., Ichinose, Y., Fukashiro, S., Fukunaga, T., 1998. Nonisometric behavior of fascicles during isometric contractions of a human muscle. J Appl Physiol 85, 1230-1235.

Iwanuma, S., Akagi, R., Kurihara, T., Ikegawa, S., Kanehisa, H., Fukunaga, T.,

Kawakami, Y., 2011. Longitudinal and transverse deformation of human Achilles tendon induced by isometric plantar flexion at different intensities. J Appl Physiol 110, 1615-1621.

Jeon, M., Youn, K., Yang, S., 2018. Reliability and quantification of gastrocnemius elasticity at relaxing and at submaximal contracted condition. Med Ultrason 20, 342-347.

Kari Kauranen, 1999. Human motor performance and physiotherapy. Oulu: University of Oulu.

Kawakami, Y., 2012. Morphological and functional characteristics of the muscle-tendon unit. J Phys Fitness Sports Med 1, 287-296.

Kawakami, Y., Abe, T., Fukunaga, T., 1993. Muscle-fiber pennation angles are greater in hypertrophied than in normal muscles. J Appl Physiol 74, 2740-2744.

Kawakami, Y., Ichinose, Y., Fukunaga, T., 1998. Architectural and functional features of human triceps surae muscles during contraction. J Appl Physiol 85, 398-404.

Kawakami, Y., Lieber, R.L., 2000. Interaction between series compliance and sarcomere kinetics determines internal sarcomere shortening during fixed-end contraction. J Biomech 33, 1249-1255.

Kostyukov, A.I., Cherkassky, V.L., Tal'nov, A.N., 1995. Hysteresis of muscle contraction and effects of uncertainty in proprioceptive activity and motor performance. Alpha and Gamma Motor Systems, 115-117.

Kubo, K., Kanehisa, H., Fukunaga, T., 2002. Effect of stretching training on the viscoelastic properties of human tendon structures in vivo. J Appl Physiol 92, 595-

601.

Kumakura, H., Inokuchi, S., 1991. Lay-out of the human triceps surae muscle: with special concern for the origin of the human bipedal posture. Showa Univ. J. Med. Sci. 3, 79-89.

Kumar, P., Pandey, A.K., Kumar, B., Aithal, S.K., 2011. Anatomical study of superficial fascia and localized fat deposits of abdomen. Indian J Plast Surg 44, 478-483.

Kwah, L.K., Pinto, R.Z., Diong, J., Herbert, R.D., 2013. Reliability and validity of ultrasound measurements of muscle fascicle length and pennation in humans: a systematic review. J Appl Physiol (1985) 114, 761-769.

Lacourpaille, L., Nordez, A., Hug, F., 2017. The nervous system does not compensate for an acute change in the balance of passive force between synergist muscles. The Journal of experimental biology 220, 3455-3463.

Lake, S.P., Miller, K.S., Elliott, D.M., Soslowsky, L.J., 2010. Tensile properties and fiber alignment of human supraspinatus tendon in the transverse direction demonstrate inhomogeneity, nonlinearity, and regional isotropy. J Biomech 43, 727-732.

Lauri Stenroth, 2016. Structure and function of human triceps surae muscle and tendon in aging. Jyväskylä: University of Jyväskylä.

Levine, T.R., Hullett, C.R., 2002. Eta Squared, Partial Eta Squared, and Misreporting of Effect Size in Communication Research. Human Communication Research 28, 612-625.

Lewis, G., Shaw, K.M., 1997. Tensile properties of human tendon Achillis: effect of donor age and strain rate. J Foot Ankle Surg 36, 435-445.

Lichtwark, G.A., Bougoulias, K., Wilson, A.M., 2007. Muscle fascicle and series elastic element length changes along the length of the human gastrocnemius during walking and running. J Biomech 40, 157-164.

Lieber, R.L., Brown, C.G., Trestik, C.L., 1992. Model of muscle-tendon interaction during frog semitendinosis fixed-end contractions. J Biomech 25, 421-428.

Lieber, R.L., Leonard, M.E., Brown-Maupin, C.G., 2000. Effects of muscle contraction on the load-strain properties of frog aponeurosis and tendon. Cells Tissues Organs 166, 48-54.

Louis-Ugbo, J., Leeson, B., Hutton, W.C., 2004. Tensile properties of fresh human calcaneal (Achilles) tendons. Clin Anat 17, 30-35.

Lynch, H.A., Johannessen, W., Wu, J.P., Jawa, A., Elliott, D.M., 2003. Effect of fiber orientation and strain rate on the nonlinear uniaxial tensile material properties of tendon. J Biomech 125, 726-731.

Maas, H., Sandercock, T.G., 2010. Force transmission between synergistic skeletal muscles through connective tissue linkages. J Biomed Biotechnol 2010, 575672.

Maeo, S., Saito, A., Otsuka, S., Shan, X., Kanehisa, H., Kawakami, Y., 2017. Localization of muscle damage within the quadriceps femoris induced by different types of eccentric exercises. Scand J Med Sci Sports.

Maeo, S., Shan, X., Otsuka, S., Kanehisa, H., Kawakami, Y., 2018a. Neuromuscular Adaptations to Work-matched Maximal Eccentric versus Concentric Training.

Med Sci Sports Exerc 50, 1629-1640.

Maeo, S., Shan, X., Otsuka, S., Kanehisa, H., Kawakami, Y., 2018b. Single-joint eccentric knee extension training preferentially trains the rectus femoris within the quadriceps muscles. Translational Sports Medicine 1, 212-220.

Maganaris, C.N., 2002. Tensile properties of in vivo human tendinous tissue. J Biomech 35, 1019-1027.

Maganaris, C.N., Baltzopoulos, V., Sargeant, A.J., 1998. In vivo measurements of the triceps surae complex architecture in man: implications for muscle function. J Physiol 512, 603-614.

Maganaris, C.N., Kawakami, Y., Fukunaga, T., 2001. Changes in aponeurotic dimensions upon muscle shortening: in vivo observations in man. J Anat 199, 449-456.

Maganaris, C.N., Paul, J.P., 2000. Hysteresis measurements in intact human tendon. J Biomech 33, 1723-1727.

Magnusson, S.P., Aagaard, P., Rosager, S., Dyhre-Poulsen, P., Kjaer, M., 2001. Load–displacement properties of the human triceps surae aponeurosis in vivo. J Physiol 531, 277-288.

Magnusson, S.P., Hansen, P., Aagaard, P., Brønd, J., Dyhre-Poulsen, P., Bojsen-Moller, J., Kjaer, M., 2003. Differential strain patterns of the human gastrocnemius aponeurosis and free tendon, in vivo. Acta Physiol Scand 177, 185-195.

Magnusson, S.P., Narici, M.V., Maganaris, C.N., Kjaer, M., 2008. Human tendon behaviour and adaptation, in vivo. J Physiol 586, 71-81.

Marieswaran, M., Mansoori, N., Digge, V.K., Jhajhria, S.K., Behera, C., Lalwani, S., Kalyanasundaram, D., 2018. Effect of preservation methods on tensile properties of human femurACL-tibial complex (FATC) – A cadaveric study on male subjects. Acta Bioeng Biomech 20.

Martin, D.C., Medri, M.K., Chow, R.S., Oxorn, V., Leekam, R.N., Mckee, N.H., 2001. Comparing human skeletal muscle architectural parameters of cadavers with in vivo ultrasonographic measurements. J Anat 199, 429-434.

Martin, J.A., Biedrzycki, A.H., Lee, K.S., DeWall, R.J., Brounts, S.H., Murphy, W.L., Markel, M.D., Thelen, D.G., 2015. In Vivo Measures of Shear Wave Speed as a Predictor of Tendon Elasticity and Strength. Ultrasound Med Biol 41, 2722-2730.

Mendes, B., Firmino, T., Oliveira, R., Neto, T., Infante, J., Vaz, J.R., Freitas, S.R., 2018. Hamstring stiffness pattern during contraction in healthy individuals: analysis by ultrasound-based shear wave elastography. Eur J Appl Physiol.

Miller, K.S., Connizzo, B.K., Feeney, E., Soslowsky, L.J., 2012. Characterizing local collagen fiber re-alignment and crimp behavior throughout mechanical testing in a mature mouse supraspinatus tendon model. J Biomech 45, 2061-2065.

Miyamoto, N., Hirata, K., Kanehisa, H., Yoshitake, Y., 2015. Validity of measurement of shear modulus by ultrasound shear wave elastography in human pennate muscle. PLoS One 10, e0124311.

Mogi, Y., Torii, S., Kawakami, Y., Yanai, T., 2013. Morphological and mechanical properties of the Achilles tendon in adolescent boys. Jpn J Phys Fitness Sports Med 62, 303-313.

Morrow, D.A., Haut Donahue, T.L., Odegard, G.M., Kaufman, K.R., 2010. Transversely isotropic tensile material properties of skeletal muscle tissue. Journal of the Mechanical Behavior of Biomedical Materials 3, 124-129.

Muramatsu, T., Muraoka, T., Takeshita, D., Kawakami, Y., Hirano, Y., Fukunaga, T., 2001. Mechanical properties of tendon and aponeurosis of human gastrocnemius muscle in vivo. J Appl Physiol 90, 1671-1678.

Narici, M.V., Binzoni, T., Hiltbrand, E., Fasel, J., Terrier, F., Cerretelli, P., 1996. In vivo human gastrocnemius architecture with changing joint angle at rest and during graded isometric contraction. J Physiol 496, 287-297.

Narici, M.V., Maffulli, N., Maganaris, C.N., 2008. Ageing of human muscles and tendons. Disabil Rehabil 30, 1548-1554.

Narici, M.V., Maganaris, C., Reeves, N., 2005. Myotendinous alterations and effects of resistive loading in old age. Scand J Med Sci Sports 15, 392-401.

Neptune, R.R., Kautz, S.A., Zajac, F.E., 2001. Contributions of the individual ankle plantar flexors to support, forward progression and swing initiation during walking. J Biomech 34, 1387-1398.

Ninh, L.N., Tangkawattana, S., Sukon, P., Takahashi, N., Takehana, K., Tangkawattana, P., 2018. Neutralizing formaldehyde in chicken cadaver with urea and urea fertilizer solution. J Vet Med Sci 80, 606-610.

Oda, T., Hisano, T., Hay, D.C., Kinugasa, R., Yamamura, N., Komatsu, T., Yokota, H., Takagi, S., 2015. Anatomical geometry and thickness of aponeuroses in human cadaver triceps surae muscles. Advanced Biomedical Engineering 4, 12-15.

Onambele, G.L., Narici, M.V., Maganaris, C.N., 2006. Calf muscle-tendon properties and postural balance in old age. J Appl Physiol (1985) 100, 2048-2056.

Otsuka, S., Shan, X., Kawakami, Y., 2019. Dependence of muscle and deep fascia stiffness on the contraction levels of the quadriceps: An in vivo supersonic shear-imaging study. Journal of Electromyography and Kinesiology 45, 33-40.

Otsuka, S., Yakura, T., Ohmichi, Y., Ohmichi, M., Naito, M., Nakano, T., Kawakami, Y., 2018. Site specificity of mechanical and structural properties of human fascia lata and their gender differences: A cadaveric study. J Biomech 77, 69-75.

Prasetyono, T.O.H., Sisca, F., 2019. Achilles tendon reconstruction with a half-width Achilles graft and wrap-around fascial flap. Arch Plast Surg.

Purslow, P.P., 2003. The structure and functional significance of variations in the connective tissue within muscle. Comparative Biochemistry and Physiology Part A 133, 947-966.

Raiteri, B.J., 2018. Aponeurosis behaviour during muscular contraction: A narrative review. Eur J Sport Sci 18, 1128-1138.

Raiteri, B.J., Cresswell, A.G., Lichtwark, G.A., 2016. Three-dimensional geometrical changes of the human tibialis anterior muscle and its central aponeurosis measured with three-dimensional ultrasound during isometric contractions. PeerJ 4, e2260.

Rehorn, M.R., Blemker, S.S., 2010. The effects of aponeurosis geometry on strain injury susceptibility explored with a 3D muscle model. J Biomech 43, 2574-2581.

Roberts, T.J., Azizi, E., 2011. Flexible mechanisms: the diverse roles of biological springs in vertebrate movement. The Journal of experimental biology 214, 353-

361.

Royer, D., Gennisson, J.L., Deffieux, T., Tanter, M., 2011. On the elasticity of transverse isotropic soft tissues (L). J Acoust Soc Am 129, 2757-2760.

Ryu, J., Jeong, W.K., 2017. Current status of musculoskeletal application of shear wave elastography. Ultrasonography 36, 185-197.

Saavedra, A.C., Zvietcovich, F., Lavarello, R.J., Castaneda, B., 2017. Measurement of surface acoustic waves in high-frequency ultrasound: preliminary results. Conf. Proc. IEEE Eng. Med. Biol. Soc., 3000-3003.

Saito, A., Ema, R., Inami, T., Maeo, S., Otsuka, S., Higuchi, M., Shibata, S., Kawakami, Y., 2016. Anatomical cross-sectional area of the quadriceps femoris and sit-to-stand test score in middle-aged and elderly population: development of a predictive equation. J Physiol Anthropol 36, 3.

Scott, S.H., Loeb, G.E., 1995. Mechanical properties of aponeurosis and tendon of the cat soleus muscle during whole-muscle isometric contractions. J Morphol 224, 73-86.

Segal, R.L., Song, A.W., 2005. Nonuniform activity of human calf muscles during an exercise task. Arch Phys Med Rehabil 86, 2013-2017.

Shan, X., Otsuka, S., Yakura, T., Naito, M., Nakano, T., Kawakami, Y., 2019. Morphological and mechanical properties of the human triceps surae aponeuroses taken from elderly cadavers: Implications for muscle-tendon interactions. PLoS One 14, e0211485.

Shinohara, M., Sabra, K., Gennisson, J.L., Fink, M., Tanter, M., 2010. Real-time

visualization of muscle stiffness distribution with ultrasound shear wave imaging during muscle contraction. Muscle Nerve 42, 438-441.

Shiotani, H., Yamashita, R., Mizokuchi, T., Naito, M., Kawakami, Y., 2019. Site- and sex-differences in morphological and mechanical properties of the plantar fascia: A supersonic shear imaging study. J Biomech.

Slane, L.C., DeWall, R., Martin, J., Lee, K., Thelen, D.G., 2015. Middle-aged adults exhibit altered spatial variations in Achilles tendon wave speed. Physiol Meas 36, 1485-1496.

Slane, L.C., Martin, J., DeWall, R., Thelen, D., Lee, K., 2017. Quantitative ultrasound mapping of regional variations in shear wave speeds of the aging Achilles tendon. Eur Radiol 27, 474-482.

Song, S., Geyer, H., 2018. Predictive neuromechanical simulations indicate why walking performance declines with ageing. J Physiol 596, 1199-1210.

Sta, H.U., Schatzmann, L., Brunner, P., Rincon, L., Nolte, L.-P., 1999. Mechanical tensile properties of the quadriceps tendon and patellar ligament in young adults. The American Journal of Sports Medicine 27, 27-34.

Stenroth, L., 2016. Structure and Function of Human triceps surae Muscle and Tendon in Aging. University of Jyväskylä, 87 p.

Stenroth, L., Peltonen, J., Cronin, N.J., Sipila, S., Finni, T., 2012. Age-related differences in Achilles tendon properties and triceps surae muscle architecture in vivo. J Appl Physiol (1985) 113, 1537-1544.

Stenroth, L., Sillanpaa, E., McPhee, J.S., Narici, M.V., Gapeyeva, H., Paasuke, M.,

Barnouin, Y., Hogrel, J.Y., Butler-Browne, G., Bijlsma, A., Meskers, C.G., Maier, A.B., Finni, T., Sipila, S., 2015. Plantarflexor Muscle-Tendon Properties are Associated With Mobility in Healthy Older Adults. J Gerontol A Biol Sci Med Sci 70, 996-1002.

Stenroth, L., Sipila, S., Finni, T., Cronin, N.J., 2017. Slower Walking Speed in Older Men Improves Triceps Surae Force Generation Ability. Med Sci Sports Exerc 49, 158-166.

Svensson, R.B., Heinemeier, K.M., Couppe, C., Kjaer, M., Magnusson, S.P., 2016. Effect of aging and exercise on the tendon. J Appl Physiol (1985) 121, 1237-1246.

Takaza, M., Moerman, K.M., Gindre, J., Lyons, G., Simms, C.K., 2013. The anisotropic mechanical behaviour of passive skeletal muscle tissue subjected to large tensile strain. J Mech Behav Biomed Mater 17, 209-220.

Taljanovic, M.S., Gimber, L.H., Becker, G.W., Latt, L.D., Klauser, A.S., Melville, D.M., Gao, L., Witte, R.S., 2017. Shear wave elastography: basic physics and musculoskeletal applications. RadioGraphics 37, 855-870.

Ting, C.E., Yeong, C.H., Ng, K.H., Abdullah, B.J.J., Ting, H.E., 2015. Accuracy of Tissue Elasticity Measurement using Shear Wave Ultrasound Elastography: A Comparative Phantom Study. World Congress on Medical Physics and Biomedical Engineering.

Tokuno, C.D., Carpenter, M.G., Thorstensson, A., Garland, S.J., Cresswell, A.G., 2007. Control of the triceps surae during the postural sway of quiet standing. Acta Physiol (Oxf) 191, 229-236.

Trotter, J.A., Samora, A., Baca, J., 1985. Three-dimensional structure of the murine muscle-tendon junction. The Anatomical Record 213, 16-25.

Valenti, G., Bonomi, A.G., Westerterp, K.R., 2016. Walking as a Contributor to Physical Activity in Healthy Older Adults: 2 Week Longitudinal Study Using Accelerometry and the Doubly Labeled Water Method. JMIR Mhealth Uhealth 4, e56.

Vergari, C., Pourcelot, P., Holden, L., Ravary-Plumioen, B., Gerard, G., Laugier, P., Mitton, D., Crevier-Denoix, N., 2011. True stress and Poisson's ratio of tendons during loading. J Biomech 44, 719-724.

Woo, S.L.-Y., Hollis, J.M., Adams, D.J., Lyon, R.M., Takai, S., 1991. Tensile properties of the human femuranterior cruciate ligament-tibia complex: The effects of specimen age and orientation. The American Journal of Sports Medicine 19, 217-225.

Yonei, Y., Takahashi, Y., Hibino, S., Watanabe, M., Yoshikawa, T., 2008. The effects of walking with pedometers on quality of life and various symptoms and issues relating to aging. Anti-aging Medicine, 5, 22-29.

Yoshida, K., Itoigawa, Y., Maruyama, Y., Saita, Y., Takazawa, Y., Ikeda, H., Kaneko, K., Sakai, T., Okuwaki, T., 2017. Application of shear wave elastography for the gastrocnemius medial head to tennis leg. Clin Anat 30, 114-119.

Yoshitake, Y., Takai, Y., Kanehisa, H., Shinohara, M., 2014. Muscle shear modulus measured with ultrasound shear-wave elastography across a wide range of contraction intensity. Muscle Nerve 50, 103-113.

Zhang, G.J., Yang, J., Guan, F.J., Chen, D., Li, N., Cao, L., Mao, H., 2016a. Quantifying the effects of formalin fixation on the mechanical properties of cortical bone using beam theory and optimization methodology with specimen-specific finite element models. J Biomech Eng 138, 0945021-0945028.

Zhang, L.N., Wan, W.B., Wang, Y.X., Jiao, Z.Y., Zhang, L.H., Luo, Y.K., Tang, P.F., 2016b. Evaluation of Elastic Stiffness in Healing Achilles Tendon After Surgical Repair of a Tendon Rupture Using In Vivo Ultrasound Shear Wave Elastography. Med Sci Monit 22, 1186-1191.

Zuurbier, C.J., Everard, A.J., Wees, P.d., Huijing, P.A., 1994. Length-force characteristics of the aponeurosis in the passive and active muscle condition and in the isolated condition. J Biomech 27, 445-453.

Acknowledgement

First and foremost, I would like to express my heartfelt thanks to my distinguished and cordial supervisor, Prof. Yasuo Kawakami, who agreed me to come to Japan and study in his laboratory, influenced me with his insightful ideas and meaningful inspirations, and guided me patiently with practical academic advice and feasible instructions while I was confused about my research. His thought-provoking comments and patient encouragements are indispensable for my accomplishment of this thesis. Without his dedicated assistance and insightful supervision, this thesis would have gone nowhere.

Besides my supervisor, I would like to express my special thanks to Profs. Takashi Nakano and Munekazu Naito, Dr. Tomiko Yakura, and all the staff members of the Anatomy Department of Aichi Medical University for providing me an opportunity to do cadaveric studies there, giving me much advice and helping me a lot. Without their precious support it would not be possible to conduct this research.

My sincere thanks also go to Ms. Fumiko Tanaka, Dr. Sumiaki Maeo, Dr. Akira Saito, Dr. Takaki Yamagishi, Dr. Ateş Filiz, Dr. Pavlos Evangelidis, Dr. Naoki Ikeda, Dr. Natsuki Sado, Dr. Junya Saeki, Mr. Weihuang Qi, Mr. Shun Otsuka, Mr. Hiroto Shiotani, Miss. Hoshizora Ichinose, Mr. Gaku Aizawa, Mr. Chi Yang, Miss Apibantawesakul Sudarat, Miss Hui Lyu, Miss Moemi Kikuchi, Ms. Mitsuko Oshige and other members in Kawakami laboratory of Waseda University, who offered me great help, and for all the fun we have had in the last four years.

Also, I am greatly indebted to China Scholarship Council (CSC) and Ministry of

Education, Culture, Sports, Science and Technology · Japan (MEXT) who provided financial aid for my abroad study.

Last but not the least, thanks go to my beloved parents and sister, whose care and support motivate me to move on and make me want to be a better person.